

RADIO ASTRONOMY

Journal of the Society of Amateur Radio Astronomers
March - April 2023

Members at OVRO



SARA's First Live Conference Since 2019!



Dr. Richard A. Russel
SARA President and Editor

Whitham D. Reeve
Contributing Editor

Radio Astronomy is published bimonthly as the official journal of the Society of Amateur Radio Astronomers. Duplication of uncopyrighted material for educational purposes is permitted but credit shall be given to SARA and to the specific author. Copyrighted materials may not be copied without written permission from the copyright owner.

Radio Astronomy is available for download only by SARA members from the SARA web site and may not be posted anywhere else.

It is the mission of the Society of Amateur Radio Astronomers (SARA) to: Facilitate the flow of information pertinent to the field of Radio Astronomy among our members; Promote members to mentor newcomers to our hobby and share the excitement of radio astronomy with other interested persons and organizations; Promote individual and multi station observing programs; Encourage programs that enhance the technical abilities of our members to monitor cosmic radio signals, as well as to share and analyze such signals; Encourage educational programs within SARA and educational outreach initiatives. Founded in 1981, the Society of Amateur Radio Astronomers, Inc. is a membership supported, non-profit [501(c) (3)], educational and scientific corporation.

Copyright © 2023 by the Society of Amateur Radio Astronomers, Inc. All rights reserved.

Cover Photo:
Richard Russel

Contents

President's Page	2
Editor's Notes.....	3
SARA NOTES	3
SARA 2023 Eastern/Annual Conference	6
News: (March - April 2023)	9
Technical Knowledge & Education (March - April 2023)	11
Announcements (March - April 2023)	13
SuperSID.....	17
Announcing Radio JOVE 2.0.....	20
John Cook's VLF Report.....	26
BAA RA Section Summer programme 2023.....	42
VINTAGE SARA	43
<i>SERENDIP's Common Thread - Charles Osborne, SARA Historian</i>	43
The Parallel Port and MAX-186/187 – James Van Prooyen.....	47
Featured Articles	49
A story, tangentially related to Radio Astronomy - Marcus Leech.....	49
Lunar radiation observed by a small dish at 80 GHz. Part 1, the telescope and conditions. - <i>Dimitry Fedorov UA3AVR and Joachim Köppen DF3GJ</i>	51
Another Look at the System Noise Temperature of a Radiometer - Peter W East.....	58
Planning for the 2023 and 2024 Solar Eclipses at VHF, UHF and Ku-band - Christian Monstein and Whitham D. Reeve.....	63
Catalogue of the brightest astrophysical maser sources - <i>Eduard Mol</i>	90
Observation Reports	94
Observations in Alaska of Solar Radio and Magnetic Activity During February 2023 - Whitham D. Reeve.....	94
Solar Radio Observations at Anchorage, Alaska in March 2023 - Whitham D. Reeve... ..	96
Journal Archives and Other Promotions	98
What is Radio Astronomy?.....	99
Radio Astronomy Constants, Variables and Formulas – Parabolic Dish Gain.....	100
Officers, directors, and additional SARA contacts.....	103
Resources	104
Great Projects to Get Started in Radio Astronomy.....	104
Radio Astronomy Online Resources.....	106
For Sale, Trade and Wanted	107
SARA Advertisements	109
SARA Brochure.....	110

President's Page



Outstanding Live Western Conference at Owens Valley Radio Observatory!

David Westman did another fabulous job of organizing the event. You can view the conference on the SARA YouTube channel: https://www.youtube.com/playlist?list=PLCEbOD5_znsINwecrEN3o_PUnW89-vVwK

I want to personally thank Whitham Reeve for being the journal's contributing editor for 10+ years. He has been my mentor for editing and producing the journal. Whit is taking a break as the contributing editor to pursue a very cool project involving long wavelength arrays. **Thanks Whit!**

SARA's next big event is the Eastern Conference at the Greenbank Observatory. Your esteemed vice president Jay Wilson is organizing this event. We will use the live/zoom approach again to get the maximum number of presentation and participants. Sign up on the SARA store.

Thanks!

Rich
SARA President

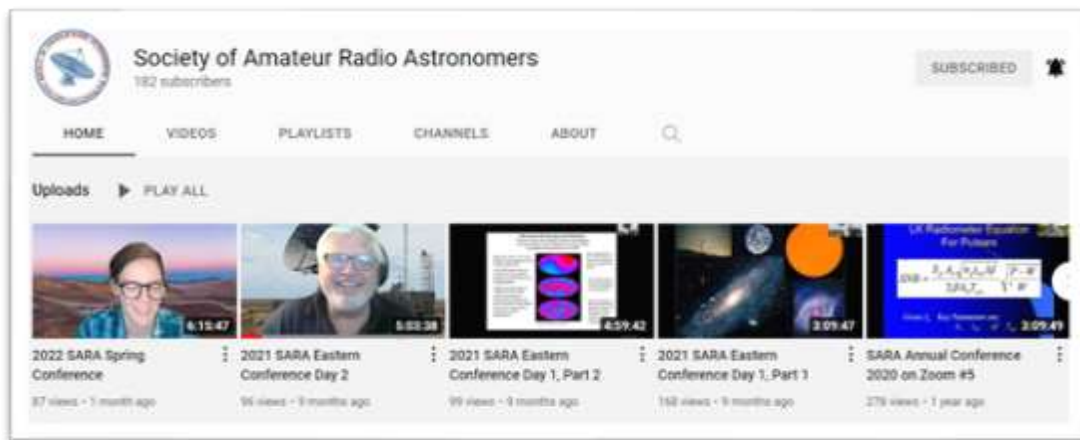
Editor's Notes

We are always looking for basic radio astronomy articles, radio astronomy tutorials, theoretical articles, application and construction articles, news pertinent to radio astronomy, profiles and interviews with amateur and professional radio astronomers, book reviews, puzzles (including word challenges, riddles, and crossword puzzles), anecdotes, expository on "bad astronomy," articles on radio astronomy observations, suggestions for reprint of articles from past journals, book reviews and other publications, and announcements of radio astronomy star parties, meetings, and outreach activities.

Subscribe to the SARA YouTube Channel

SARA has a YouTube channel at: <https://www.youtube.com/channel/UC-SzptAQZ-20c9CkRb9ZPpw/videos>

We are also looking to add content to the site. Anyone who wants to help produce a series of 5 - minute videos relating to radio astronomy technology or observations please contact me. (drrichrussel@netscape.net)



Observation Reports

We are now accepting 1-2 page observation reports. These reports should include the astronomical object's RA/DEC plus UTC of the observation. Also include the telescope configuration, process used to observe the object and results. Picture of the setup and plots of the observation are a plus to the report.

If you would like to write an article for Radio Astronomy, please follow **the newly updated Author's Guide** on the SARA web site:

http://www.radio-astronomy.org/publicat/RA-JSARA_Author's_Guide.pdf.

Let us know if you have questions; we are glad to assist authors with their articles and papers and will not hesitate to work with you. You may contact your editors any time via email here: edit@radio-astronomy.org.

The editor(s) will acknowledge that they have received your submission within two days. If they do not reply, assume they did not receive it and please try again.

Please consider submitting your radio astronomy observations for publication: any object, any wavelength. Strip charts, spectrograms, magnetograms, meteor scatter records, space radar records, photographs; examples of radio frequency interference (RFI) are also welcome.

Guidelines for submitting observations may be found here: http://www.radio-astronomy.org/publicat/RA-JSARA_Observation_Submission_Guide.pdf

SARA Student & Teacher Grant Program

All, SARA has a grant program that is, sad to say very underutilized. We will provide kits or money to students and teachers including college students to help them with a radio telescope project. SARA can supply any of the following kits:

- [1] SuperSID
- [2] Scope in a Box
- [3] IBT (Itty Bitty Telescope)
- [4] Radio Jove kit
- [5] Inspire
- [6] Sky Scan

We can also provide up to five hundred dollars (\$500.00 USD) for an approved radio telescope project.

We have on occasion provided more money based on the merits of the project and the SARA Grant Committee approval.

More information on the grant program can be found at the URL below.

[SARA Student and Teacher Project Grants | Society of Amateur Radio Astronomers \(radio-astronomy.org\)](#)

All that is required is the SARA grant request form be filled out and sent in. If it needs more work for approval, we will work with the student to help ensure their success.

Please pass the word that SARA will fund any legitimate radio telescope project anywhere in the world.

If you have a question, contact me at [crowleytj at hotmail](mailto:crowleytj@hotmail.com) dot com.

Tom Crowley
SARA Grant Program Administrator

NEW Drake's Lounge Australia

This new zoom forum is geared to the Melbourne, Australia time zone (UTC+10) in order to improve coordination with our Australia, New Zealand, and Japanese members. The meetings are scheduled for the 4th Friday of every month, 9 AM Melbourne time (2000 UTC December 23). A zoom announcement will be sent out to all SARA members before the meeting.

Radio Telescope Observation Party (RTOP)

RTOP is designed to demonstrate how to take observations using various radio telescopes. It will also cover how to record and analyze data.

RTOP is every month on the 1st Sunday at 2 pm Eastern time (1800 UTC). ZOOM email notifications will be sent to all members.

Drake's Lounge

Join the SARA community as we discuss the latest astronomy and radio astronomy news. The lounge also provides a forum to share and get advice on your radio astronomy projects from very experienced amateur radio astronomers.

Drake's Lounge is every month on the 3rd Sunday at 2 pm Eastern time (1800 UTC). ZOOM email notifications will be sent to all members.

**2023 SARA Annual Conference
Green Bank Observatory
Green Bank, West Virginia,
2023 20-23 August 2023**

The 2023 SARA Annual Conference will be held at the Green Bank Observatory, West Virginia, Sunday through Wednesday, 20-23 August 2023.

SARA has traditionally held our Eastern Conferences at GBO, and we are very pleased to return following a two-year hiatus due to COVID.

With radio astronomy as its foundation, the Green Bank Observatory (GBO) is a world leader in advancing research, innovation, and education.

The first trailblazers of American radio astronomy called Green Bank Observatory home over 60 years ago. Today, their legacy is alive and well. Nestled in the mountain ranges and farmland of West Virginia, within the National Quiet Zone, radio astronomers are listening to the remote whispers of the universe, in order to discover answers to our most astounding astronomical questions.



Call for Papers

Papers are invited on all subjects related to amateur, scholastic, or professional radio astronomy including hardware, software, education, tutorial, outreach, research strategies, observation, data collection, philosophy, theoretical or practical challenges, and related subjects.

If you wish to present a paper or provide an exhibit, please email a proposal including a title and abstract to the conference coordinator at vicepresident@radio-astronomy.org no later than 30 April 2023.

Please include your full name, affiliation, CV if appropriate, postal address, and email address, and indicate your preference to present to the conference in person or virtually. You will receive an email response within about a week.

Complete papers are due on July 15, 2023. Presentation Slides / PowerPoints are due on August 10, 2023.

Basic Schedule: Conference meetings will be held in the main auditorium of the Jansky Laboratory at Green Bank Observatory with presentations by SARA members, GBO staff and distinguished speakers. Security and COVID restrictions permitting, tours of the facility, radio telescopes and laboratories will be conducted. Certain locations are open only to U.S. citizens who submit for a security review two weeks prior; however, other areas will be open to all attendees. Virtual participation in the conference will be available for those who cannot attend in person.

Key advantage of in-person attendance is training and hands-on use of the historical 40-foot radio telescope as well as user tutorial on the 20 meter radio telescope.

On Sunday and Monday evenings, round table discussions and refreshments are scheduled in the Drake Lounge, and there will be space outside for attendees to set up and display their own portable radio astronomy systems and optical telescopes.

Meals in the GBO cafeteria are included in the registration fee.

Lodging is not included in the conference registration fee. A few GBO dormitory rooms may be available and can be requested on a first-come-first-served basis when you register for the conference. All available rooms are usually needed for conference presenters and SARA officers working at the conference, but if additional rooms become available, they will be offered to other attendees on a first-come basis about 10 days before the conference. Attendees staying in GBO rooms pay the observatory housing office by check or charge card on Monday afternoon of the conference. Expected rates are \$75 single occupancy or \$95 double.

No-frills rooms and RV/camping sites are available at the nearby Boyer Station Motel and Campground. The Elk Springs Resort is about 12 miles away. Many chain accommodations are located about 30 miles away in Elkins, but that drive takes at least an hour due to mountainous roads.

Registration: Registration for in-person attendance by SARA members at the Conference is \$275.00 (USD) if received by July 20, 2023, which includes meals but not lodging. The fee for family members or other guests who do not participate in conference sessions is \$75.00, which includes meals plus evening activities.

Registration by July 20th for non-members is \$295.00, which includes a year's membership in SARA.

SARA members wishing to renew their membership at the same time as they register may also pay \$295 and should include a renewal comment with their payment.

Late registration after July 20, 2023, is \$325.00, with very little chance of on-campus housing. Walk-in registration at the conference is \$350.00 with no on-campus housing option.

Payment can be made through PayPal, www.paypal.com by sending payment to treas@radio-astronomy.org Please include in comments that the payment is for the **2023 Annual Conference** and indicate if you would like on campus housing for single or double occupancy if it becomes available.

COVID Restrictions. GBO reserves the right to impose requirements for vaccinations and masks. SARA will notify all registrants should GBO issue a policy statement. Should GBO policies adversely impact a conference registrant, they may change their registration from in-person to virtual / online and receive a refund for the difference. Should GBO close the campus for any reason, all registrations will be changed to virtual / online.

Cancellations. Full refund minus PayPal transaction fees will be issued for cancellations received by July 31, 2023. After July 31, cancellations will be handled on a case-by-case basis. SARA will strive to issue partial refunds based on the non-refundable obligations we have made.

No Cellular Phone Service. GBO is in the National Radio Quiet Zone and there is no wireless phone service in the area. Use of wi-fi devices and satellite phones such as Iridium, Globalstar, StarLink or similar devices near the facility is not allowed, and severe restrictions are placed on digital cameras, although film cameras without electronic flash are allowed in most areas of the site. Some dorm rooms have wired internet connections for portable computers and there is a computer lab available during the day. Some dorm rooms have phones for incoming calls. Outgoing calls require a calling card. In case of family or business emergencies, GBO Operations can be reached at 304-456-2150.

Pre-Conference Activities. Suggested pre-conference activities include free self-guided tours of the Green Bank Observatory Science Center and reasonably priced guided tours of the radio telescope area. Full details with a link for ticket purchase: <https://greenbankobservatory.org/visit/>

An overall guide to other activities and attractions in the area: <https://pocahontascountywv.com/things-to-do/>

Contact: Please contact the conference coordinator, B.J. Wilson, if you have any questions or if you would like to help with the conference: vicepresident@radio-astronomy.org

Additional Information: Additional details and updates will be published online at www.radio-astronomy.org and in the SARA journal, *Radio Astronomy*, as we get closer to the conference date.



Universe Today ~ *The World's Largest Radio Telescope Just Scanned 33 Exoplanets for a Signal From Aliens:*
<https://www.universetoday.com/159855/the-worlds-largest-radio-telescope-just-scanned-33-exoplanets-for-a-signal-from-aliens/>

Universe Today ~ *A Green Bank Telescope Prototype Radar System Can Image the Moon in High-Resolution and Detect Asteroids:* <https://www.universetoday.com/160048/a-green-bank-telescope-prototype-radar-system-can-image-the-moon-in-high-resolution-and-detect-asteroids/>

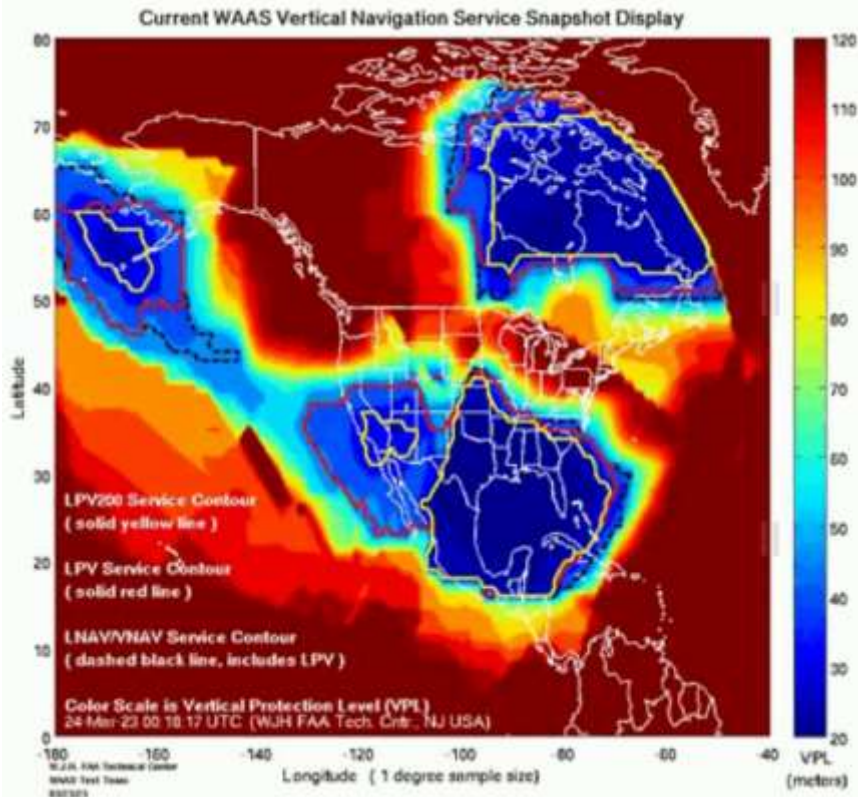
NASA ~ *Ham Radio Operators, We Need Your Help During Solar Eclipses!:*
<https://science.nasa.gov/science-news/citizenscience/ham-radio-operators-we-need-your-help-during-solar-eclipses>



History of Geo- and Space Sciences ~

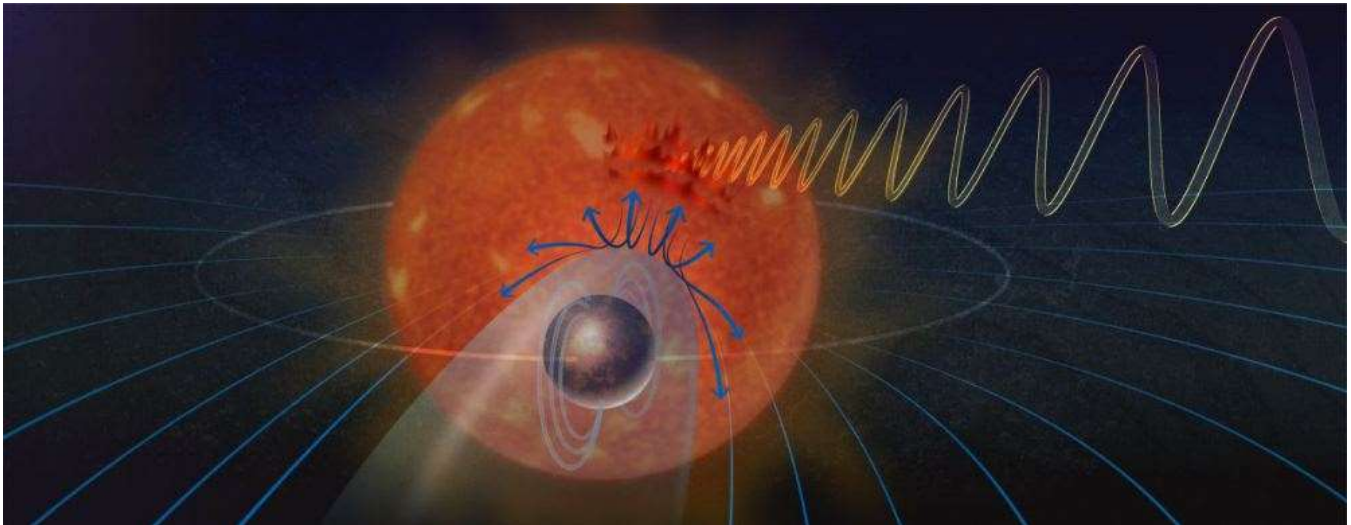
⚙ *History of the Potsdam, Seddin and Niemegek geomagnetic observatories – Part 1: Potsdam:* <https://hgss.copernicus.org/articles/14/23/2023/>

⚙ *History of the Potsdam, Seddin and Niemegek geomagnetic observatories – Part 2: Seddin:* <https://hgss.copernicus.org/articles/14/43/2023/>



STCE ~ Severe geomagnetic storm!: <https://www.stce.be/news/638/welcome.html>

Universe Today ~ Gravitational Waves From Colliding Neutron Stars Matched to a Fast Radio Burst:
<https://www.universetoday.com/160752/gravitational-waves-from-colliding-neutron-stars-matched-to-a-fast-radio-burst/>

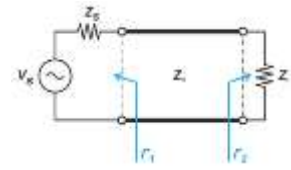


Universe Today ~ Do Repeating Radio Signals Indicate an Exoplanet with a Magnetosphere?:
<https://www.universetoday.com/160864/do-repeating-radio-signals-indicate-an-exoplanet-with-a-magnetosphere/>

Technical Knowledge & Education (March - April 2023)

All About Circuits ~ *Mismatch Loss and Mismatch Uncertainty in RF Systems:*

<https://www.allaboutcircuits.com/technical-articles/mismatch-loss-and-mismatch-uncertainty-in-rf-systems/>



All About Circuits ~ *Mismatch Loss: Two Different Definitions:*

<https://www.allaboutcircuits.com/technical-articles/mismatch-loss-effect-on-radio-frequency-power-measurement-and-gain-of-cascaded-amplifiers/>

SARA ~ *Complete 3-part tutorial for the SARA ezRA – Easy Radio Astronomy:*

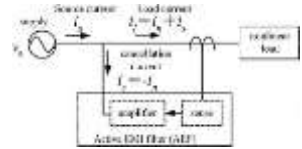
- ⚙ Part 1) <https://youtu.be/2DbS5A42OJQ>
- ⚙ Part 2) <https://youtu.be/N1TRyJ9w0As>
- ⚙ Part 3) <https://youtu.be/8EUmCQAIBLg>



Rohde & Schwarz ~ *The Cold Source Technique for Noise Figure Measurements:* https://www.rohde-schwarz.com/us/applications/the-cold-source-technique-for-noise-figure-measurements-application-note_56280-1160641.html

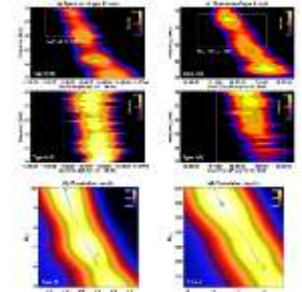
Electronic Design ~ *Exploring Op Amps:*

<https://www.electronicdesign.com/magazine/51497>



CESRA ~ *The frequency ratio and time delay of fundamental and harmonic components in solar radio bursts:*

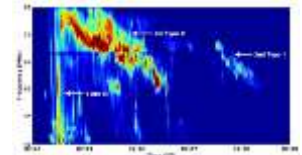
<https://www.astro.gla.ac.uk/users/eduard/cesra/?p=3493>



arXiv ~ *The First CHIME/FRB Fast Radio Burst Catalog; CHIME/FRB Collaboration; updated with an erratum affecting the sky rate:* <https://arxiv.org/abs/2106.04352>

Copper Mountain Technologies ~ *Optimizing VNA Measurement Speed:*

<https://coppermountaintech.com/wp-content/uploads/2023/01/Optimizing-VNA-Measurement-Speed-v2.pdf>



CESRA ~ *Solar coronal density turbulence and magnetic field strength at the source regions of two successive metric type II radio bursts:*

<https://www.astro.gla.ac.uk/users/eduard/cesra/?p=3501>

EE Times ~ *Ebook: Advancements in Wideband in RF Receiver Signal Chain Design:*

<https://aspencore.uberflip.com/i/1489750-adi-na-q1-2023-adv-in-wideband-rf/0>

SARA ~ *2023 Western Conference Video Recordings:*

https://www.youtube.com/playlist?list=PLCEbOD5_znsINwecrEN3o_PUnW89-vVwK



SigidWiki ~ *Signal Identification Guide:*

https://www.sigidwiki.com/wiki/Signal_Identification_Guide

All About Circuits ~ *Learn by Example—Using an Impedance Smith Chart:*

<https://www.allaboutcircuits.com/technical-articles/learn-to-use-the-impedance-smith-chart-through-examples/>



KA1GT

VHF/UHF/Microwave Information
and Resources for Radio Amateurs



Stable 25 MHz Reference: http://www.bobatkins.com/radio/25MHz_reference.html

Low cost 10Ghz EME Rx System: http://www.bobatkins.com/radio/10Ghz_EME_rx.html

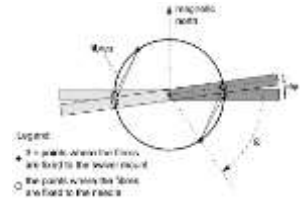
History of Geo- and Space Sciences ~ *Historical geomagnetic observations from Prague observatory (since 1839) and their contribution to geomagnetic research:*

<https://hgss.copernicus.org/articles/14/51/2023/>

SARA ~ *Radio Astronomy Video Series: Constants, Variables and Formulas, Radio Astronomy Formulas:*

⚙ Lesson 1- *Parabolic Dish Gain:* https://www.youtube.com/watch?v=2bx5K9jUc_w

⚙ Lesson 2 -*Parabolic Dish Half Power Beamwidth:* <https://www.youtube.com/watch?v=XWOMRrwlk18>



Announcements (March - April 2023)



**Foundations of Citizen Science
Tutorial**

Start with the self-guided Foundations of Citizen Science Training and badge, a prerequisite for follow-on trainings. Learn the basics, participate in projects, and make the most of SciStarter.

[Get Started](#)



April is Citizen Science Month — are you ready?

A great way to get your head in the game is to join thousands of others who have completed our short training module: [Foundations of Citizen Science](#) (https://scistarter.org/training?utm_campaign=UM54&utm_medium=Email&utm_source=User%20Messages).

Presented by SciStarter, created by the talented instructional designers at Arizona State University and funded by the National Library of Medicine, the interactive overview walks you through what citizen science is all about. You'll even get started on two of our most popular projects: Stall Catchers and Project Squirrel. Most people finish the module in less than an hour.

If you've graduated from Foundations, find your next training adventure on our [training page](#) (https://scistarter.org/training?utm_campaign=UM54&utm_medium=Email&utm_source=User%20Messages).

Find a module on Building Data Literacy Through Community and Citizen Science. Practitioners can find trainings too: Libraries as Community Hubs for Citizen Science, Teaching in Higher Education with Citizen Science and Data Ethics for Practitioners.

If you're logged into SciStarter when you engage with the training, you'll earn a free, printable, personalized certificate and a digital badge linked to skills you can share on social media. Head to our [training page](#) to get started.

Are you interested in a future training that would prepare you to be a SciStarter Ambassador? SciStarter Ambassadors are people who complete the Foundations training and one additional training to help others learn about SciStarter and citizen science at their local library, museum, science club, etc. We'll provide you with

training slides, talking points and activities. [Complete this brief Google Form](#) if this is something you might be interested in in the future!

And be sure to check out all the events we have in store for you this April during [Citizen Science Month 2023!](#)



It is our pleasure to announce the ninth incarnation of Science at Low Frequencies (SALF IX), which will be a hybrid conference held from the 11th to the 15th of December 2023. The in-person component will be hosted at Amsterdam Science Park, The Netherlands. Amsterdam Science Park is easily accessible via public transport from Schiphol international airport and is only a 10-minute train ride (or 20-minute bike ride) from the centre of the city.

Thanks to several low-frequency telescopes maturing in their scientific output, the low-frequency radio astronomy community has been developing rapidly. In particular, there is a large amount of effort going into all-sky surveys and towards studying/detecting the Epoch of Reionisation, transients, pulsars, exoplanets, and radio stars as well as studies of active galactic nuclei, solar physics, and space physics. With the next generation low-frequency telescopes in mind, we also need to understand the achievements and challenges presented by the existing telescopes. This is particularly pertinent considering Square Kilometre Array will start construction imminently. SALF IX is to act as the premier forum to share scientific results and techniques for low-frequency astronomy.

Talks at SALFIX will be recorded, so you can also peruse the presentations afterwards. There will also be a Slack channel dedicated to the meeting to encourage conversations to extend over different time zones. We are aiming to keep the registration costs of the conference as low as possible, but it is expected to be no more than 150 euro (depending on our success in securing external funding).

More details about the conference can be found here: <https://salfconference.org/2020-9th-annual-science-at-low-frequencies-salf-conference/> . A direct link to registration is available here: [https://urldefense.com/v3/https://indico.astron.nl/event/313/registrations/124/;!!IKRxdwAv5BmarQ!cxKTFNAjrLUeB3hSvCscb03gAFZlzoYgI-gCnYrRGAiVcWmdUw2lwadJARM4BKeNzYNhz5AylgwJWekxquVkYixu\\$](https://urldefense.com/v3/https://indico.astron.nl/event/313/registrations/124/;!!IKRxdwAv5BmarQ!cxKTFNAjrLUeB3hSvCscb03gAFZlzoYgI-gCnYrRGAiVcWmdUw2lwadJARM4BKeNzYNhz5AylgwJWekxquVkYixu$)

IMPORTANT DATES:

Abstract submission deadline: 11th of September, 2023

Registration deadline: 12th of October, 2023

Conference period: Monday 11th to Friday 15th of December, 2023

Scientific Organising Committee:

Natasha Hurley-Walker (Curtin University)

Jason Hessels (ASTRON/UvA)

Joe Callingham (ASTRON/Leiden), Chair

Poonam Chandra (NRAO/NCRA)

Leah Morabito (University of Durham)

Bryan Gaensler (University of Toronto)

Cherry Ng (CNRS)

Peijin Zhang (University of Helsinki)

Wendy Williams (SKAO)

George Heald (CSIRO)

Oleg Ul'yanov (Institute of Radio Astronomy, Ukraine)

Local Organising Committee:

Jason Hessels (ASTRON/UvA)

Joe Callingham (ASTRON/Leiden)

Marjan Tibbe (ASTRON)

Liesbet Elpenhof (ASTRON)

Please forward to anyone who may be interested in attending and please let me know if you have any questions.

Space Weather and Upper Atmospheric
Data analysis **Training Workshop**
for East African Community

25th - 29th September 2023
@MUNI UNIVERSITY

URSI GASS 2023

SAPPORO, JAPAN

XXXVth URSI General Assembly and Scientific Symposium

| Dates

August 19 (Sat) – 26 (Sat), 2023

| Venues

Sapporo Convention Center
Sapporo Business Innovation Center

▶ HOME

▶ Invitation

▶ Organization

▶ Committees

▶ Program

▶ Call for Papers

▶ Paper Submission

▶ Registration

▶ Accommodation

▶ Sponsors and Exhibitors

▶ Venue

▶ VISA &
Useful Information

▶ Contacts

▶ Poster
Download



▶ Logo
Download



Information

- 2023.03.28 [Registration](#) page has been updated.
- 2023.03.17 [Program](#) page is now open.
[Registration](#) page and [VISA & Useful Information](#) page have been updated.
- 2023.02.24 [VISA & Useful Information](#) page is now open.
- 2023.02.20 [Accommodation](#) page is now open.
- 2023.02.14 Paper Submission has been closed.
Thank you for your submission.
- 2023.01.25 The deadline of paper submissions has been extended. **The new deadline is 23:59, February 10, 2023, Brussels time!**
- 2023.01.23 The deadline of [paper submissions](#) is **January 25, 2023**. Please go to the Paper Submission Website for details. The list of sessions and their descriptions are found [here](#).
- 2022.12.19 The [Registration](#) webpage has been updated.
- 2022.12.07 The [Call for Papers](#) and [Committees](#) webpages have been updated.
- 2022.12.01 The [Paper Submission](#) and [Sponsors and Exhibitors](#) webpages have been updated.
- 2022.07.29 Website is Now Open.

Host

Japan National Committee of URSI (JNC-URSI)

Sponsors

The Institute of Electronics, Information and Communication Engineers (IEICE),
Science Council of Japan (SCJ)(under process),
International Union of Radio Science (URSI)

General Chair

Prof. Kazuya Kobayashi, Chuo University, Tokyo, Japan

Conference Secretariat

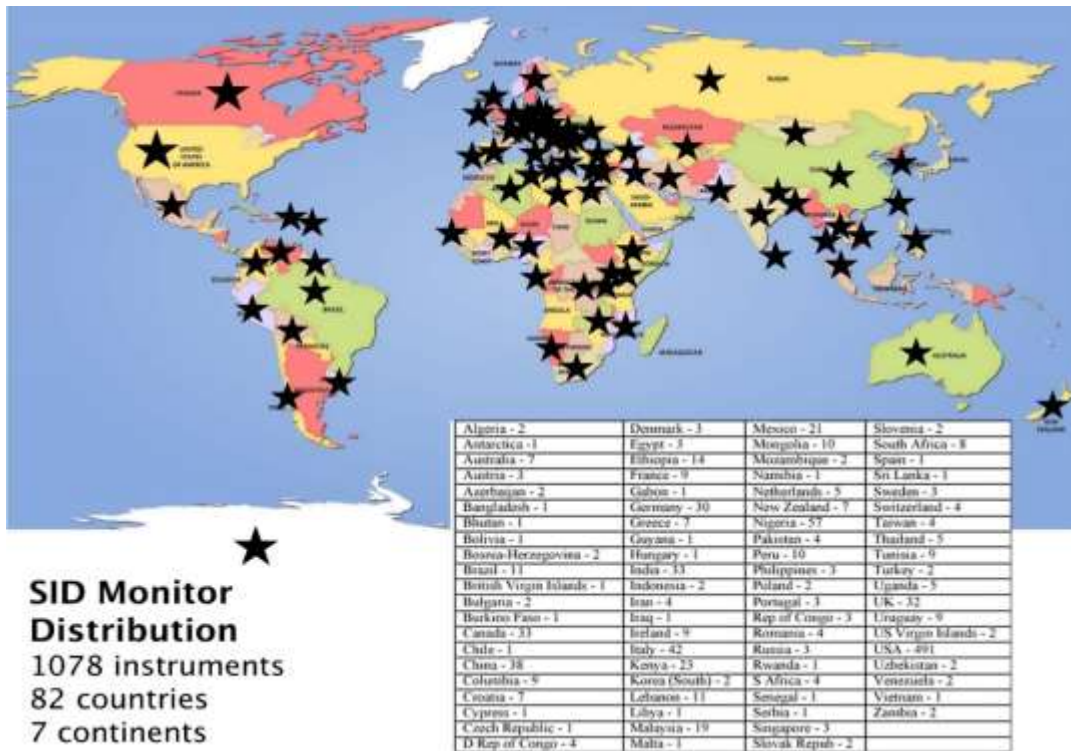
Convention Linkage, Inc., Sapporo, Japan



SuperSID
*Collaboration of Society
of Amateur Radio
Astronomers and
Stanford Solar Center*



- Stanford provides data hosting, database programming, and maintains the SuperSID website
- Society of Amateur Radio Astronomers (SARA) sells the SuperSID monitors for 48 USD to amateur radio astronomers and the funds are then used to support free distribution to students all over the world (image below as of Fall 2017)
- Jonathan Pettingale at SARA is responsible for building and shipping the SuperSID monitor kits: SuperSID@radio-astronomy.org
- SuperSID kits may be ordered through the SARA SuperSID webpage: <http://radio-astronomy.org/node/210>
- Questions about the SuperSID project may be directed to Steve Berl at Stanford: steveberl@gmail.com
- Jaap Akkerhuis at Stanford is responsible for the SuperSID software and SARA has provided financial support for his efforts
- SuperSID website hosted by Stanford: <http://solar-center.stanford.edu/SID/sidmonitor/>
- SuperSID database: <http://sid.stanford.edu/database-browser/>
- The data is searchable by time, station, date, and multiple plots may be placed on the same graph for comparison.



For official use only
 Monitor assigned: _____
 Site name: _____
 Country: _____

SuperSID Space Weather Monitor Request Form

Your information here	
Name of site/school (if an institution):	
Choose a site name: <i>(3-6 characters) No Spaces</i>	
Primary contact person:	
Email:	
Phone(s):	
Primary Address:	Name School or Business Street Street City Country
	State/Province Postal Code
Shipping address, if different:	Name School or Business Street Street City Country
	State/Province Postal Code
Shipping phone number:	
Latitude & longitude of site:	Latitude: _____ Longitude: _____

I understand that neither Stanford nor the Society of Amateur Radio Astronomers is responsible for accidents or injuries related to monitor use. I will assure that a surge protector and other lightning protection devices are installed if necessary.

Signature: _____ **Date:** _____

I will need:

What	Cost	How many?
SuperSID distribution USB Power	\$48 (assembled)	
USB Sound card 96 kHz sample rate (or provide this yourself)	\$40 (optional)	
Antenna wire (120 meters) (or you can provide this yourself)	\$23 (optional) with connectors attached and tested	
RG 58 Coax Cable (9 meters) (or provide this yourself)	\$14 (optional) with connectors attached and tested	
Shipping	US \$12 Canada & Mexico \$40 all other \$60	
	TOTAL	\$

_____ I have included a \$_____ check (payable to SARA)

_____ I will make payment thru www.paypal.com to treas@radio-astronomy.org

or

_____ If you are a Minority-serving institution, in a Developing or economically deprived nation, and/or you are using the monitor with students for educational purposes, you may qualify for obtaining a monitor at reduced or no cost. Check here if you wish to apply for this designation. Then tell us how you want to use the SuperSID monitor. Include type of site, number of students involved, whether public or private school, grade levels, etc. and describe your program. The goal of the SuperSID project is to provide as many students with systems as possible. If you are able to pay for a system, even if you qualify for a free one, please do so and help support our goal.

For more details on the Space Weather Monitor project, see: <http://sid.stanford.edu>

To set up a SuperSID monitor you will need:

¹ Access to power and an antenna location that is relatively free of electric interference (could be indoors or out)

² A **PC**** with the following minimal specifications:

- a. A sound card that can record (sample) up to 96 kHz, or a USB port to connect such a sound card (for North and South America)
 - i. All other countries can use AC97 sound card with 48 kHz record (sample) rate. Most computers made after 1997 will have AC97.
- b. Windows 2000 or more recent operating system
- c. 1 GHz Processor with 128 mb RAM
- d. Ethernet connection & internet browser (desirable, but not required)
- e. Standard keyboard, mouse, monitor, etc.

³ An inexpensive antenna that you build yourself. You'll need about 120 meters (400 feet) of **insulated** wire. Solid wire is easier to wind than stranded. Magnet wire will work but be more fragile. You can use anything from #18 to #26 size wire. The antenna frame can be made of wood, PVC pipe, or similar materials. We'll provide instructions. You can purchase the wire from us or obtain your own.

⁴ RG58 coax cable with a BNC connector at one end to run from the antenna to the SuperSID receiver. 9 meters is recommended, but the length will depend on where you place the antenna. You can purchase the coax from us or obtain your own.

⁵ Surge protector and other protection against a lightning strike

Return this form to: SuperSID@radio-astronomy.org

or mail to: SARA
Brian O'Rourke, SARA Treasurer
337 Meadow Ridge Rd,
Troy, VA 22974-3256

Announcing Radio JOVE 2.0

The Radio JOVE Team



Radio JOVE students and amateur scientists from around the world observe and analyze natural radio emissions of Jupiter, the Sun, and our galaxy using their own easy to construct radio telescopes.

Our Project announces Radio JOVE 2.0, where participants assemble a 16-24 MHz radio spectrograph to observe solar, Jupiter, Galactic, and Earth-based natural radio emissions and share their observations with fellow participants.

In the Beginning

Radio JOVE started as a NASA sponsored educational outreach project in 1999. We developed a radio telescope kit suitable for receiving signals from Jupiter, the Sun, the Galaxy, and Earth-based radio emissions. The original kit comprised a radio receiver (RJ1.1) and a dual dipole antenna for 20.1 MHz. An important goal was to teach electronic principles including how to build, solder, and assemble the radio receiver and antenna.

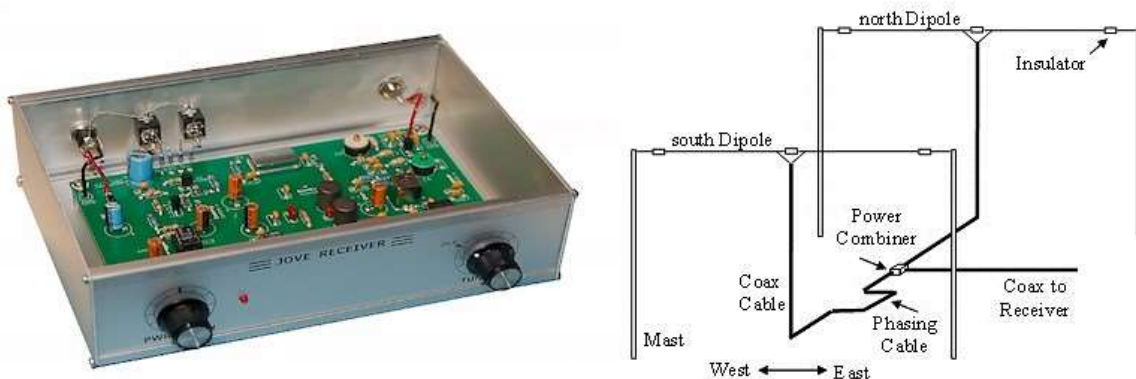


Figure 1. A Radio JOVE RJ1.1 receiver and a schematic of the dual-dipole antenna.

In addition to the hardware, three software packages were developed. These were Radio Jupiter Pro (Jupiter emission prediction program), Radio-SkyPipe (strip chart program) and Radio Sky Spectrograph (control and display of radio spectrograph data).

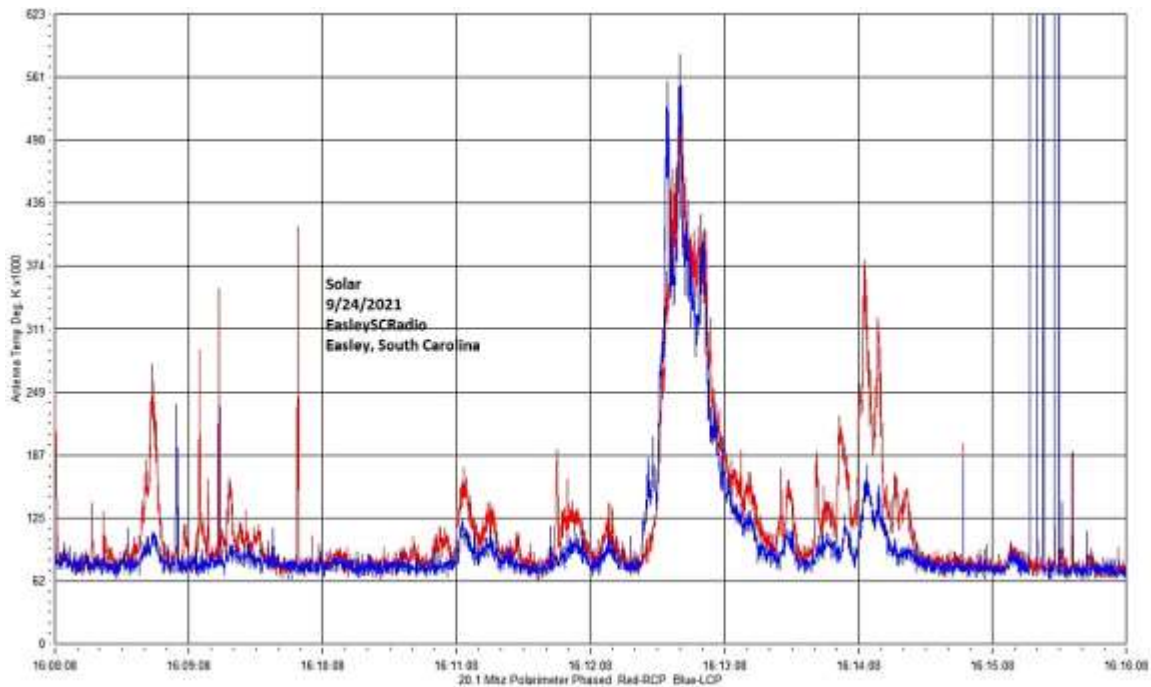


Figure 2. A SkyPipe strip chart showing multiple solar bursts using a JOVE receiver. John Cox, SC.

The Growth of Radio JOVE

As of Autumn 2021, over 2,500 kits have been sold at cost to schools and individuals around the world. Thousands of data submissions from observers have been made to the Radio JOVE data archive.

The Radio JOVE web site has always provided a wealth of information describing observation methods and various educational materials intended to teach radio astronomy techniques and scientific methods. Biannual newsletters are produced and several telephone help sessions are held each year.

A sub-group of experienced observers known as the Spectrograph Users Group (SUG) evolved from the core JOVE group. These observers developed data collection and analysis techniques using more advanced equipment and techniques. SUG members have contributed to articles published in peer-reviewed scientific journals. This group remains active under the Radio JOVE listserv at <https://groups.io/g/radio-jove/>.

Moving Forward with New Technology

In the past, Radio JOVE provided the hands-on experience of building a radio kit. We have many RJ1.1 receivers in operation successfully contributing scientifically valuable data. It has, however, become increasingly difficult to obtain parts for the RJ1.1 receiver kits and we therefore decided to replace the RJ1.1 receiver with a new SDR-based design for the receiver portion of our radio telescope kits. While we continue to support the hardware and software for the original RJ1.1 receivers, the only kits now available for purchase from Radio JOVE contain this newly designed system.

In recent years, new technologies have made software defined radios (SDRs) ever more affordable. These radios can operate on a single frequency like the original JOVE receiver but can also generate spectrograms which depict radio activity as a function of both time and frequency. Such displays offer new insights into our studies of the Sun, Jupiter, the Galaxy, and both natural and artificial Earth-based radio emissions.

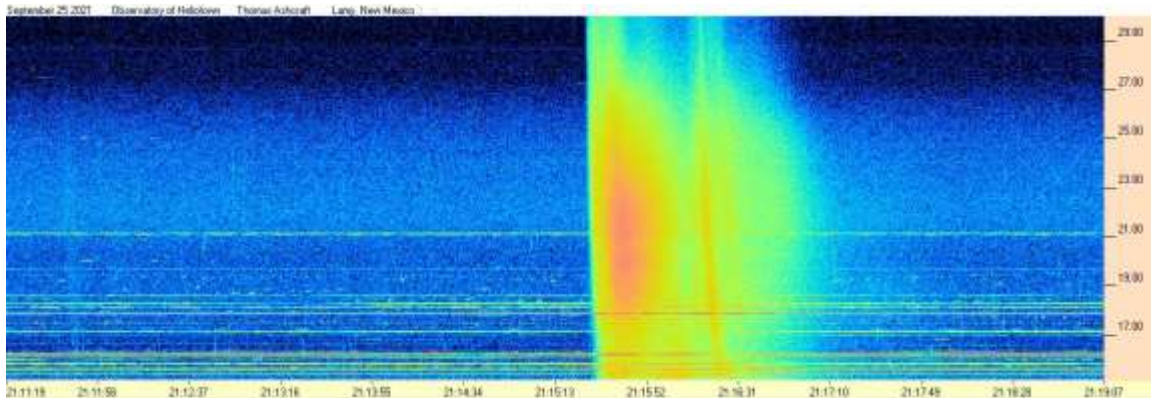


Figure 3. Radio spectrogram showing multiple solar bursts received by Tom Ashcraft in New Mexico. Horizontal scale is time, and the vertical scale is frequency. Amplitude is displayed using different colors corresponding to the strength of signals.

Radio JOVE continues to sell radio telescope packages including an antenna, receiver, and software; however, the receiver is now a commercially built SDR.



Figure 4. The JOVE team has had considerable success with the SDRPlay RSP1A unit and will provide support for using this instrument for our radio astronomy program. Not all SDR types can be supported, but it is our intent to provide support for some other SDRs as they become available during this period of rapid SDR development.

It continues to be our goal to introduce new observers to the scientific method and help them experience the thrill of receiving cosmic radio signals. Through a series of educational training modules and observing and analysis projects we aim to guide new observers to levels where they can contribute to Citizen Science projects.

We continue to support our large user base that uses JOVE RJ1.1 receivers – both in terms of technical support for the receivers but also with new and exciting observing projects for both RJ1.1 and SDR users.

We welcome both new and experienced observers to the JOVE 2.0 program as we share the excitement of receiving, studying, and understanding radio signals from our corner of the galaxy.

Please see the Radio JOVE web site at <https://radiojove.gsfc.nasa.gov> for more information.



RADIO JOVE 2.0 RADIO TELESCOPE KIT ORDER FORM

Order Online using PayPal™

* * * Please allow 2 to 3 weeks for delivery. * * *

IMPORTANT: Before you order the Jove receiver kit and/or the antenna kit, we suggest that you read the on-line manuals. You will need to provide additional materials and tools to complete the antenna. The cost of additional materials for the antenna support structure (masts, etc.) may be in the range of US\$75 to US\$100. Also note that the optimal antenna height can be up to 20ft, depending upon your latitude.

<p>Item # RJK2u – Complete 2.0 Kit: Receiver + Unbuilt Antenna Kit + Software</p> <p>This kit includes an SDRplay RSP1A, USB Cable, SMA/BNC cable, F-adapter, unbuilt Antenna Kit (RJA), printed assembly manuals, and Radio-Sky Spectrograph (RSS) software.</p> <p>Note: Kit does not include antenna support structure.</p> <p>Price: \$215 + Shipping (See reverse for shipping)</p>	<p>Item # RJK2p – Complete 2.0 Kit: Receiver + Professionally Built Antenna Kit + Software</p> <p>This kit includes an SDRplay RSP1A, USB Cable, SMA/BNC cable, F-adapter, Professionally Built Antenna Kit (RJA2), printed assembly manuals, and Radio-Sky Spectrograph (RSS) software.</p> <p>Note: Kit does not include antenna support structure.</p> <p>Price: \$384 + Shipping (See reverse for shipping)</p>
<p>Item # RJA – Unbuilt Antenna Kit</p> <p>The RJA Radio JOVE Antenna Kit includes a printed construction manual, stranded copper easy-to-solder antenna wire, ceramic insulators, RG-59 easy-to-solder coax cable, screw-on Fconnectors, and a power combiner.</p> <p>Note: Kit does not include antenna support structure. Assembly requires a soldering gun and other tools.</p> <p>Price: \$90 + Shipping (See reverse for shipping)</p>	<p>Item # RJA2 – Professionally Built Antenna Kit</p> <p>The RJA2 Radio JOVE Antenna Kit includes a printed installation manual, two professionally assembled dipole antennas constructed of #14 Copperweld wire with Budwig center insulators and center support rope attachment points, high quality RG-6 coax with pre-installed commercial grade connectors, and a power combiner.</p> <p>Note: Kit does not include antenna support structure.</p> <p>Price: \$249 + Shipping (See reverse for shipping)</p>
<p>Item # LTJ2 – Listening to Jupiter, 2nd Ed. by R. S. Flagg</p> <p>PDF download of Richard Flagg's book "Listening to Jupiter, 2nd Ed., 2005". The file is downloaded from a secure website.</p> <p>Price: \$10 + \$0 shipping (PDF file download)</p>	<p>Item # RJR2 – Radio JOVE 2.0 Receiver-Only Kit</p> <p>This kit includes one SDRplay RSP1A SDR receiver, USB Cable, SMA/BNC cable, and F-adapter, printed assembly manuals, and Radio-Sky Spectrograph (RSS) software.</p> <p>Price: \$135 + Shipping (See reverse for shipping)</p>

RADIO JOVE 2.0 RADIO TELESCOPE KIT ORDER FORM (continued)

Order Online at https://radiojove.net/kit/order_form.html OR
Complete this form and mail with payment

Payment may be made by Credit Card via PayPal™, U.S. Check, U.S. Money Order, International Money Order in U.S. funds drawn on a U.S. bank, or Western Union Money Transfer made payable to **The Radio JOVE Project**. No bank-to-bank wire transfers are accepted. Purchase Orders are accepted from U.S. Institutions.

Send to: The Radio JOVE Project
 1301 East Main St
 MTSU Box 412
 Murfreesboro, TN 37132, USA
 email: chiggins@mtsu.edu
 FEIN: 20-5239863

Item	Description	Quantity	Item Price	Shipping (see below)	Subtotal
RJK2u	Complete Radio JOVE 2.0 Kit Receiver + unbuilt Antenna		\$215		
RJK2p	Complete Radio JOVE 2.0 Kit Receiver + Professionally Built Antenna		\$384		
RJA2	Professionally Built Antenna-Only Kit		\$249		
RJA	Unbuilt Antenna-Only Kit		\$90		
RJR2	Receiver-Only Kit		\$135		
LTJ2	Listening to Jupiter, 2 nd Ed., by R.S. Flagg (PDF download)		\$10	\$0	
Total:					

Shipping Fees for Radio JOVE: We ship all packages using USPS Priority Mail flat rate boxes.

U.S.A.: \$17.00
 Canada: \$57.00
 All Other International Shipping: \$85.00

Ship to: (Please print clearly)

Name: _____
 Address: _____
 City, State, Postal Code: _____
 Province, Country: _____
 Email: _____

Visit the Radio JOVE web site and fill out the team application form at https://radiojove.net/sign_up_form.php even if you are just an interested individual so that you can receive important information about kit updates, online services, and activities within the project as they occur!



The British Astronomical Association
A company limited by guarantee Registered Charity No. 210769

Burlington House, Piccadilly, London, W1J 0DU

Telephone: 020 7734 4145

Fax No.: 020 7439 4629

Email: office@britastro.org

Website: www.britastro.org



Please send questions, reports and observations to John Cook: jacook@jacook.plus.com

John Cook's VLF Report

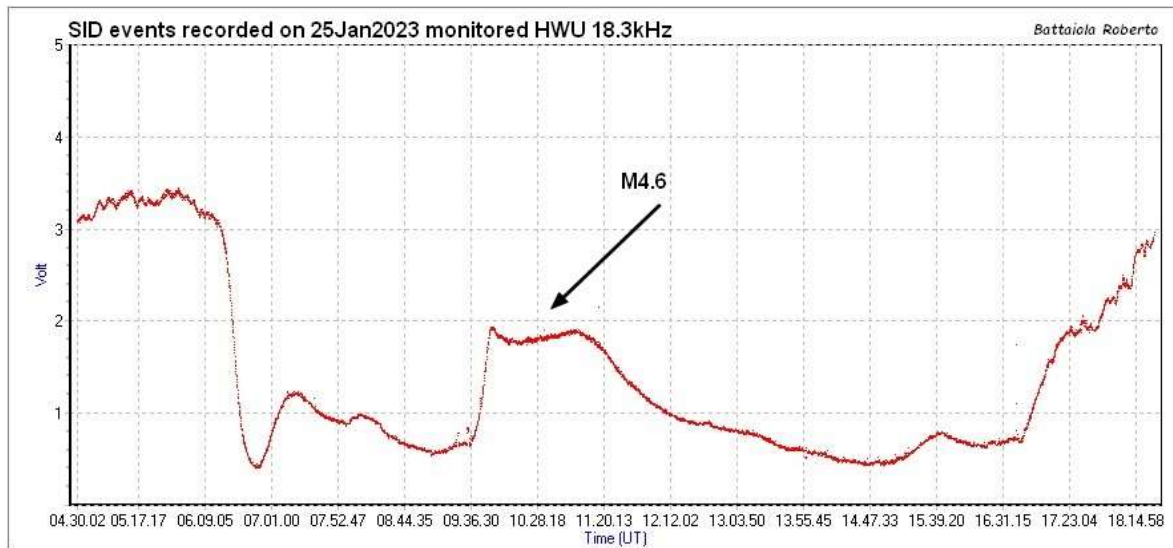
BAA Radio Astronomy Section, Director: Paul Hearn

RADIO SKY NEWS

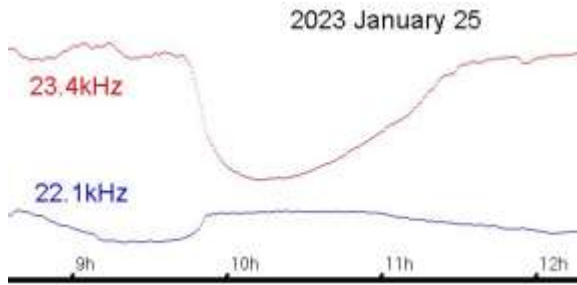
2023 January

VLF SID OBSERVATIONS

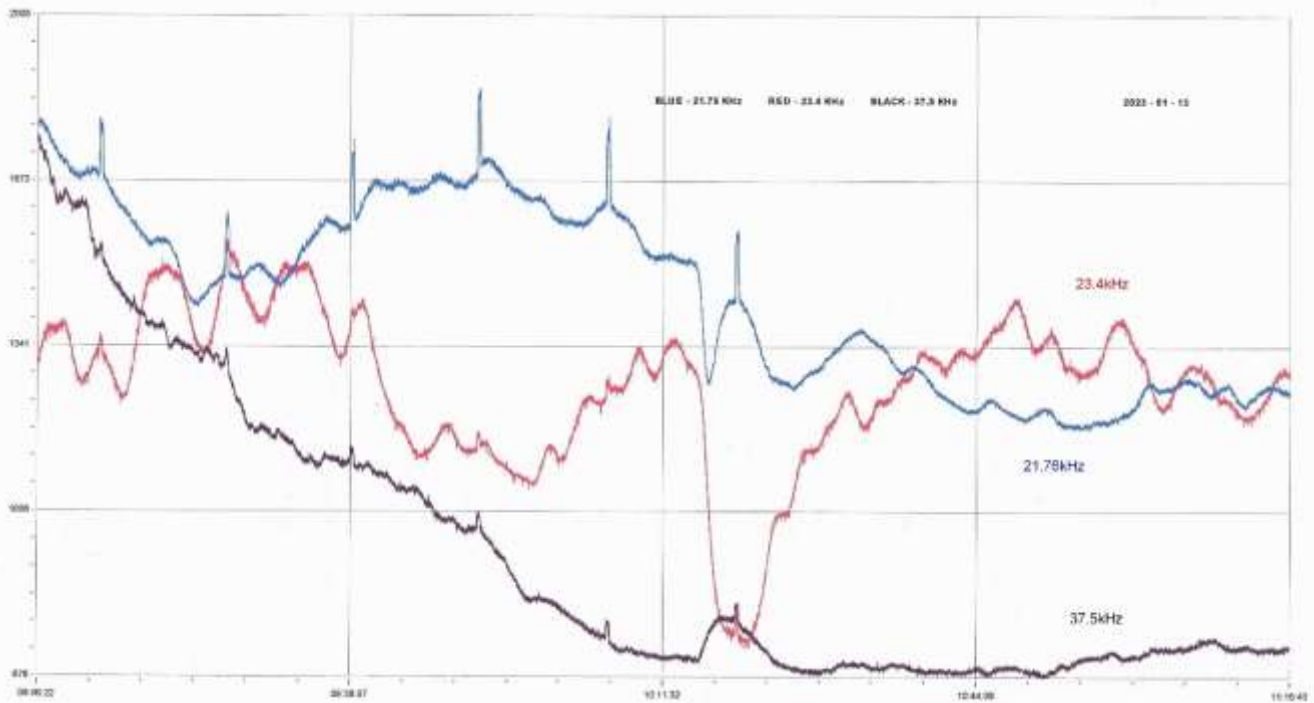
Solar activity in January was very similar to that in December, with another 'fireworks' display of M-class flares. Roberto Battaiola recorded one of the stronger flares on the 25th:



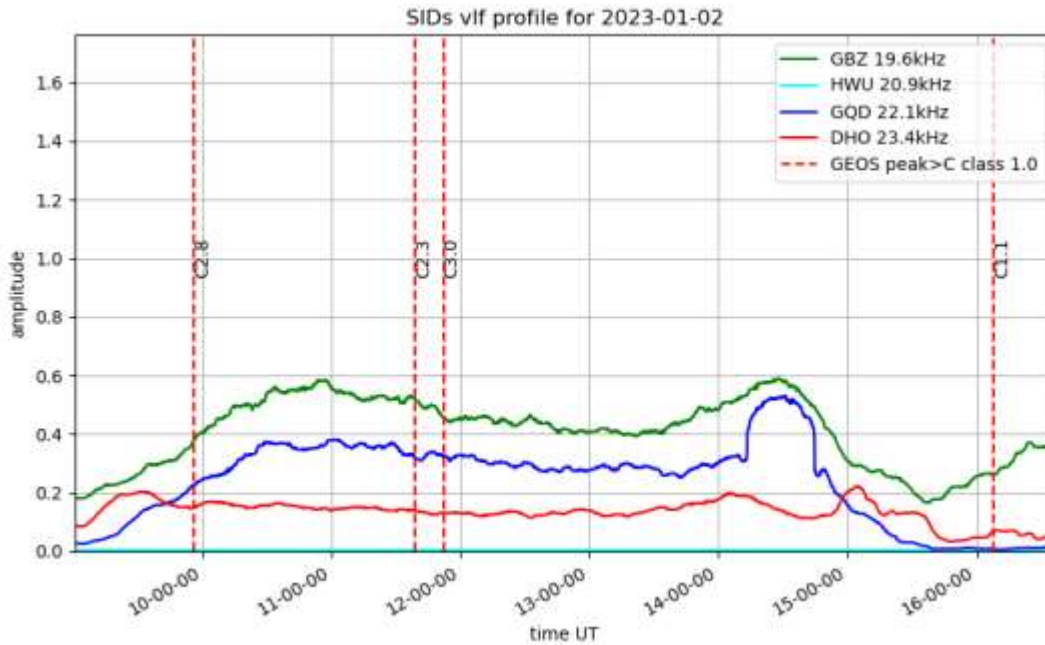
This was a very slow flare, and shows a spike and wave SID lasting well over an hour. This has caused a wide spread in our timings of the peak, from 09:47 to 10:15UT.



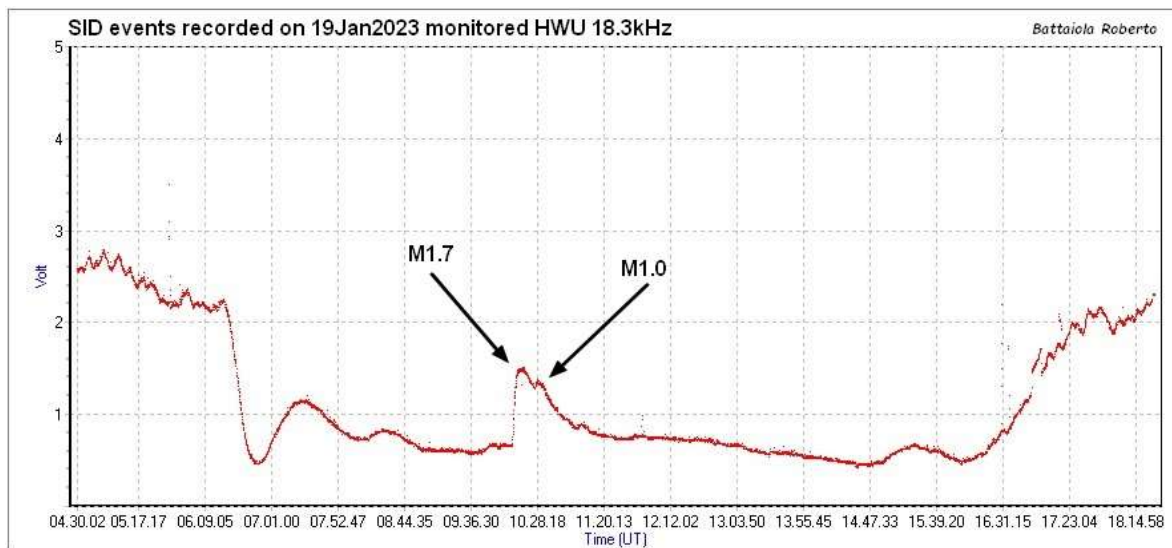
My own recording also shows how the peak of the SID appears to vary with the signal path, appearing earlier at 22.1kHz. The background X-ray flux was also quite high at times, so that even the M-class flares often represented only a relatively small increase. Many C-class flares remained well hidden during these periods and did not show as SIDs.



The M3.9 flare on the 13th shows well on this recording by Colin Clements. The 23.4kHz SID is very strong, while 21.75kHz is less clear with a rather noisier signal. There are also some interference spikes on all three signals, a common problem.



This recording by Mark Prescott does not show any SIDs but does have a very unusual response to the sunset. The large 'bump' on the 22.1kHz signal is unlike any other sunset effect that we have recorded. The other two signals have a much smaller response, more as expected. It does not appear to be a transmitter effect, as it does not appear on my own recording. There is a small dip in the signal at the start and end of the bump, and these do show on my recording and so can be assumed as transmitter effects.

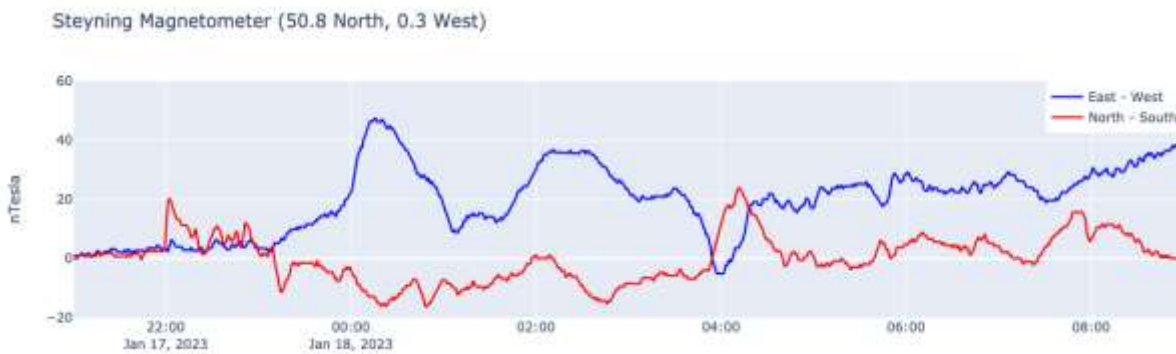


This recording by Roberto Battaiola from the 19th shows the two M-class flares overlapping. The peaks are only 15 minutes apart, although they did appear as individual SIDs on some frequencies.

MAGNETIC OBSERVATIONS

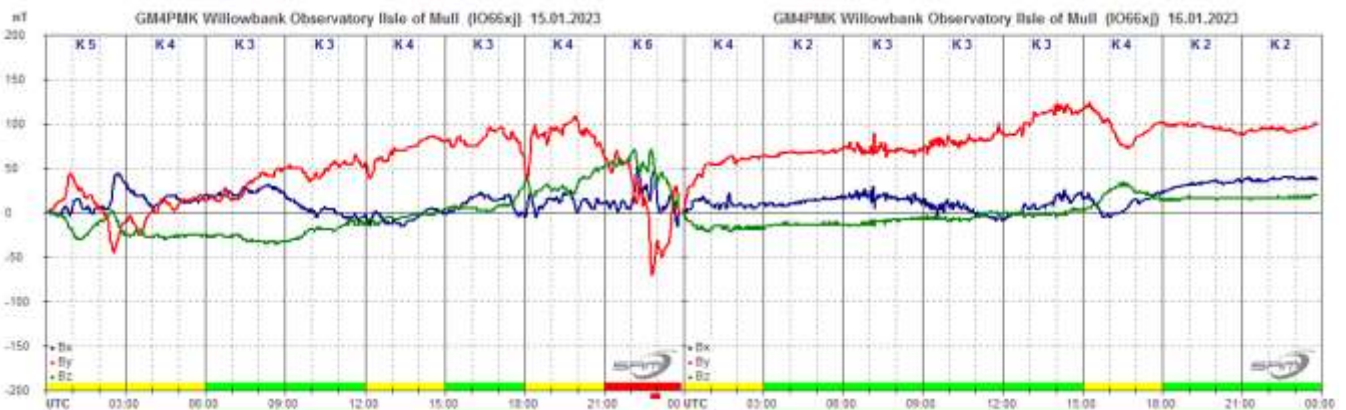
Unfortunately, Stuart Green lost most of his January data due to water getting into the sensor. Despite being in a waterproof enclosure, this has failed over time. Over the years I have heard similar stories from other observers with outdoor sensors. At one of the BAA autumn meetings, we had an opportunity to visit the BGS Eskdalemuir magnetic observatory. Their sensors are hidden deep inside a cave in one of the hills, an option not really available in our domestic garden sites.

Several of the stronger flares did produce CMEs, but the majority were again not Earth-directed. Most of the activity seems to have been from turbulent solar winds. We did record one distinct CME impact, although its source is not clear. The chart by Nick Quinn from the 17th and 18th shows a very sharp rise of about 20nT in the N-S component at 22:00UT on the 17th:

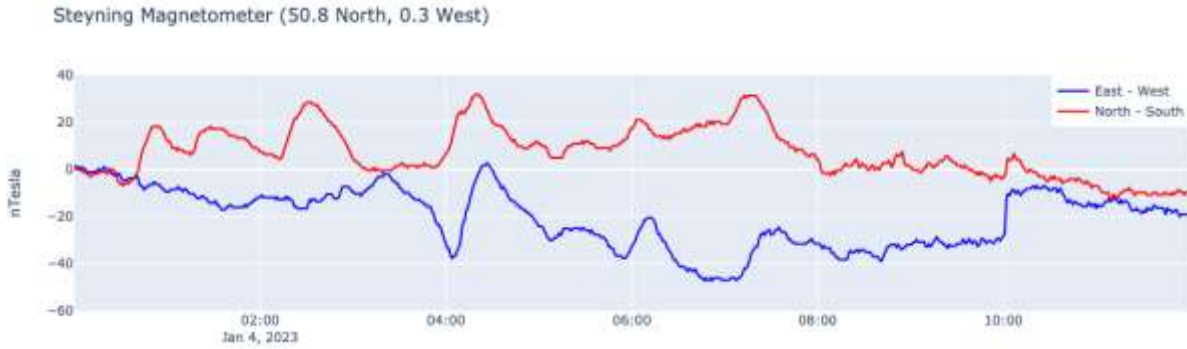


A similar transient is visible in Roger Blackwell's recording as well as my own, eliminating any local interference source. Mild disturbance of about +/- 50nT continued through to mid-afternoon on the 18th. Satellite data shows potential glancing blows from a number of CMEs, including a large filament eruption in the preceding days.

The Bartels diagram shows an extended period of mild disturbance from the 10th to the 18th, including a short active period on the 15th. It also highlights the number of flares contributing to the activity.



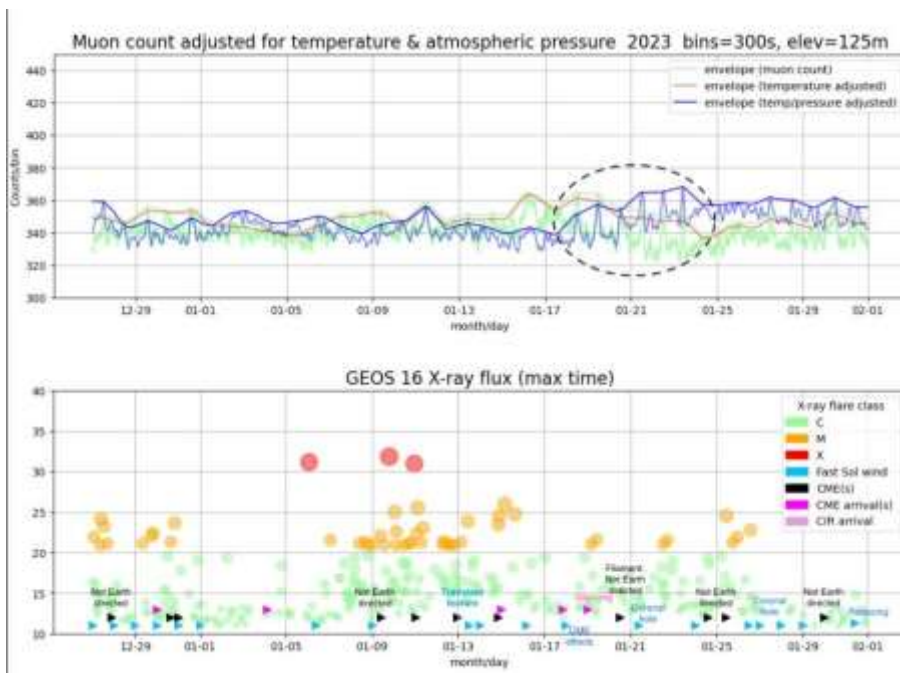
Roger Blackwell's chart shows this peak in activity. There is also a very rapid spike just after 07UT on the 16th, also visible in my own recording. It is not clear whether this is CME related, or just very rapid turbulence.



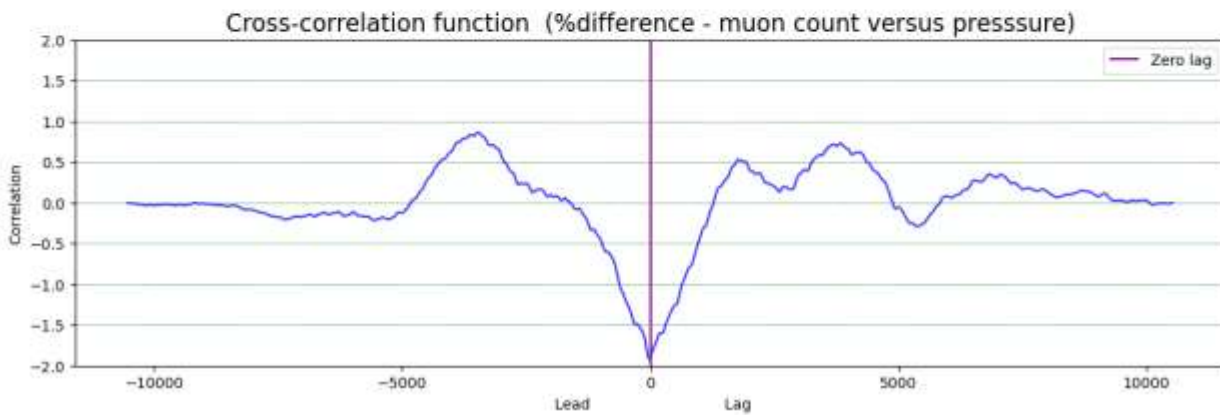
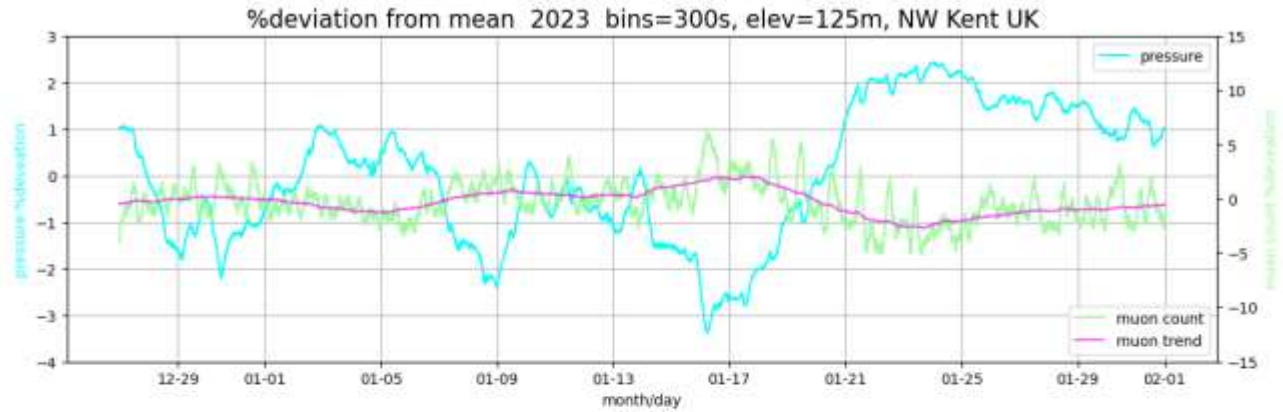
Nick Quinn's chart from the 4th shows magnetic disturbance from a fast solar wind and glancing CME. Activity faded out in the afternoon, but continued again overnight on the 5th and into the 6th.

Magnetic reports received from Roger Blackwell, Colin Clements, Stuart Green, Nick Quinn and John Cook.

MUONS



Mark Prescott's chart of Muon counts shows a distinct increase over the 18th to 23rd January when the raw data is compensated for temperature and pressure variations. This was also during the long period of magnetic disturbance.



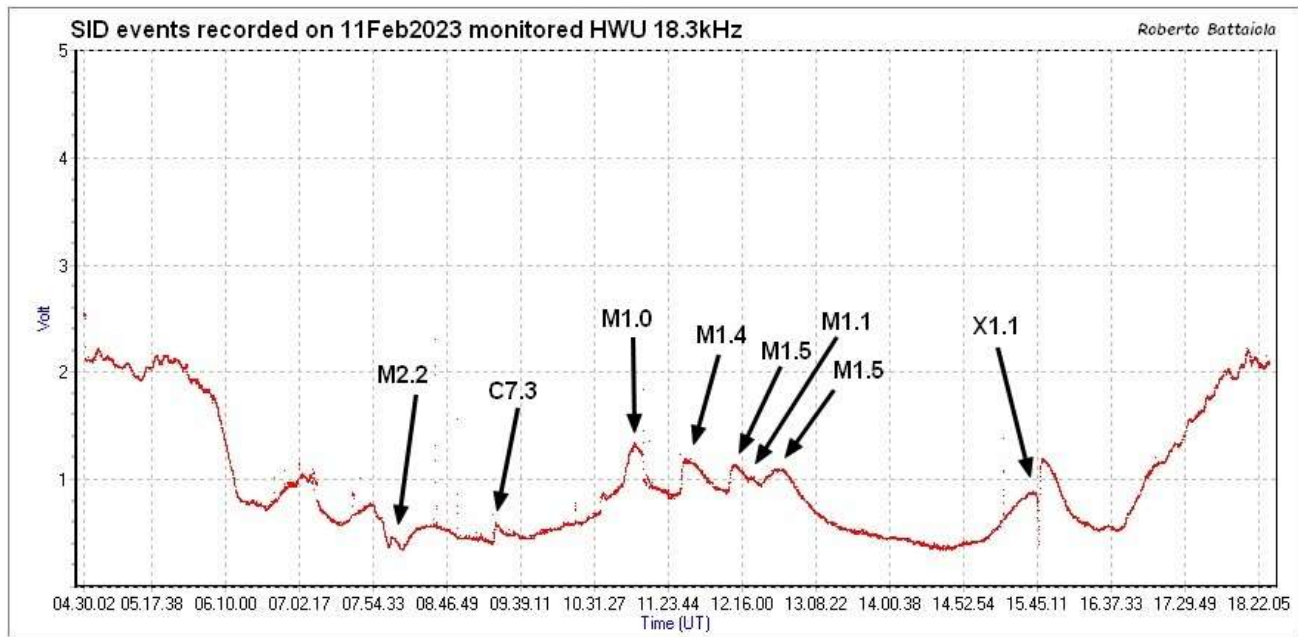
The upper panel shows the pressure variations along with the raw muon counts and averaged trend. The 17th to 21st shows a large increase in pressure, and there were also some much colder nights. The more rapid (daily) temperature changes would not be removed using the longer term correlation applied to the data, perhaps accounting for the increased muon counts shown in the first chart. With large daily temperature variations, the muon counts would be expected to vary as explained last month. The lower panel is a cross correlation of muon count versus pressure. I am afraid that my statistical knowledge does not allow me to add further descriptions. Mark is still working on analysing his full set of data recordings.

VLF SID OBSERVATIONS

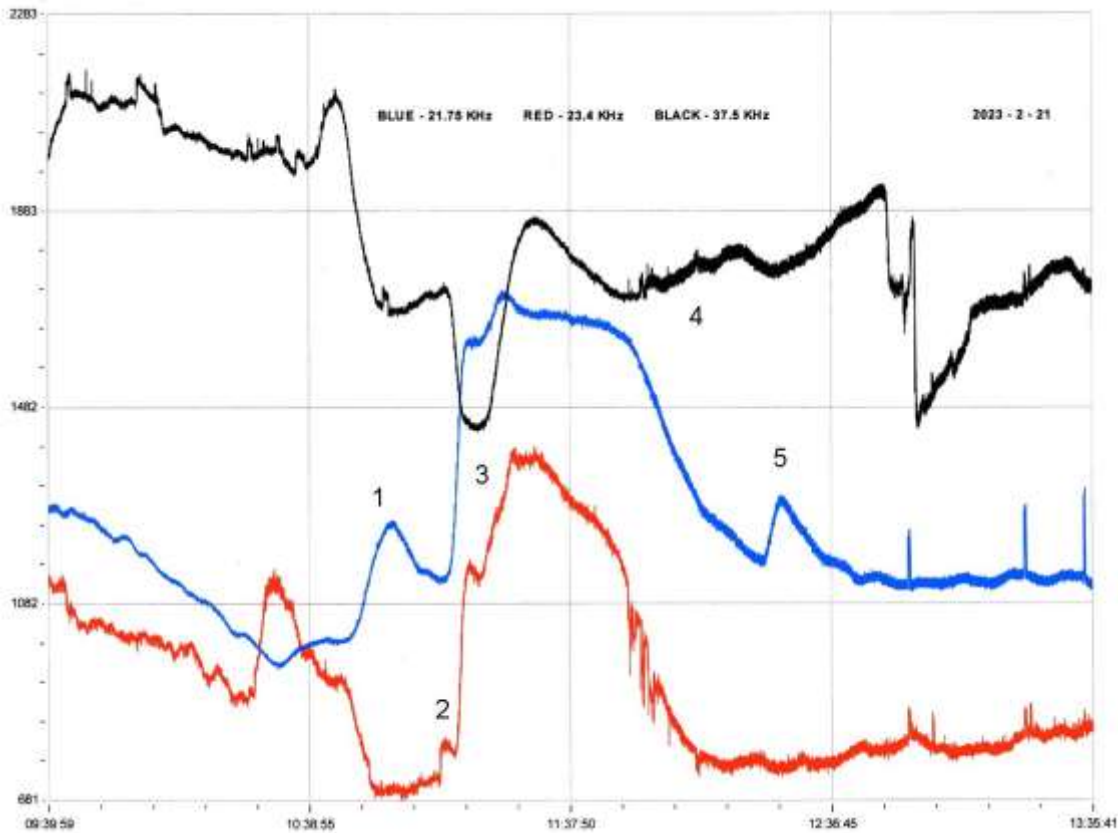
Solar flare activity increased significantly in February, with many M-class flares and two of X-class that were suitably timed for us to record. The general X-ray flux background was very high, and so many of the smaller flares were lost. Many of the larger flares were also quite complex, with multiple peaks. These have shown up on some signal paths, but not all. There were also two simultaneous flares from the same active region, hence showing as just a single SID, but listed in the SWPC independently at C6.2 and C6.1. This was the SID peaking at 17:52UT on the 9th, only recorded on the 24kHz Atlantic path, shown in the timing tables as just 'C'. The X2.2 flare on the 17th was also rather late, just showing on 24kHz, but the X1.1 on the 11th was more widely recorded.



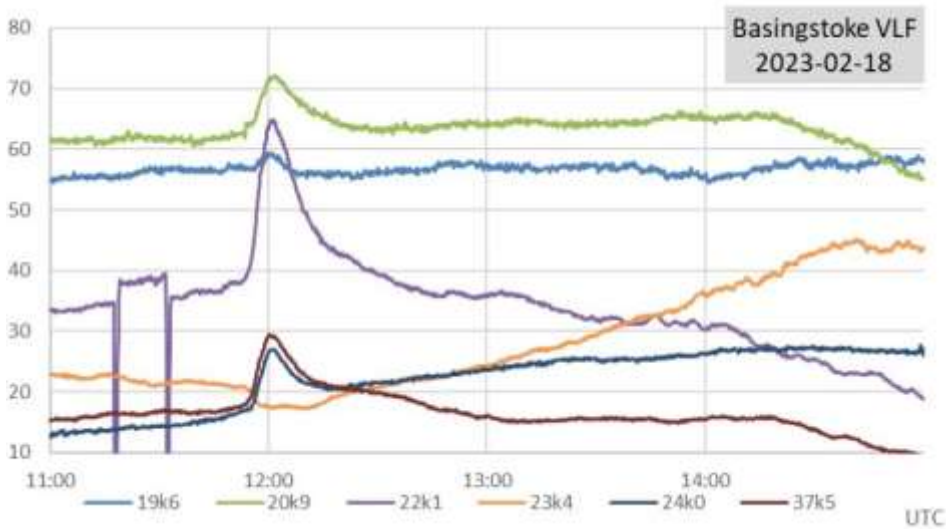
This chart by Mark Edwards shows the X1.1 flare in detail over six signals, just merging into the afternoon sunset on the European signals.



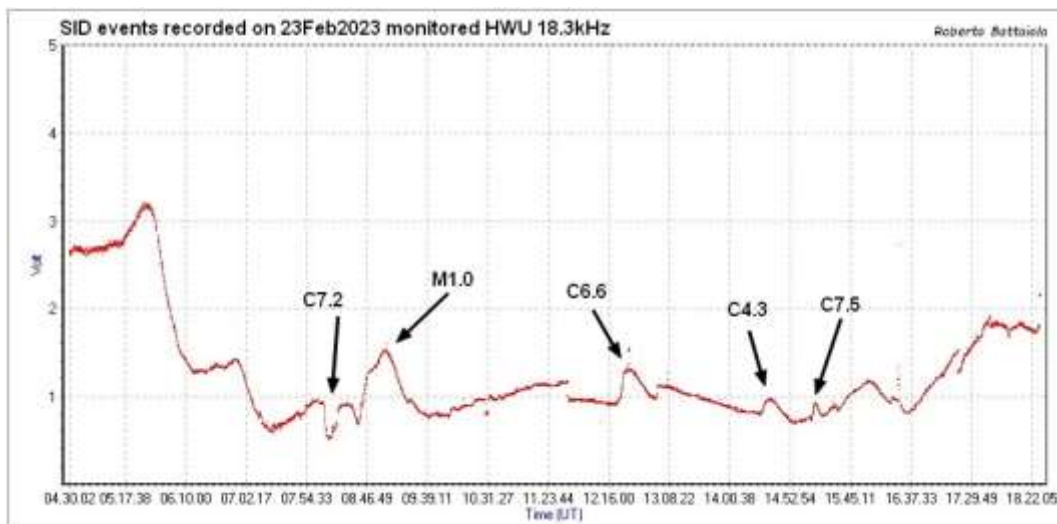
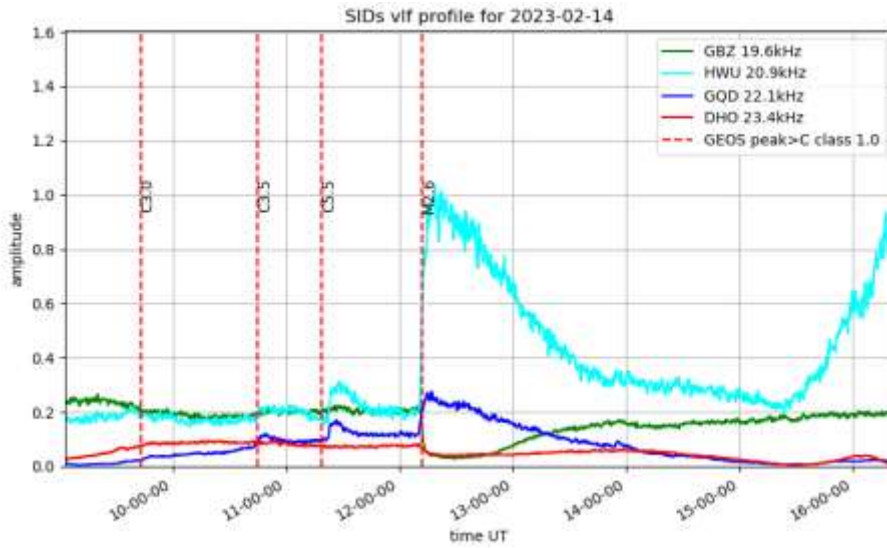
The recording from Roberto Battaiola shows it in context to the rest of the day's activity, including a barrage of M-flares from 11:00 to 13:00UT.



The timing tables show a complex set of flares on the 21st, shown in this recording by Colin Clements. I have labelled the timing entries 1..5, as listed in the tables. Not all of flares show as clear SIDs, with three active regions responsible. Entries 2 and 3 both appear to be from M-class flares, although only 2 is given a magnitude (M4.7). I suspect that both 2 and 3 were fairly slow flares, so merging into a single larger SID. A complex system to analyse.

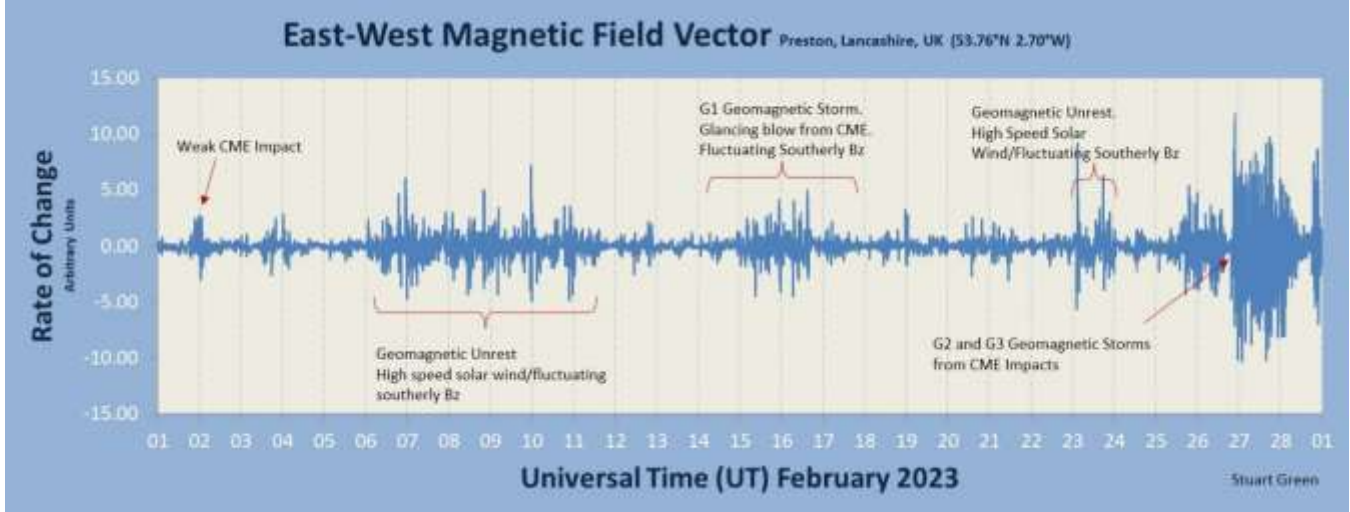


This recording by Paul Hyde shows a much better defined SID from the C7.7 flare at 12:02UT on the 18th. The SWPC bulletin does list a lot more flares on the 18th, but without magnitudes.



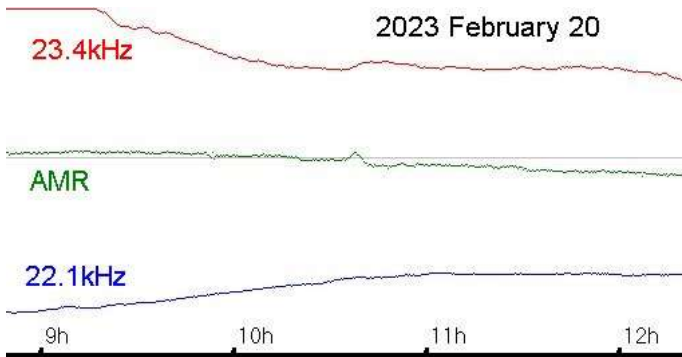
The recording from Mark Prescott shows the M2.6 flare on the 14th with a strong response at 20.9kHz. The recording from Roberto Battaiola shows another busy day on the 23rd, including the M1.0 flare with two peaks at 08:44 and 09:02UT.

MAGNETIC OBSERVATIONS



Stuart Green has repaired his leaking sensor and has it back in operation again. The month's summary shows a fairly quiet start, with a much more active period in the last week.

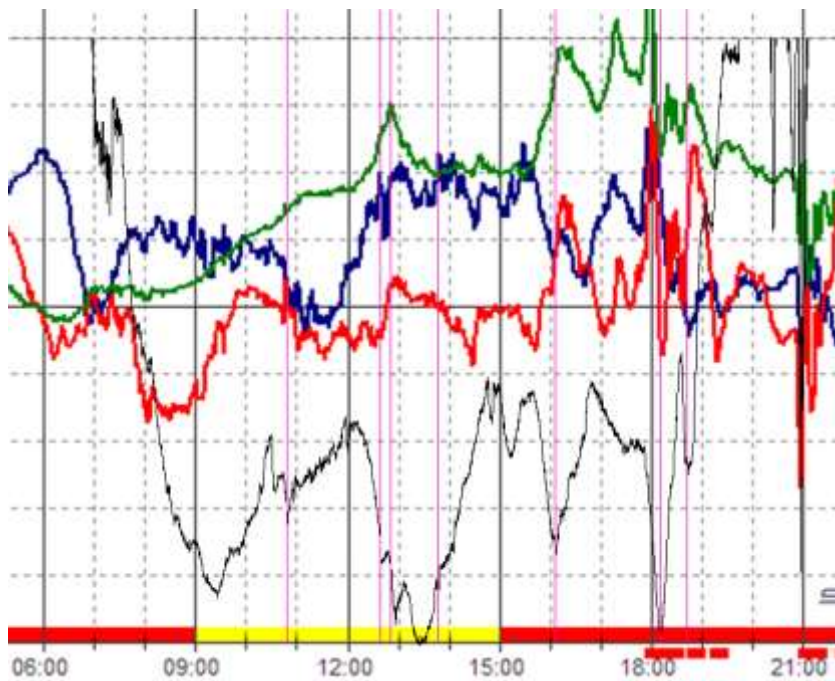
The X2.2 flare at 20:16UT on the 17th was too late in the evening to be recorded as a SID, but it did produce a CME arriving on the 20th. My own recording shows the sudden impact at 10:38UT on the 20th, with a magnitude of about 14nT. Subsequent magnetic disturbances were very mild lasting into the morning of the 21st.



A combination of a high speed solar wind and a number of CMEs produced very active conditions at the end of the month. The recording by Nick Quinn shows the start at about 19:30UT on the 26th with a very sharp shock. The disturbance grew in strength through the following days.

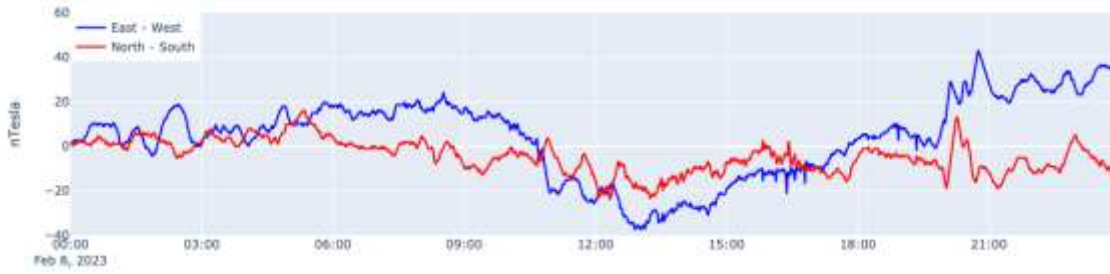


The chart by Roger Blackwell for the 27th and 28th shows the very active period in the evening of the 28th. Note the change in scale on the vertical axis between the days, +/-250nT on the 27th and +/-200nT on the 28th. The sensor reset at midnight has also led to the three axes being a little offset on the 28th. As might be expected, this level of activity caused a notable disturbance on the 37.5kHz signal from Iceland.



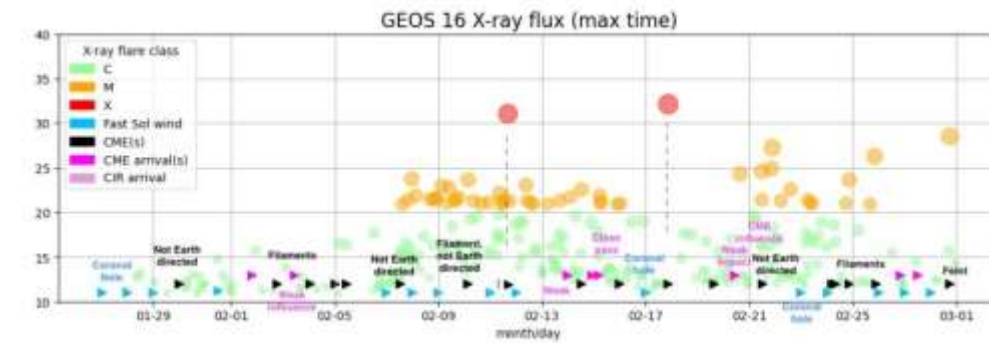
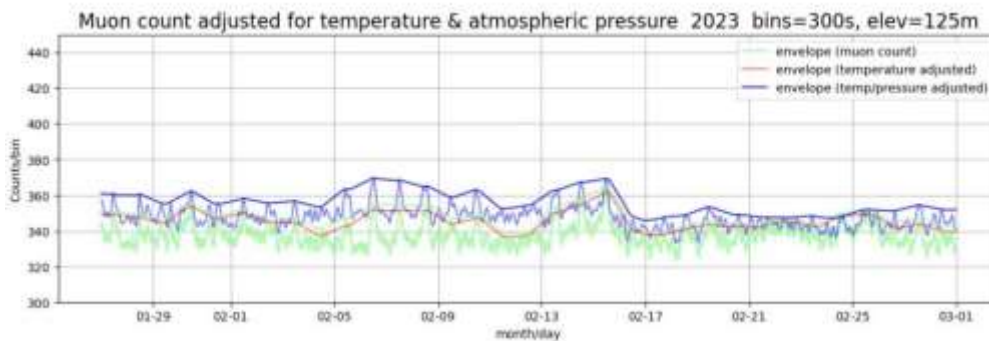
Mark Edwards has overlaid his 37.5kHz trace (black) onto Roger Blackwell's magnetometer. The vertical pink lines highlight some of the matching dips and peaks. The C4.5 flare at 10:27UT is also visible.

Steyning Magnetometer (50.8 North, 0.3 West)

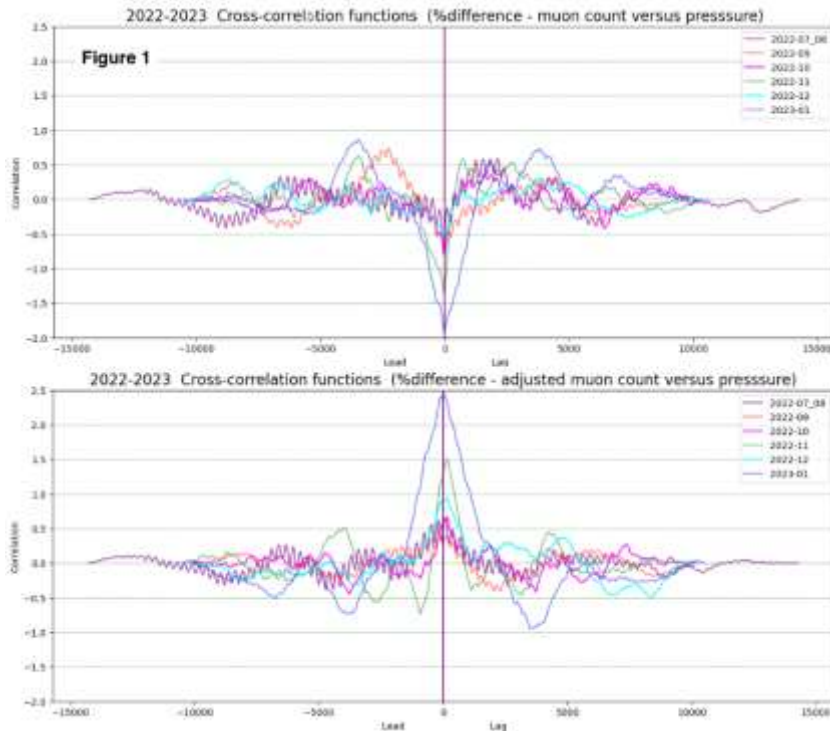


CMEs from flares earlier in the month were mostly not Earth-directed, a stronger solar wind causing short periods of mild magnetic disturbance. The recording of the 8th by Nick Quinn shows just a sample of this activity. Magnetic observations received from Roger Blackwell, Stuart Green, Andrew Thomas, Nick Quinn and John Cook.

MUONS



Mark Prescott has provide his Muon counts for February. The two X-class flares are marked in the lower panel. As already noted, the second one produced an Earth-directed CME, which may be reflected in the Muon counts, corrected for pressure and temperature, in the upper panel.



These charts show the cross-correlation of Muon count versus atmospheric pressure. The upper panel uses the raw Muon counts, giving a negative match. This shows that the Muon trend is mirrored in the long-term pressure trend. The lower panel uses the corrected Muon data shown in the first chart. This has a good positive cross-correlation, showing that there is a good match following the corrections applied.

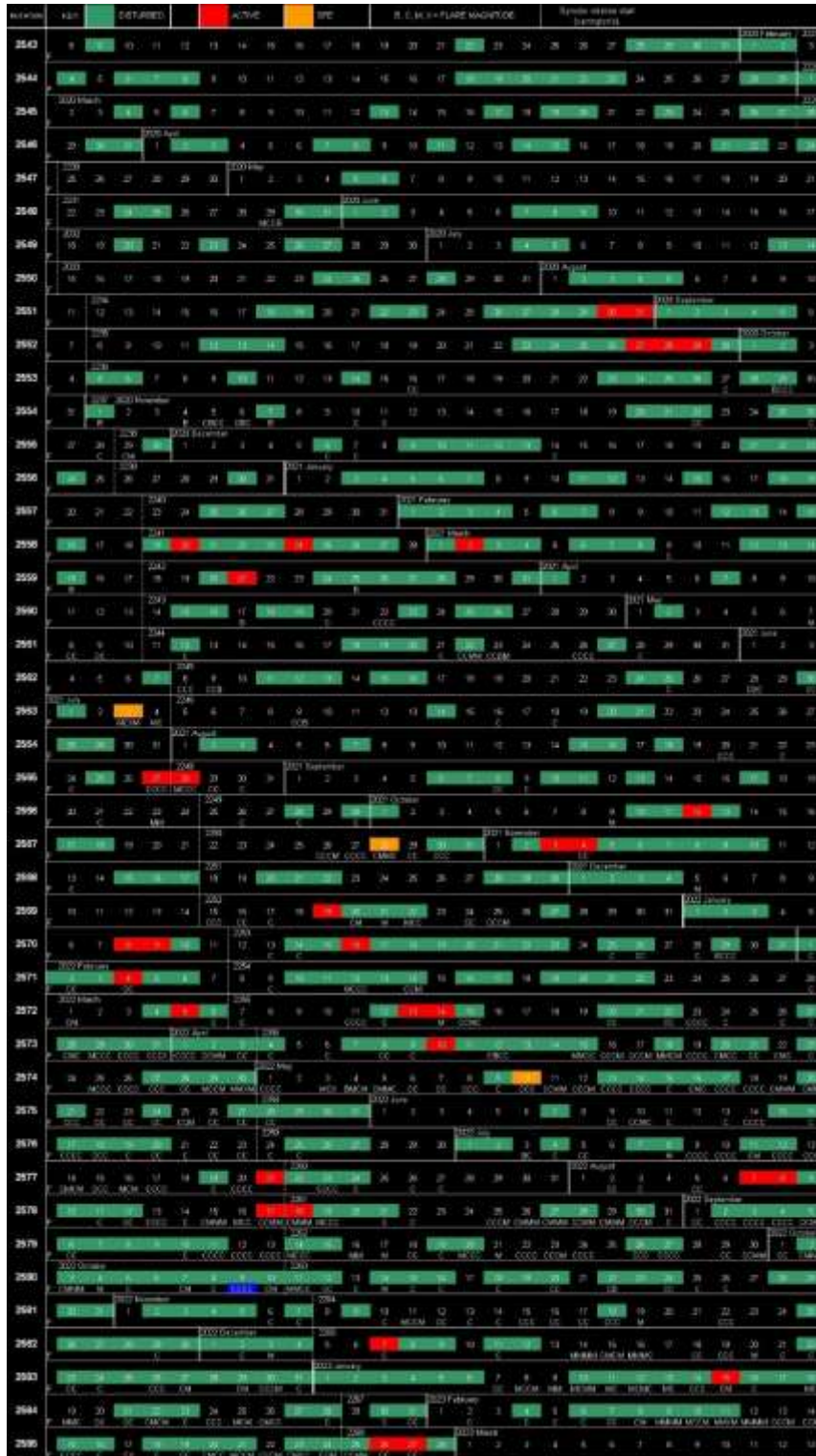
For those interested in particle interactions with the atmosphere, there is an interesting tutorial titled "Capturing cosmic rays with a digital camera." on the BAA web site (www.britastro.org). The link can be found towards the bottom of the page.

ANY IDEAS?

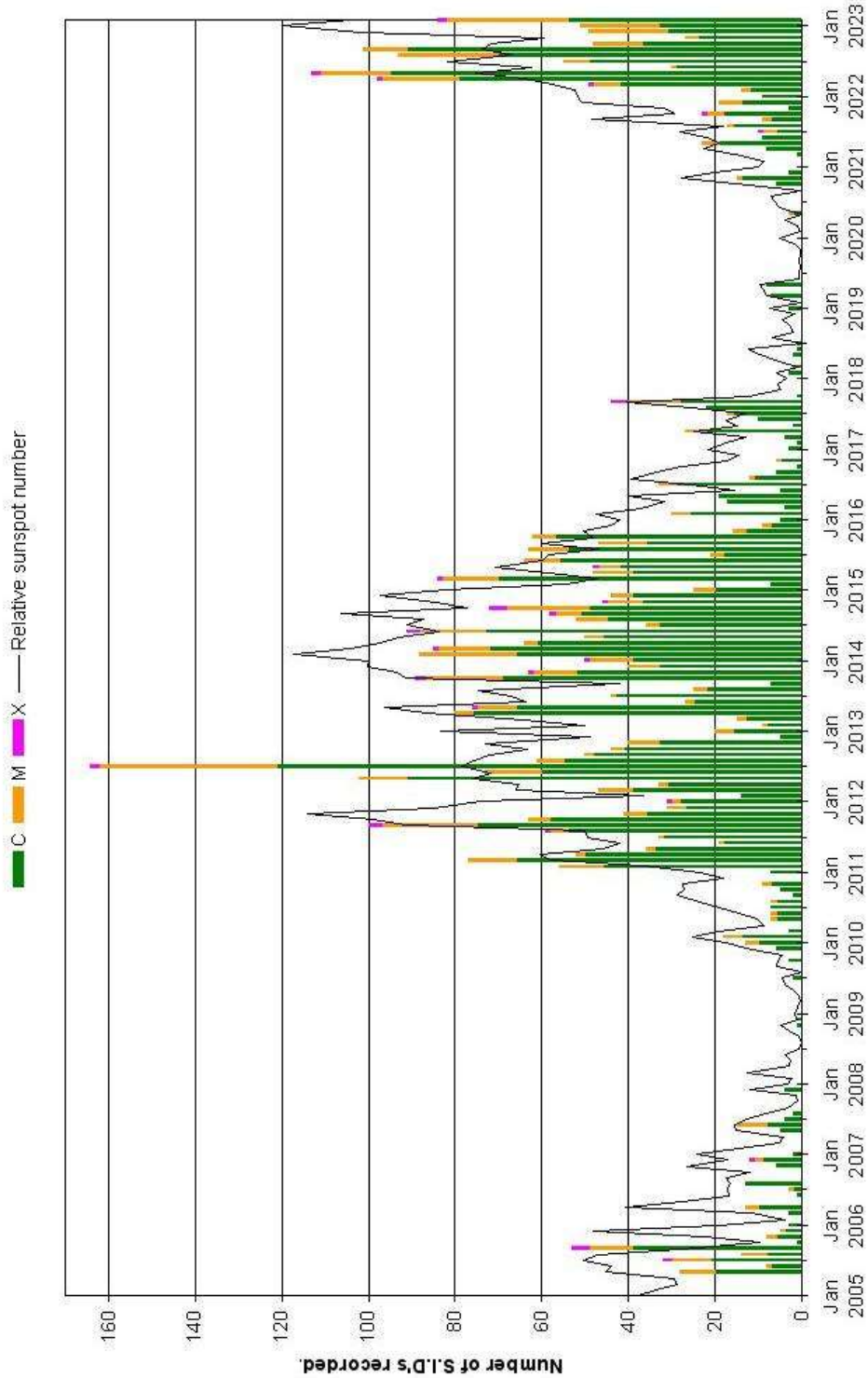


One of our members recently made a visit to Esperance in southwestern Australia, where there is a museum including wreckage from the 1979 skylab that crashed into the sea nearby. The item in the picture is clearly not from that source, but its history is completely unknown to the museum staff. The heading at the top of the cabinet reads: "SOLAR RADIATION MEASUREMENT EQUIPMENT". Have any of our readers come across this before?

BARTELS CHART



VLF flare activity 2005/23





BAA RA Section Summer programme 2023

<p>May 5th 19:30 BST 18:30 UTC</p>	<p>Dr Luke Daly MSc Geology, ARSM, FRAS</p> <p>Lecturer Planetary Geoscience co-lead of the UK Fireball Network School of Geographical and Earth Sciences University of Glasgow</p>	<p><i>The UK Fireball Alliance</i> aims to recover freshly fallen meteorites in the UK. Led by staff of the Natural History Museum, UKFAIL is a collaboration between the UK's meteor camera networks.</p>
<p>June 8th 19:30 BST 18:30 UTC</p>	<p>Prof. Karen Aplin BSc. Hons, PhD, FInstP</p> <p>Space Science and Technology, Department of Aerospace Engineering Bristol Univ. an interdisciplinary physicist with expertise in innovative instrumentation as applied to problems in space and atmospheric science.</p>	<p>Space Weather, Cosmic Radiation, instrumentation and science'.</p>

The summer programme can be downloaded [here](#).

Useful links.....

[Join the RA conversation](#)

[Join the muon conversation](#)

[Join the UK Beacon conversation](#)

[Society of American Radio Astronomers](#)

[UK Radio Astronomy Association \(UKRAA\)](#)

[BAA RA YouTube channel](#)

If you have any suggestions for the winter 2023 term do let me know.

Our meetings are open to all. Once you are registered on the RA Section email list the Zoom link will be sent out to you before the meeting. If you are not on the email list, please request registration from Paul Hearn (paul@hearn.org.uk).

VINTAGE SARA

CHARLES OSBORNE, SARA HISTORIAN

SERENDIP's Common Thread

While looking at a video (contributed by Gene Greneker K4MOG) of the 1985 Green Bank SARA Conference I realized a thread which has surfaced again and again across SARA's history, is that of a project called SERENDIP. It's the brainchild of UC Berkeley Space Sciences Lab Professor Dan Werthimer. SERENDIP is the acronym for: Search for Extra Terrestrial Radio Emissions from Nearby Developed Intelligent Populations. No wonder he abbreviated it. That must be a record for number of letters in a project name.

Dr. Werthimer is also the Principal Investigator for CASPER: Collaboration for Astronomy Signal Processing and Electronics Research. And also, he is the Co-Founder and Chief Scientist of the SETI@Home Project.

The SETI-Institute awarded Dan Werthimer (picture below left) the 2021 Frank Drake Prize.



In the video I'm editing from 38 years ago, Dan Werthimer is the scientist at Green Bank explaining the SERENDIP hardware (picture above right). At the time the signal processing was being done with an IBM PC-AT. That's an 80286 10 MHz processor! The signal being sliced and diced was a signal split off the 300 ft dish IF chain I believe at 30 MHz if I'm interpreting the video and hardware correctly.

The SERENDIP technique involves taking whatever Frequency and ra/dec the Principal Investigator is looking at and processing that RF. It's not totally random luck if something was found. But certainly, adds a level of chance to the pointing, timing, and frequencies. Werthimer has on an Arecibo T shirt and was talking about doing pulsar observations using the 300 ft dish. The pulsar work was why he was there at Green Bank. SERENDIP was just another project he was doing, which at the time was NASA funded.

Over the years I've seen later incarnations of the SERENDIP hardware on the Arecibo 1000 ft dish while we were there for a SARA Regional Conference in 2004.

The SETI Institute has periodically used the 140 ft dish at Green Bank and briefly the Woodbury 100ft dish in Georgia, subject of last month's column.

All that has evolved into the ten year \$100Million Breakthrough Listen Project at the Green Bank 100meter and Parks 64meter telescope and a host of others: 500m FAST, MeerKAT, Jodrell Bank, VERITAS, LOFAR, Allen Telescope Array, and many more, with Dan Werthimer and SETI@Home still key players.

It's interesting to see the data now is 6 GHz of bandwidth and 24 GB per second of capture rate per Wikipedia. And having seen it at Green Bank a few years ago they were having trouble cooling the room due to the number of server grade CPUs Breakthrough Listen was using. Contrast that to the subject of this article, SERENDIP on the 300 foot dish and an IBM PC-AT. The 286 had a 10 MHz clock rate, 20 MB hard drive, and 1 MB of RAM.





SERENDIP II+ was 64,000 BINS across the bandwidth of the telescope IF they were using. Pretty sure an RTL-SDR would outperform it today. In fact, somewhere I saw that the PC AT would be equivalent to a \$16K computer correcting for inflation.

I can recall about the time this video was taken in 1988 a modem designer at a company I was working at needed to do some development simulations and asked to buy a PC AT. They turned him down because it cost too much. Management forced him to use a mainframe to do the project as a time share which charges by the seconds of CPU time used. When finished they found out the PC would have cost less than the hours of mainframe time it took to do the simulations. Today a RaspberryPi would be like a supercomputer from 1988. Well maybe not a supercomputer, but at least 100x the PC-AT.



Drive gear and counterweight below the 300ft transit dish in June 1988. November 15th, 1988, the dish collapsed due to a gusset plate stress fracture which had been cracking slowly for a long time. The dish was put up as a temporary antenna due to delays in the completion of the 140ft dish twenty-five years before. The 300ft telescope was built in 1962.

That concludes this month's Vintage SARA trip back in time.
--the end--

More Vintage

The Parallel Port and MAX-186/187

James Van Prooyen

The PC Parallel Port and MAX-186/187 A/D's (or DAC) played a major role in the development of radio astronomy in the 90's and 00's, it have been superseded by other interfaces types between the radio and computer, but there is still a lot of equipment out there that uses this type of interface, so documentation is needed and the best place in the SARA Journal.

The parallel port are available on many single board computers (Raspberry Pi for example) and for Desktop PC's, parallel port card are available (details below). Technical details on the parallel port may be found here: https://en.wikipedia.org/wiki/Parallel_port

The MAX-186/187 chips are available for ~ \$15 to \$20 (US). Note that the MAX-186 has multiple A/D input channels where's as the MAX-187 only has one input channel.

Currently I know of two differences interface for the MAX-187, RAS – Radio Astronomy Supplies and Radio Sky Publishing – Radio Sky Pipe. The differ in the pins used on the parallel port

Radio Sky Pipe Parallel Port wiring for MAX-187 A/D

MAX 187	DB-25 Male	
Chip Pin	Connector Pin	
6 (Dout)	12 PE	
7 (CS)	2 Bit 0 8 (SCLK)	3 Bit 1
5 (REF-)	24 Ground	

See the RSP web page here for more details: <http://www.radiosky.com/dcla2d.html> Most version of Radio Sky Pipe support the both the MAX-186/187

Radio Astronomy Supplies Parallel Port wiring for MAX-187 A/D

MAX 187	DB-25 Male	
Chip Pin	Connector Pin	
6 (Dout)	12 PE	
7 (CS)	14 Auto Feed	
8 (SCLK)Purple	1 Strobe	
5 (REF-) Black	25 Ground	

A MAX-187 can be built on a prototyping board or ordered from this source as a kit listed below:

MTM Scientific <http://www.mtmscientific.com/max187.html>

Image of the completed A/D shown below, cost for the kit is ~ \$40.



There are many sources for Parallel Ports Interface Card for the IBM compatible PC a few are listed below:

Amazon ~ \$30 (US)

Staples ~ \$30 (US)

New Egg ~ \$21 (US)

Jim Sky has a post on using the Arduino Nano to create a wireless interface using a parallel port
It can be found here. <http://cygnusa.blogspot.com/2021/02/rescue-that-printer-port-adc.html>

In summary this is still a very useful interface for doing radio astronomy.

James Van Prooyen grro@sbcglobal.net

Featured Articles

A story, tangentially related to Radio Astronomy

Marcus Leech

Sometime around 2007 or so, I met a guy called Trond Trondsen, while waiting for a flight to Calgary. He'd attracted my attention because he was carrying a conference bag for a recent physics conference (atmospheric plasma physics as I recall). I said "hey, you a physicist?". He regarded me, somewhat aloof and suspicious. Lots of kooks will "buttonhole" physicists and rant at them about the standard model being all wrong, and it's really the lizard-people, etc. He relaxed considerably when he realized that I was no such kook (a weirdo, perhaps, but not a kook).

We (by some miracle I still cannot understand) were seated next to one another on the flight. Trond, it turned out, was VP of a company in Calgary that (among other things) built EUV imagers for upper-atmosphere and auroral research. We exchanged animated nerdlings for the rest of the flight about the things we obsessed about. I spent a lot of time talking about SDR and radio astronomy, he about modern imaging hardware.

We agreed to stay in touch, and subsequently became friends.

A year or two passed, and Nortel had graduated me and a thousand of my closest friends. Trond contacted me to see if I'd be interested in working on an exploratory contract to design a riometer using "modern techniques" with a view to replacing the stone-knives-and-axes technology that was currently in the field at the time (designed in 1973). I designed an early system, tested it in my backyard, and the back-yards of all my friends who would cooperate. Still, no "ready market".

A riometer is an instrument that measures the Relative Ionospheric Opacity -- using the galactic background synchrotron radiation as a kind of "standard candle". Over a wide-enough field-of-view, those emissions are basically invariant. During the course of a day, as the sky moves through the field-of-view, a typical brightness curve is produced. The shape of that curve is characteristic of the antenna pattern and particular location on the planet. Deviations from that curve are produced usually by solar events that change the absorption of the ionosphere--sometimes quite dramatically. Very occasionally (like on October 9th, 2022), by distant cosmic cataclysms...

The government science departments that deployed riometers all over the world were a conservative bunch and those "tin cans" from 1973 worked "well enough".

A year or two after that, we got an opportunity to go to Puerto Rico to visit Arecibo and set up some riometer tests there. It was a scientific fiasco in many ways, but I learned a bunch of things about the RFI environment in YET ANOTHER location. This caused me to design prototype number 2 or 3, depending on how you're counting. STILL no "ready customers". The 1973 (all-analog, of course) design was fairly-well entrenched even at this late date.

A couple of years later, my not-for-profit (CCERA) got a chance to work on a small Government of Canada contract to review their existing riometer network (still, the 1973 tin-cans), make recommendations to "keep it going", establish requirements for future networks, and repair a few of them that had come back in from the field. I also

had an opportunity to do more "field" work--literally at their geomagnetics field station in the far east end of Ottawa. This was another learning opportunity, and I took ruthless advantage of it. When the contract was done, I wrote an extensive report for them, and naturally recommended my designs, but that they'd have to purchase them through Keo Scientific. That field experience drove even more changes, and the 4th generation design ended up being sent to Keo for review and to come up with a "manufacturable platform". This was 4 years ago. Still nothing moving on the actually-selling-these-things front.

Then a couple of months ago, this all changed. I worked with Keo remotely and via e-mail to get the prototype back up and running while they in parallel prepared to make a manufacturable version that used a modified LWA antenna, and they'd made some hardware improvements--the noise source had active rather than passive thermal management, and the filters were improved, and a couple of nice "system management" things were added.



Their first customer, the British Antarctic Survey is deploying a unit to the Halley VI research station on the Brunt Ice Shelf in Antarctica:

<https://www.bas.ac.uk/polar-operations/sites-and-facilities/facility/halley/>

If you don't think that research station looks like a Gerry Anderson "Moon Base" then you're not nerd enough to be reading this message :) :)

Lunar radiation observed by a small dish at 80 GHz. Part 1, the telescope and conditions.
by Dimitry Fedorov UA3AVR and Joachim Köppen DF3GJ

The Moon is the nearest celestial body, which is heated by the Sun. As the illumination of the lunar surface changes during a month, we can see it by eyes how the Moon looks in different phases. A heated celestial body has to emit the thermal radiation at radio frequencies too. The Moon's radiation, in principle, can be detected by small dishes like in Itty-Bitty Telescopes (IBT, <http://www.aoc.nrao.edu/epo/teachers/ittybitty/>). IBT is usually built for frequencies 11-12 GHz using Sat TV equipment, but it is interesting how the lunar radiation behaves at higher frequencies.

The Moon can be considered as a radiating blackbody. A brightness temperature of the detected radiation can be extracted from observation data, when antenna and receiver performance characteristics are known. The lunar radiation behaves differently for different frequencies due to properties of the lunar soil (regolith). The lunar radio flux and its surface temperature are almost constant (~ 210 K, [1]) during a month at low frequencies (up to several GHz); the phase-dependent variation of the temperature becomes much stronger at higher frequencies, including 80 GHz. Changes in temperature are already detectable with a small dish at frequencies about 11 GHz [2]. The distribution of temperature across the lunar disk is also uneven at higher frequencies and depends on the phase. Such behavior of the lunar radiation is due to lunar soil properties: the regolith is a poor thermal conducting substance, and its radio absorption rises with frequency. For low frequencies the lunar radiation is formed mainly by deep layers under the Moon surface with almost constant physical temperature, but at higher frequencies the radiation comes mainly from layers closer to the surface which is subject to changing temperatures. At 80 GHz the range of variations could be expected about 150-250 K [3].

The temperature variations with the Moon phase can be detected by the 80 GHz small dish telescope. Such a telescope may remind of the IBT, but its building is a bit more complex than the original IBT. This paper is about building of such telescope, measuring lunar radiation at different phases, collecting data, and how to extract the lunar radio brightness temperatures from the collected data. The Earth atmosphere plays a significant role in the experiments and data post-processing due to the high levels of atmospheric absorption of mm-wave radiation and difficult weather conditions.

The paper is based on the detailed investigation [4]; the lunar measurements and raw data processing are performed by Dimitry Fedorov UA3AVR in 2021-2022, the post processing procedures were reworked, systematized and polished by Joachim Köppen DF3GJ in 2022.

The small dish telescope (radiometer) at 80 GHz, how it looks like

The radiometer's offset dish 0.9 m (from Russian manufacturer 'Supral', originally intended for Sat TV) and the feed are shown in Fig.1; the receiving system structure is shown as a schematic in Fig.2.



Figure 1: The antenna and the feed of the 80 GHz radiometer

The radiometer consists of a dish reflector with a feed, a Low Noise Amplifier (LNA) followed by a band-pass filter, next a sequence of two frequency converters (downconverters) and, as the end of the chain, a noise power meter. The receiver characteristics are collected in Table 1. The reflector feed is homemade from a crimping cap for RF coaxial connectors and soldered to a 3.6x1.8 mm waveguide flange; the feed beam width needed for the dish (with equivalent $F/D=0.5$, with -10 dB taper at the dish edge) has been confirmed by calculations with Comsol (2D axisymmetric RF module). VSWR of the feed was measured as <1.3 .

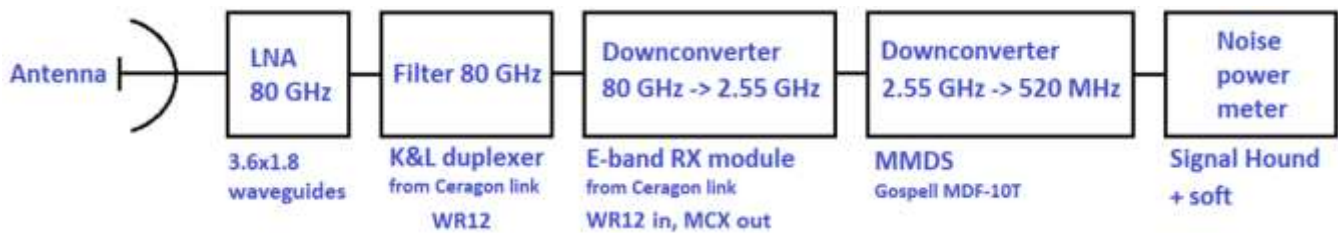


Figure 2: Schematic diagram of the receiving system of the 80 GHz radiometer

Table 1: The 80 GHz radiometer characteristics

Offset antenna reflector, dish diameter	0.9 m
Half Power Beam Width (HPBW)	0.3°
Main Beam Efficiency η	0.65
Aperture efficiency $\eta_A \approx 0.75 \eta$ [5]	0.49
Side and back lobes coefficient k (see the text below)	0.5
RX Noise Figure, NF	5.5 dB
Receiver frequency	80.5 GHz

Table 1a: The telescope characteristics

Dish antenna sensitivity (the 'Forward Gain')	0.11 mK/Jy
System temperature, T_{SYS}	≈ 840 K
SEFD (System Equivalent Flux Density = T_{SYS} / 'Forward Gain')	$\approx 7.6 \cdot 10^6$ Jy

The Main Beam Efficiency $\eta=0.65$ was measured once (July 2021) using the method described in [6], while enjoying a rare chance of a bit after the Full Moon and perfectly clear weather. Although the telescope characteristics of the radiometer are not immediately applied in considerations below, they have collected in Table 1a for reference. The LNA was assembled using broadband UMS die chips (courtesy to Sergey Zhutyaev RW3BP) with 3.6x1.8 mm waveguide apertures at the input and output. Initial tests of the LNA gave noise figure NF=3.5 dB and gain Ga=15 dB at 76 GHz; despite of our working frequencies being somewhat higher these NF and Ga could be used as a reference. The noise figure of the receiver as a whole of 5.5 dB was determined by the ‘Golden Device’ method [7]; this method de-facto compares the receiver with a device of known noise figure. These NF measurements did not take into account a connecting waveguide from the LNA to the feed; so, a real NF of the receiver may be a bit higher (by several tenths of dB).

The working frequencies are limited by the following RF filter and downconverter. A filter was extracted from a Ceragon E-band link head (‘Ceragon Fibear Gigamax 80AR low’, the duplex filter ‘K&L M/W 7WZ01-00065). The input of this filter is of WR12 size. It is immediately connected to the LNA output with 3.6x1.8 mm aperture; the flanges are mechanically compatible, and the EM-analysis with Comsol, 3D RF module shows only a small mismatch – return loss is more than 26 dB from both ends for basic TE₁₀ (H₁₀) mode. The next downconverter device was also extracted from the same head; it does not require an external local oscillator as it contains its own parametric oscillator tuned by an external DC voltage. Despite its poor frequency stability and phase noise, such downconverter can well be suitable for radio astronomy applications exploring broadband sources. It does not well work at frequencies below 80 GHz, so the measurements were made at a slightly higher frequency. The second frequency conversion uses a MMDS receiving device (with marking ‘Gospell MDF-10T’; modified by a separate SMA input); it gives an additional gain of almost 40 dB, and has an output on 520 MHz for transmission over a lengthy cable to the indoor located power meter. This power meter based on the Signal Hound analyzer SA-44b with a LabVIEW software written especially for noise measurements [8].

The antenna beam width (0.3° HPBW) is comparable with the seen angular size of the Moon (~0.5°).

Observational procedures and lunar noise measurements

Three measurements were being done with this instrument for every observation:

1. The power at the receiver output (Moon noise power) was measured when the antenna beam is directed to the Moon. A maximum power level was searched by slight adjustments of the dish in azimuth and elevation.
2. Next, the empty sky power level at the same elevation was measured. The same elevation is needed to provide the same amount of atmospheric losses for a measured radiation.
3. The flux calibration of the instrument is performed when a sheet or a box of RF-absorbing material (a calibrating load) is placed in front of the feed (see Fig.3). This measurement gives a possibility to compare a receiver response to the case when a blackbody source emits with a known temperature.



Figure 3: Flux calibration of the 80 GHz IBT: a plastic box (a calibration load) with a foam RF absorber sheet inside (left) and just a RF-absorbing sheet covering the feed (right).

The lunar data were collected between December 2021 and June 2022, from a location near Moscow (56°8'46"N, 37°29'47"E), when the Moon was mainly in south-west to west directions (azimuth >210 deg) and with elevations 20-43°. The lunar signal was 0.25-0.65 dB above the neighboring empty sky, and the flux calibrations were in the range 0.7-0.95 dB above the sky.

Interpretation of the Moon noise power

When the antenna beam is directed to the Moon the receiver response is defined by several factors besides the Moon itself. First, the receiver has its own noise described by its Noise Figure. Second, the atmosphere also emits its thermal noise, which must be taken into account, especially for mm-waves. And third, the antenna receives the thermal noise from its surroundings by back and side lobes. The total can be described as

$$P_{moon} = g * (\eta * (T_{moon}/L(e) + T_{sky}(e)) + (1-\eta) * k * T_{amb} + T_{RX}), \quad (1)$$

which contains a receiver gain factor g . The Main Beam Efficiency η of the antenna [5,9,10] describes how much a dish receives by the main lobe only in comparison to the entire radiation pattern, including back and side lobes, hence $0 < \eta < 1$. The Moon's contribution is represented by

$$\eta * T_{moon} / L(e), \quad (2)$$

where $L(e)$ is the attenuation in the atmosphere along the line of sight at elevation angle e , and T_{moon} – is the Moon beam temperature, i.e. the radiative temperature which the antenna beam sees from the Moon. The contribution Eq. (2) depends on the elevation angle e of the Moon and, certainly, on atmospheric conditions (air temperature, pressure, and humidity). A well detailed and suitable for practical use description of atmospheric

losses can be found in ITU recommendations [11]; there is a JavaScript of the calculation procedure available [12]. The value $L(e)$ is expressed via zenith losses in dB, $L_{dB}(90^\circ)$, and used as a reference of atmospheric losses,

$$L_{dB}(e) = L_{dB}(90^\circ) / \sin(e), \quad L(e) = 10^{(L_{dB}(e)/10)}. \quad (3)$$

A typical value for the zenith loss is about 0.4 dB. The ITU recommendations [11] are well applicable for clear weather when almost no clouds present in the sky. At working elevations, the loss is higher than at the zenith and rises dramatically towards low elevations.

The sky radiation is contributed by atmospheric thermal emission,

$$T_{sky}(e) = T_{sky0} * (1 - 1/L(e)), \quad (4)$$

with T_{sky0} being a mean temperature of the atmosphere. We adopted the value $T_{sky0} = 275 \text{ K}$ [13], although, as expected, it may depend on the atmospheric conditions too. The atmospheric contribution in Eq. (1) lies between 30 and 100 K, and we note these values can be substantial for 80 GHz. The Cosmic Microwave Background (CMB) would also contribute to the sky temperature, but we omit it because of relatively small temperatures of CMB, which are definitely below 2.7 K.

The next term to be taken into account describes what the dish receives by back and side lobes from the warm ground and other surroundings with temperature T_{amb} . If the back lobe and all side lobes see the temperature T_{amb} the noise picked up by the dish would be $T_{amb} (1-\eta)$. But really only a part of lobes outside the main beam collects the ambient thermal noise from surroundings. This is described by the back and side lobes coefficient k with typical value $k = 0.5$,

$$T_{amb} * (1-\eta)*k. \quad (5)$$

This contribution is about 50 K.

Finally, the most important contribution is the internal noise of the receiver, which is described by the noise figure NF ,

$$T_{RX} = 290 \text{ K} * (10^{(NF/10)} - 1), \quad (6)$$

The previously measured receiver noise figure of 5.5 dB gives a rather high value $T_{RX} = 739 \text{ K}$; this is the most significant contribution to the system temperature T_{SYS} and the output receiver noise.

Direct extraction of the Moon contribution when Noise Figure is known well (method NF)

The Moon noise power is represented by Eq. (1). To extract the Moon contribution and the beam temperature T_{moon} we need the second measurement of the empty sky at the same elevation. This power is represented by

$$P_{sky}(e) = g * (\eta * T_{sky}(e) + (1-\eta)*k*T_{amb} + T_{RX}). \quad (7)$$

It differs from Eq.(1) only by not having the Moon contribution. Introducing the Moon Y-factor

$$Y_{moon} = P_{moon}/P_{sky}(e) \quad (8)$$

and substituting the explicit expression for $T_{sky}(e)$ from Eq.(4) one can derive from (1) and (7)

$$T_{moon} = L(e) * (Y_{moon} - 1) * (\eta * T_{sky0} * (1 - 1/L(e)) + (1-\eta)*k*T_{amb} + T_{RX}) / \eta. \quad (9)$$

The receiver gain factor g is gone due to using the Y-factor in Eq. (8). Note that the Moon beam temperature T_{moon} is proportional to $L(e)$, and therefore, the accuracy of atmospheric attenuation value also determines the accuracy of T_{moon} . Let us consider the atmospheric losses more closely.

Calibration and atmospheric attenuation

The ITU Recommendations [11] describe the gaseous attenuation in the Earth atmosphere, but do not take into account specific phenomena in the radio propagation path like clouds, fog, precipitations etc. Some presence of clouds in the sky happens often. This is a rare chance of having a perfectly clear weather and the desired Moon phase happening at the same time.

The actual attenuation at the atmospheric path for given antenna elevation can be obtained with the calibration procedure. This procedure uses a source with a priori known temperature and can be realized placing RF-absorbing objects in front of the dish feed (see Fig.3). Under usual assumption that temperature of absorber T_{cal} is approximately equal the ambient temperature T_{amb} , $T_{cal} = T_{amb}$ we can measure a power at the receiver output with the calibration load

$$P_{cal} = g * (T_{cal} + T_{RX}). \quad (10)$$

Together with Eq. (7) one can get an actual value for atmospheric losses for given elevation angle e

$$L(e) = 1 / (1 - ((T_{amb} + T_{RX}) / Y_{cal} - T_{RX} - (1 - \eta) * k * T_{amb}) / (\eta T_{sky0})), \quad Y_{cal} = P_{cal} / P_{sky}(e). \quad (11)$$

Here we have introduced the calibration Y-factor Y_{cal} . We find that the value $L(e)$ from Eq.(11) is usually larger than obtained by the ITU procedure [11]. We interpret this introducing a correction factor $L_{clouds\ dB} > 0$ for result of ITU procedure $L_{ITU\ dB}$, $L_{dB} = L_{ITU\ dB} + L_{clouds\ dB}$, caused by clouds or haze in the sky.

Therefore, the calibration procedure is able to give more accurate value of the atmospheric attenuation.

(to be continued)

References

- [1] J. Köppen DF3GJ, *The 2015 Lunar Eclipse Observed at Radio Frequencies*, DUBUS 2/2020, p. 78.
- [2] C. Monstein, *The Moon's Temperature at $\lambda=2.77$ cm*, 2001, <https://doi.org/10.3929/ethz-a-004322130>, <https://www.research-collection.ethz.ch/handle/20.500.11850/146152>.
- [3] J. Köppen DF3GJ, *Noise from the Moon*, DUBUS 3/2021, p. 100.
- [4] D. Fedorov UA3AVR and J. Köppen DF3GJ, *Lunar Noise at 80 GHz*, DUBUS 4/2022, pp. 22-41.
- [5] D. Fedorov UA3AVR, *Solar Flux and Temperature at Millimetre Wavelengths*, DUBUS 3/2016, p. 41.
- [6] D. Fedorov UA3AVR, *Calibrations of mm-wave antennas and RX systems using Moon radiation*, 5th Sweden EME Meeting by SM4IVE, Örebro, 19-21 May 2017, see at the page <https://moonbouncers.org/>.
- [7] D. Fedorov UA3AVR, *Notes from the noise test lab, part 3*, DUBUS 3/2020, p. 38.
- [8] D. Fedorov UA3AVR, *Notes from the noise test lab, part 2*, DUBUS 1/2020, p. 30.
- [9] J. D. Kraus, *Radio Astronomy*, 2nd ed, 1986.
- [10] T.L. Wilson, K. Rohlfs, S. Hüttemeister, *Tools of Radio Astronomy*, 6th ed, Springer, 2013.
- [11] ITU Recommendations P.676-10 (09/2013), *Attenuation by atmospheric gases*, Annex 2.
- [12] J. Köppen DF3GJ, *Approximate Atmospheric Attenuation 1-350 GHz (uses ITU recommendations P676-10)*, <https://portia.astrophysik.uni-kiel.de/~koeppen/JS/AtmosAtten.html>, 2022.
- [13] ITU Recommendations P.372-11 (09/2013), *Radio Noise*.

About the authors



Dimitry Fedorov was first licensed as radio amateur since 1982, as UA3AVR since 1983. In 1990 graduated as MS in electronics in Moscow Power Engineering University. Now works as research and development engineer in wireless industry, LTE/5G NR, RF and microwave modules development. Previous scientific experience in nuclear and particle physics, worked in Moscow State University, Institute of Nuclear Physics and Universität Tübingen, Institut für Theoretische Physik, see profile blog at <https://www.researchgate.net/profile/Dimitry-Fedorov-2>. Radio Astronomy hobby since 2012, mainly in applications for weak signals reception. You can contact the author at ua3avr@yandex.ru.



Joachim Köppen (DF3GJ) is a retired astrophysicist having worked in theory and observations of planetary nebulae and in evolution of galaxies in Heidelberg, Kiel, and Strasbourg. Having been infected by the radio and electronics virus as a small boy, he operated two small radiotelescopes for student projects in Strasbourg. Now in Kiel he joined the DLØSHF group, also writing software for the telescope operations, and using the instruments for the observational projects of the astronomy students in our institute. Contact: koeppen@astrophysik.uni-kiel.de (Inst.Theoret.Physik u.Astrophysik, Univ. Kiel).

Another Look at the System Noise Temperature of a Radiometer

Peter W East

Introduction

This article investigates the sensitivity limitations of a typical radio telescope radiometer, usually specified by its system noise temperature (T_{SYS}). T_{SYS} defines the limiting sensitivity of a radiometer, bandwidth 'B,' observing and integrating a source for a time 't' as T_{SYS} / \sqrt{Bt} .

The importance of including a low noise amplifier (LNA) is well recognized. It is also advised to locate the LNA close to the antenna terminal and keep connection losses low and control interface mismatches.

Following a few definitions to set a baseline, the sensitivity controlling functions are derived and some results presented graphically.

Definitions

Figure 1 depicts an antenna, terminal impedance Z_a observing a region of space, temperature T_a feeding a transmission line of impedance Z_{TL} driving an LNA, input impedance Z_{LNA} , plus an RF amplifying chain with an overall noise figure F_{LNA} in a physical environment with an ambient temperature, T_{amb} (~ 290 °K un-cooled).

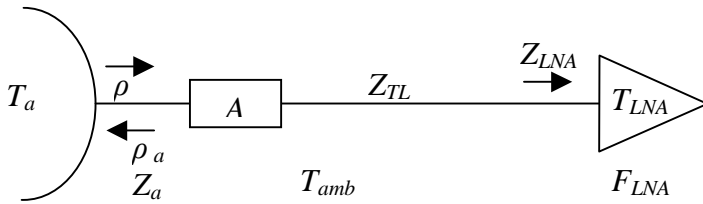


Figure 1. Radiometer Input Schematic

The equivalent noise temperature of the LNA plus following RF amplifier/filter chain is, $T_{LNA} = (F_{LNA} - 1)T_{amb}$, or $T_{LNA} = T_{Ina} + T_{RFChain}/Gain_{Ina}$, where T_{Ina} is the noise temperature of the LNA alone.

For the attenuator, 'A' represents the total resistive loss factor (<1) of the connections and cable between the antenna and LNA terminals and is usually measured in decibels, (dB), where,

$$dB_A = 10 \log_{10}(A) \text{ or } A = 10^{dB_A/10}$$

An attenuator preceding an LNA effectively increases the combined Noise Figure by the dB loss of the attenuator (see derivation in the Appendix) but the equivalent attenuator noise temperature itself is,

$$T_{atten} = (1 - A)T_{amb}$$

Mismatches between RF components and transmission lines cause power to be reflected at the junctions setting up voltage standing waves along the lines, the median representing mismatch loss.

There are two potential mismatch planes, one at the antenna terminal and the other at the LNA input with voltage reflection coefficients ρ_a and ρ where,

$$\rho_a = \left| \frac{Z_a - Z_{TL}}{Z_a + Z_{TL}} \right| \text{ and } \rho = \left| \frac{Z_{LNA} - Z_{TL}}{Z_{LNA} + Z_{TL}} \right|$$

The proportion of power transmitted is $(1 - \rho_a^2)$ and $(1 - \rho^2)$, respectively, representing mismatch power loss and can be treated as attenuations.

Finally, the relation between reflection coefficient and voltage standing wave ratio (VSWR) is,

$VSWR = \frac{(1 + \rho)}{(1 - \rho)}$ or alternatively, it is defined as the magnitude of the ratio of the interface impedances Z_1, Z_2 producing a value ≥ 1 .

These are average functions and in practice the instantaneous values fluctuate with frequency.

System Noise Temperature

Based on the definitions above, the effective noise temperature at the LNA input, when the antenna is pointed off a source, referring to Figure 1, T_{SYS} is calculated from,

$$T_{SYS} = A(1 - \rho^2)(1 - \rho_a^2)(T_{CMB} + T_{sky} + T_{Grnd}) + [1 - A(1 - \rho^2)(1 - \rho_a^2)]T_{amb} + T_{LNA} \quad (1)$$

$T_{CMB} + T_{sky} + T_{Grnd}$ represent antenna noise temperature contributions from the Cosmic Microwave Background (~ 2.7 °K), random sky contributions (~ 10 - 20 °K) and thermal noise from the physical environment via antenna spill-over, and/or side- and back-lobes (~ 10 - 100 °K). These are reduced by the product of the line attenuation and mismatch loss factors.

The second term in Equation 1 is the temperature contribution of the line/connector attenuation and mismatch losses.

The source noise temperature at the LNA input is similarly reduced by the connection losses and is,

$$T_{SRC} = A(1 - \rho^2)(1 - \rho_a^2)(T_{source}) \quad (2)$$

In terms of the source flux, 'J' Jansky and the antenna effective collecting area 'C' m²,

$$T_{source} = J.C/1380 \text{ °K.}$$

The RF output signal to noise ratio SNR is given by T_{SRC}/T_{SYS} .

The source attenuation line losses can be accounted for by further increasing the calculated system noise temperature to,

$$T_{SYS_{eff}} = \frac{T_{SYS}}{A(1 - \rho^2)(1 - \rho_a^2)} \quad (3)$$

Note that the overall sensitivity degradation due to attenuation in the antenna - LNA path is doubled, by increasing interface noise and reduction of the wanted signal level.

T_{SYS} Measurement

The standard Y-factor method of measuring T_{SYS} is to measure the ratio of the detected power when pointed at the ground ($T_{ground} = 290 \text{ °K}$) and to a cold part of the sky ($T_{sky} = 15 \text{ °K}$), then,

$$Y = T_{ground}/T_{sky} \text{ and } T_{SYS} \approx \frac{T_{ground} - Y.T_{sky}}{Y - 1} \quad (4)$$

This is obviously an approximation but it is more than adequate for most amateur requirements.

Practical Implications

Figure 2 plots the system noise temperature results for a variety of conditions and shows the importance of keeping LNA cabling short and optimising antenna and LNA match.

Side-lobes or dish feed spill-over illuminating the ground virtually adds directly to T_{SYS} as indicated by the green and magenta curves in Figure 2 and is to be controlled by antenna choice or screening.

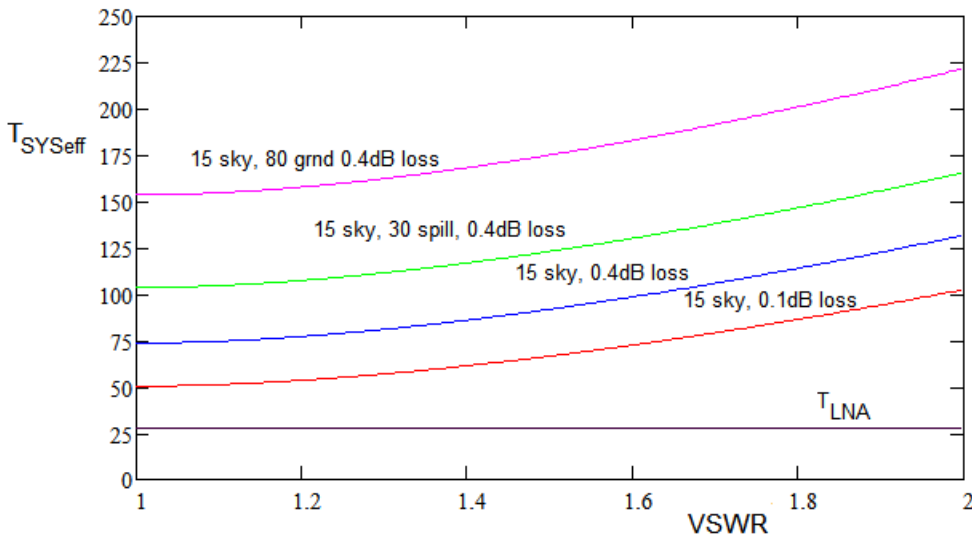


Figure 2. Effective System Noise Temperature Results for 0.4dB LNA Noise Figure (~28 °K)

Depending on a dish feed illuminating efficiency, the spill-over contribution temperature contribution is typically in the range 20 °K to 70 °K. For a long Yagi in a cluttered environment with a local horizon of some 20°, the corresponding range for side- and back-lobes is 60 °K to 120 °K, so careful siting and shielding may be necessary.

Removing the Connection Cable

The recommendation of connecting the LNA directly to the antenna or with a connection that is very short compared to the RF wavelength, effectively removes the cable loss plus one mismatch/connector plane so now it is only necessary to match the antenna to the LNA. This may be possible by antenna tuning or a short matching circuit. As a general tuning rule, it is advisable to keep the VSWR less than 1.5 and to minimize the reactive components or keep the reactive component magnitudes less than half the full impedance magnitudes.

Conclusions

To maximise sensitivity given a specified LNA, minimise losses by placing the LNA directly following the antenna terminal. It is important to ensure a good match, preferably a VSWR of less than 1.5 for the both the antenna and LNA input.

Reference

[1] W.D. Reeve Noise Tutorial, Part III ~ Attenuator and Amplifier Noise.
https://reeve.com/Documents/Noise/Reeve_Noise_3_AttenAmpNoise.pdf

Appendix

Noise Temperature of Attenuator

W. Reeve presents a rigorous method of calculating the noise temperature of passive attenuators.[1] An alternative way of understanding the performance of a passive attenuator is to notionally apply the standard method of noise figure measurement, namely to input a calibrated noise signal that doubles the output noise power. The noise factor is then simply the ratio of the input noise power required to the available resistive power, T_{amb} .

In the case of a terminated resistive attenuator with a power transfer factor, A at temperature T_{amb} , the static input and output available thermal noise powers are each $kT_{amb}B$, where k is Boltzmanns constant and B is the measurement bandwidth.



Figure A1. Noise Temperature of an Attenuator; Injected Noise power Doubles Output Power

With no input the termination input and output noise powers are, $kT_{amb}B$

To double the output noise power an extra input kT_eB is required; from Figure A1, the new total input power is, $kT_eB + kT_{amb}B$ and the doubling of the output becomes,

$$A(kT_eB + kT_{amb}B) + kT_{amb}B = 2 kT_{amb}B$$

Solving this equality, referred to the input the attenuator equivalent temperature is,

$$T_e = (1/A-1)T_{amb}$$

and the equivalent output temperature is,

$$AT_e = (1-A)T_{amb}.$$

The corresponding noise factor is, $(T_e + T_{amb})/T_{amb} = 1/A$, agreeing with Reference 1 analysis; using the identity, $T = (F - 1)T_{amb} \rightarrow F = (T + T_{amb})/T_{amb}$.

PWE March 2023



Peter East, pe@y1pwe.co.uk is retired from a Defense Electronics career in radar and electronic warfare system design. He has authored a book on Microwave System Design Tools, is a member of the British Astronomical Association since the early '70s and joined SARA in 2013. He has had a lifelong interest in radio astronomy; presently active in amateur detection of pulsars using SDRs and researching low SNR pulsar recognition and analysis. He has recently written another book, 'Galactic Hydrogen and Pulsars - an Amateurs Radio Astronomy' describing his work in Radio Astronomy. He maintains an active RA website at <http://www.y1pwe.co.uk/RAProgs/>

Planning for the 2023 and 2024 Solar Eclipses at VHF, UHF and Ku-band

Christian Monstein and Whitham D. Reeve

1. Introduction

The annular solar eclipse (ASE) and total solar eclipse (TSE) forecasted to occur on 14 October 2023 and 8 April 2024, respectively, (figure 1) provide two wonderful opportunities for observing related radio phenomena over a wide frequency range. Observations of at least partial eclipses are possible over much of North and South America (2023 eclipse) and much of North America and even Greenland (2024 eclipse). Almost all states in the USA will be able to view at least a part of the two eclipses, but observations are not limited to just the USA.

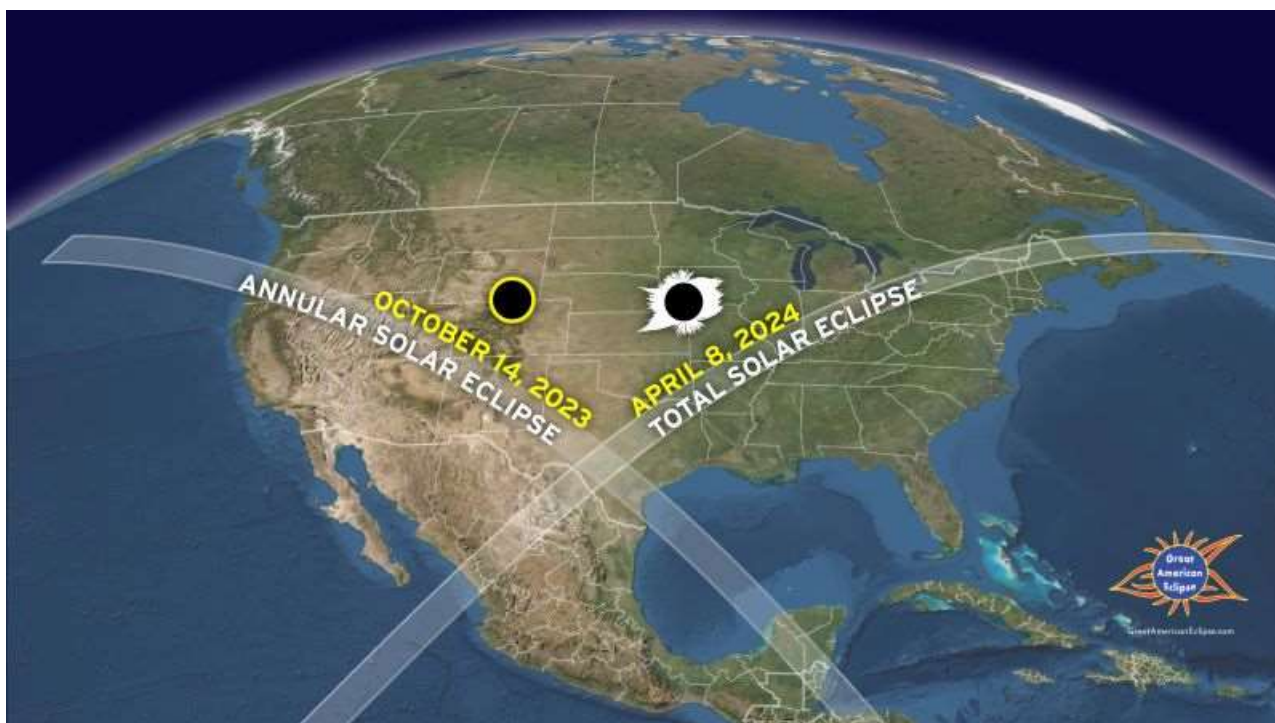


Figure 1 ~ View of the October 2023 and April 2024 eclipse paths over North America. Image source: <https://earthsky.org/sun/annular-solar-eclipse-october-14-2023/>

The current paper primarily concerns direct solar radio observations during the eclipses in the very high frequency (VHF, 30 to 300 MHz), ultrahigh frequency (UHF, 300 to 3 000 MHz) and super high frequency (SHF, 3 000 to 30 000 MHz) bands. We do not cover eclipse effects in the very low frequency (VLF, 3 to 30 kHz) and low frequency (LF, 30 kHz to 300 kHz) but these ranges are worth observing as well.

In particular, we focus on the native frequency range of the Callisto solar radio spectrometer, 45 to 870 MHz, with additional information on using an inexpensive Ku-band satellite dish antenna and associated low noise block

converter (LNB) as a down-converter with Callisto to observe in the X-band at about 10 600 MHz. The concepts described in this paper can be applied to other frequency bands with or without the Callisto as an integral part of the radio telescope.

We discuss how to observe changes in solar radio emissions received on Earth's surface as the Sun is occulted by the Moon. At the frequencies of interest, Earth's ionosphere effects are expected to be minor. However, we also discuss how to use Callisto to measure the scintillation index of satellite transmissions in the upper-VHF band during the eclipses.

The eclipses will occur during the rising portion of the current solar cycle 25, so radio observations generally will be of the *active Sun* and its broadband continuum of moderate level radio emissions. A solar radio storm or bursts could occur during the eclipses, but such events have low likelihood at X-band.

The current paper provides the forecasted physical characteristics of the two eclipses. We then turn to the higher radio frequencies. Observing a solar eclipse of any kind requires considerable planning, and now is the time to start. Some observers may wish to construct dedicated observing facilities for the eclipses, which will require additional time. Because of the relatively short notice of this article in April 2023, some observers may not have time (6 months) to fully prepare for the October 2023 eclipse, but it nevertheless will provide a good practice session for planning and system setup for the total solar eclipse in April 2024.

Observers should not wait until the last minute. It is very important to pretest the radio spectrometer system long before the event day so that there is plenty of time to become familiar with it and correct any problems. The need for adequate pretesting cannot be overemphasized.

2. Eclipse Characteristics

Solar eclipses of all types (partial, annular, total) are not particularly rare worldwide (for example, see [{Solar}](#)). Total solar eclipses (TSE), during which the Moon completely occults the Sun, occur somewhere around the world annually but for most of us the opportunity to view a TSE happens only a few times in our lifetime. Annular eclipses also are common but thought to be not as dramatic. During an annular solar eclipse, the Moon is too far from Earth to completely block the Sun but it does occult a good portion of it. During annularity (the maximum phase of an annular eclipse), the Sun appears as an extremely bright ring around the Moon.

On 14 October 2023, the annular solar eclipse will be visible, at least partially, over almost the entire North and South American continents (figure 2). In the USA, the path of annularity starts on the USA west coast in Oregon at 1613 UTC (9:13 am PDT) and ends in Texas at 1703 UTC (12:03 pm CDT). The duration of the optical eclipse will be about 5 min 17 sec at any given location along the annularity path but the duration from start to end of the partial eclipse will be almost 6 h. The Moon will cast a shadow up to 187 km wide as it crosses the United States. Because the eclipse is annular, a portion of the Sun will be visible at all times, and eye protection will be needed during radio telescope alignment.



Figure 2 ~ Path of the 2023 annular solar eclipse across Earth's surface. Annularity will be visible within the area outlined by the yellow stripe. The path width is 187.4 km. The northern and southern limits of the eclipse are shown along with the percentage of the eclipse that will be visible at a location. The greatest eclipse location (location of the longest optical eclipse duration) is $11^{\circ} 21.7' N$, $83^{\circ} 04.3' W$, just off the eastern coast of Nicaragua in the Caribbean Sea. The greatest eclipse duration occurs at 17:59:21 UTC and is 5 min 17 s. Image source: <https://earthsky.org/sun/annular-solar-eclipse-october-14-2023/>

On 8 April 2024, a total solar eclipse will be visible in the United States (figure 3). The path of totality – the path where the Moon totally obscures the Sun as viewed from Earth's surface – starts in Texas about 1727 UTC (01:27 pm CDT) and ends in Maine about 1935 UTC (03:35 pm EDT). The duration of total optical eclipse will be about 4 min 27 sec at any given location along the totality path but the duration from start to end of partial eclipse will be almost 3 h. The Moon will cast a shadow up to 197.5 km wide as it crosses the United States.

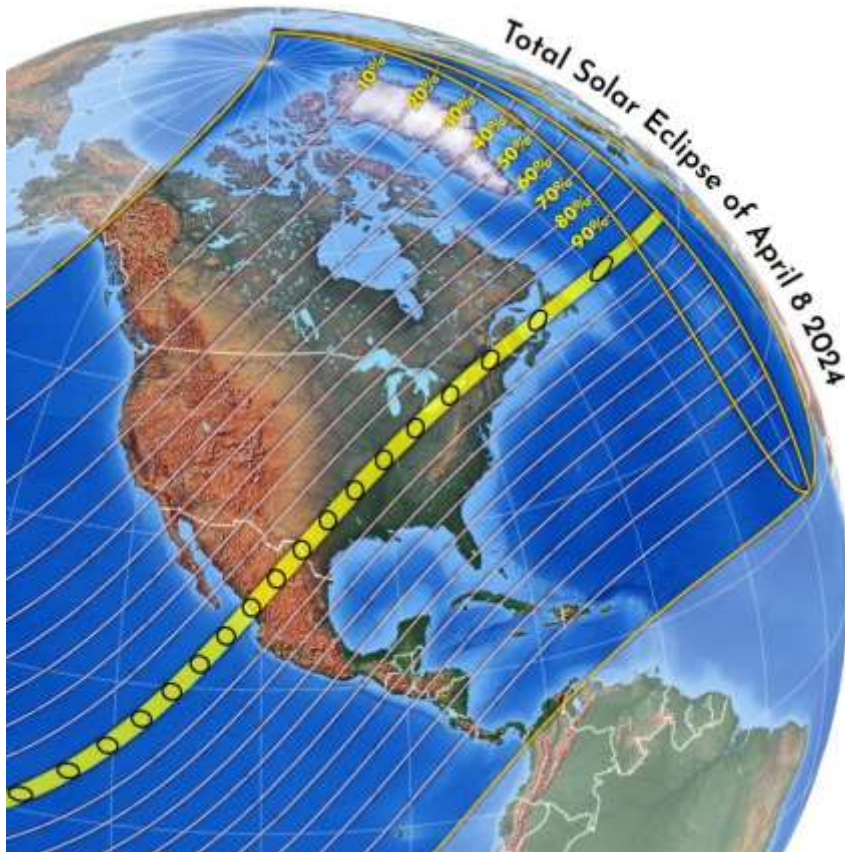


Figure 3 ~ Path of the 2024 solar eclipse across Earth's surface. It will be totally visible within the area outlined by the yellow stripe. The northern and southern limits of the eclipse are shown along with the percentage of the eclipse that will be visible at a location. The greatest eclipse location occurs at 18:17:13 UTC over Durango in northwestern Mexico at 25° 17.5' N, 104° 07.2' W. The longest optical duration is forecasted to be 4 min 27 s. Image source: <https://earthsky.org/astronomy-essentials/total-solar-eclipse-april8-24/>

2. Radio Emissions from the Quiet Sun

The radio flux from the quiet Sun is a broadband continuum consisting of a steady background component with a constant level lasting months or years and a slowly varying component that changes from day to day with a period of 27 days. These also are called the B- and S-components, respectively. By definition, the quiet Sun produces low level radio emissions.

The background is caused by thermal emissions of the solar atmosphere and is randomly polarized. At frequencies of approximately 30 to 300 MHz the background emissions originate mostly in the solar corona, which is the outer region of the Sun's atmosphere reaching a few solar radii. The corona temperature is about 10^6 kelvin. At higher frequencies up to about 3 GHz the emissions originate partly in the corona and partly in the chromosphere where the temperatures are on the order of 10^4 K. At even higher frequencies, the emissions originate mostly in the chromosphere. Frequencies below 200 MHz are often called *coronal frequencies* and above 10 000 MHz are called *chromospheric frequencies* [Smerd].

The slowly varying component also consists of randomly polarized thermal emissions, but these are produced in regions of relatively high electron densities and strong magnetic fields near sunspots and chromospheric plagues

(also called plagues). During solar minimum, disturbances from solar flares and other transient phenomena may occasionally and temporarily raise the received radio level above the quiet Sun level.

The spectral flux density of the quiet Sun varies with frequency and rapidly rolls off below about 100 MHz (table 1). The low levels require that the radio telescope has very high sensitivity, which can be attained only by using a low noise amplifier and a high-gain antenna (discussed in sections 6 and 7). The chart indicates the possibility of using a Ku-band dish antenna and associated low noise block converter (LNB) as a down-converter with Callisto (discussed in section 8).

Table 1 ~ Quiet Sun spectral flux densities in solar flux units (sfu) and watts per square meter per Hz at Earth. For reference this chart shows frequencies below and above the Callisto range. Source: [Benz]

Frequency (MHz)	Wavelength (m)	S _{Quiet} (sfu)	S _{Quiet} (W m ⁻² Hz ⁻¹)	Callisto range
30	10	0.17	0.17 · 10 ⁻²²	Up-converter
50	6	0.54	0.54 · 10 ⁻²²	Yes
100	3	2.4	2.4 · 10 ⁻²²	Yes
150	2	5.1	5.1 · 10 ⁻²²	Yes
200	1.5	8.1	8.1 · 10 ⁻²²	Yes
300	1	14.9	14.9 · 10 ⁻²²	Yes
400	0.75	21.7	21.7 · 10 ⁻²²	Yes
600	0.5	32.1	32.1 · 10 ⁻²²	Yes
1000	0.3	41.3	41.3 · 10 ⁻²²	870 MHz
1500	0.2	48.0	48.0 · 10 ⁻²²	Down-converter
3000	0.1	69	69 · 10 ⁻²²	Down-converter
3750	0.08	82	82 · 10 ⁻²²	Down-converter
5000	0.06	107	107 · 10 ⁻²²	Down-converter
10000	0.03	275	275 · 10 ⁻²²	Ku band LNB
15000	0.02	574	574 · 10 ⁻²²	Down-converter

During an eclipse, the received solar radio emissions are reduced as the Moon moves between the Sun and observer. However, unlike the total solar eclipse in visible light, the Sun's radio emissions are not completely blocked along the path of totality because the radio Sun is much larger than the visible Sun, and a total solar radio eclipse can never occur (figure 4). Similar comments hold for an annular eclipse. The radio Sun at the frequencies of interest is approximately 1.5 to 2 times as wide (east-west) as the visible Sun but roughly the same height (north-south).

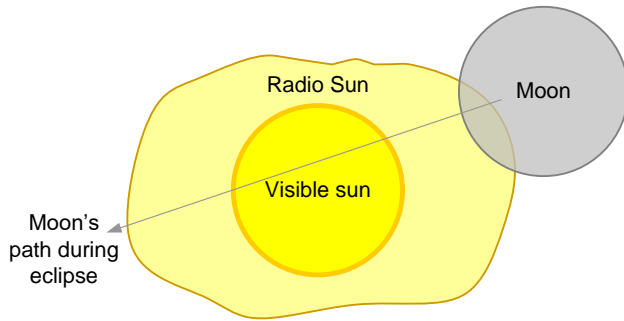


Figure 4 ~ The Moon's angular size as viewed from Earth is close to the visible Sun's size, about 0.5° . However, the radio Sun is larger so its radio emissions are not entirely blocked during an eclipse. The radio Sun is asymmetric. The reduction in received flux between the start and end of partial obscuration will span a few hours with some variation at different locations. Image adopted from [Kundu].

The received flux $\psi_{rx}(t)$ during an eclipse is of the form

$$\psi_{rx}(t) = 1 - \psi(t)$$

where $\psi(t)$ is the residual flux as a decimal fraction of the total flux (figure 5).

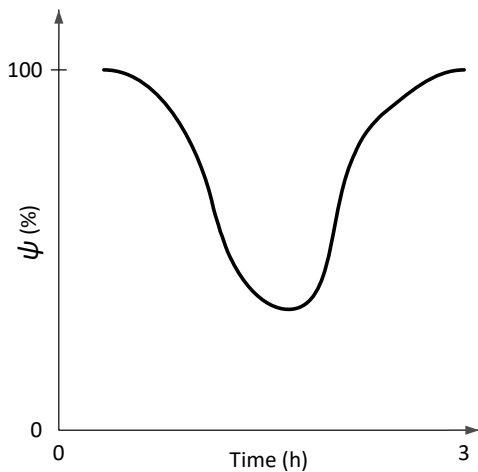


Figure 5 ~ Solar radio flux received on Earth's surface during an eclipse as a percentage of the total flux. The time scale is approximate. Radio observations of the Sun are complicated by the variable component of its emissions and asymmetry of its radio shape. Image adopted from [Kundu].

4. General Considerations

This section provides general considerations and not step-by-step procedures. Each station should formulate detailed observing strategies and procedures and rehearse them well before the eclipse. Although the total eclipse lasts only a few minutes at a given location, the Sun is partially eclipsed for several hours. To obtain comparative data, the Sun should be observed as long as possible before and after the actual eclipse. Two observing modes are described below, Sun tracking and Sun Transit.

Sun tracking mode: The Sun tracking mode requires a 2-axis antenna rotator system that can automatically track the Sun in azimuth and elevation. As a convenient alternative we can use a parallactic mount (also called equatorial mount) where tracking requires only one active drive because the declination of the Sun hardly changes

during a few days of observation. The recommended observations span a total of at least seven days – three days before, three days after and the day of the eclipse itself. The pre- and post-eclipse data will be used to establish the quiet Sun emission levels for comparison with the eclipse day. Use the collected data to produce a plot of peak transit intensity over the seven day period as follows (Eclipse day = E):

E–4 day:	Final check of antenna tracking system for proper Sun tracking
E–3, E–2, E–1 days:	Observe the Sun to obtain quiet Sun data before eclipse
Eclipse day:	Observe as in previous days but expect lower peak intensity during transit
E+1, E+2, E+3 days:	Observe the Sun to obtain quiet Sun data after eclipse

Sun transit (drift) mode: In principle one could observe the eclipse in transit or drift mode where a tracking system is not available. A fixed antenna with 10° beamwidth that is accurately pointed at the midpoint of the total eclipse will view the Sun for approximately 12 min before and 12 min after the midpoint. Therefore, in this case, the Sun will be partially eclipsed when it enters and exits the antenna beam. The observing schedule for the transit scan is very similar to the tracking mode. Note that the Sun changes position in the sky by a small but significant amount throughout the 7-day observation period:

E–4 day:	Adjust antenna to the sky position of the Sun during eclipse
E–3, E–2, E–1 days:	Observe daily transit to obtain data about quiet Sun level before eclipse
Eclipse day:	Observe as in previous days but expect lower peak intensity during transit
E+1, E+2, E+3 days:	Observe daily transit to obtain data about quiet Sun level after eclipse

The position of the Sun in the sky as seen from the observation point needs to be determined in advance, usually in terms of azimuth and elevation (or altitude). These are easily determined using online calculators such as [{NOAA}](#) or a PC software tool such as the Multiyear Interactive Computer Almanac [[MICA](#)]. In order to use these tools observers need to know their observatory’s geographical location, which can be determined either from a large scale map or Global Navigation Satellite System (GNSS) receiver such as the Global Positioning System (GPS). In addition, one of the authors (Monstein) is able to provide Python scripts for free to perform these calculations.

5. Observed Phenomena

Observations may yield interesting results even for observers who are not along the totality path. The list below provides some ideas for observation. Previous observations of solar eclipses using Callisto are described in [Monstein].

- 1) Width of the radio Sun is almost twice that of the visible Sun
 - 2) Received flux will dip but not disappear during the eclipse
 - 3) Radio brightening at the limb of the optical disk occurs at 200 MHz and above
 - 4) Effects of the eclipse on the scintillation of satellite signals
 - 5) The eclipse can be observed in radio even when the Sun is not visible due to clouds, rain or snowfall.
- Therefore, it is an ideal experiment for outreach during bad weather conditions.

6. Equipment Considerations

This section discusses the requirements for observing the quiet Sun with a radio telescope based on Callisto. Callisto (figure 6) is the instrument portion of the solar radio spectrometer. Callisto has 62.5 kHz frequency resolution throughout its 45 to 870 MHz range, 1 ms integration time, 300 kHz detection bandwidth and 7 dB noise figure. More detailed specifications are at [Callisto](#) and information on the e-Callisto network can be found at [eCallisto](#). Callisto by itself is not sensitive enough to observe the quiet Sun, so a low noise amplifier is needed. The entire spectrometer consists of only a few basic components: Callisto, a high-gain antenna, low noise amplifier and associated power coupler (bias-tee), power supply and PC running the Callisto software (figure 7).

For all calculations in this and the next section, the low noise amplifier noise figure is assumed to be 1.1 dB. Actual noise figures for any installation may be substituted with little trouble. For a temporary setup, the low noise amplifier does not have to be an elaborate weatherproof unit and can be quickly and inexpensively built (figure 8) [ReeveLNA].



Figure 6 ~ Callisto is a channelized sweep-frequency receiver. In most configurations, the channels are swept at a rate of 800 channels/s, but this can be extended to 1000 channels/s when the Callisto is connected to a 1 MHz reference clock source. The Callisto instrument dimensions are 200 x 110 x 82 mm and it weighs 0.9 kg. It is powered by a 12 Vdc power supply and controlled through an EIA-232 interface. Image ©2012 W. Reeve

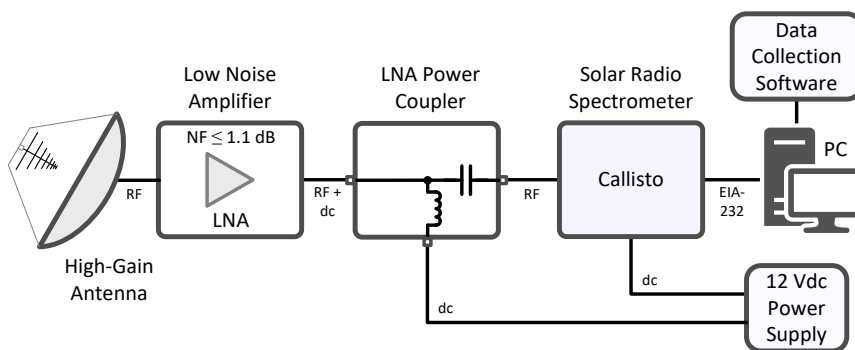


Figure 7 ~ Block diagram showing the basic solar radio spectrometer components. A low noise amplifier and high-gain antenna are critical components required to observe the radio Sun near solar cycle minimum. The LPC contains a bias-tee that allows the LNA to be powered through the coaxial cable to the antenna. Image ©2016 W. Reeve



Figure 8 ~ Inexpensive amplifier package made with a modular low noise amplifier. Dimensions are 110 x 77 x 47 mm and average measured noise figure across the frequency range 45 to 870 MHz is 0.8 dB. This unit requires 12 Vdc at 40 mA, and it can be powered through the coaxial cable using a pair of bias-tees or directly with a separate power cable. It is not weatherproof so it must be covered if there is rain during the eclipse. Image ©2015 W. Reeve

Two factors make detecting the quiet Sun during an eclipse somewhat difficult: First, the received flux levels are very low and the reduction as the Moon moves between the Sun and a terrestrial observer will be small even if the observer is on the path of totality. Thus, the radio telescope must have very high sensitivity, which is obtained by using a high-gain antenna and a low noise amplifier at the antenna. Second, a high-gain antenna may have such a narrow beamwidth that it will be required to accurately track the Sun throughout the eclipse. On the other hand, with a sufficiently sensitive radio telescope using a fixed antenna, a drift scan during the eclipse as previously discussed may yield interesting results.

Many existing Callisto stations use a log periodic dipole array (LPDA) to receive relatively strong solar radio bursts from an active Sun. The gains of typical LPDA antennas range from about 6 to 10 dB and are sufficient to detect strong transient solar radio phenomena above a few hundred solar flux units (sfu). However, the gains are not high enough to allow the Callisto to detect the quiet Sun even with a low noise amplifier at the antenna. Therefore, successful observations during the two eclipses will require both an LNA and an antenna with considerably higher gain. The next section discusses the antenna requirements.

Other Callisto stations use the Long Wavelength Array (LWA) Antenna. The sensitivity of the LWA Antenna and Callisto are approximately the same or better than the LPDA mentioned above. The LWA Antenna has a built-in low noise front end at the antenna hub, but its noise figure is 2.7 dB, somewhat higher than many other types of LNAs that are better than 1 dB.

To illustrate the need for high sensitivity, it is instructive to compare the spectral flux density of the quiet Sun to the sensitivity of a basic Callisto connected to a resistance termination at 290 K and a zero gain antenna (figure 9). For most Callisto stations the quiet Sun flux lies well below the received background when Callisto is connected to such an antenna. Above 600 MHz the quiet radio Sun is close to the noise produced by a room temperature resistance termination.

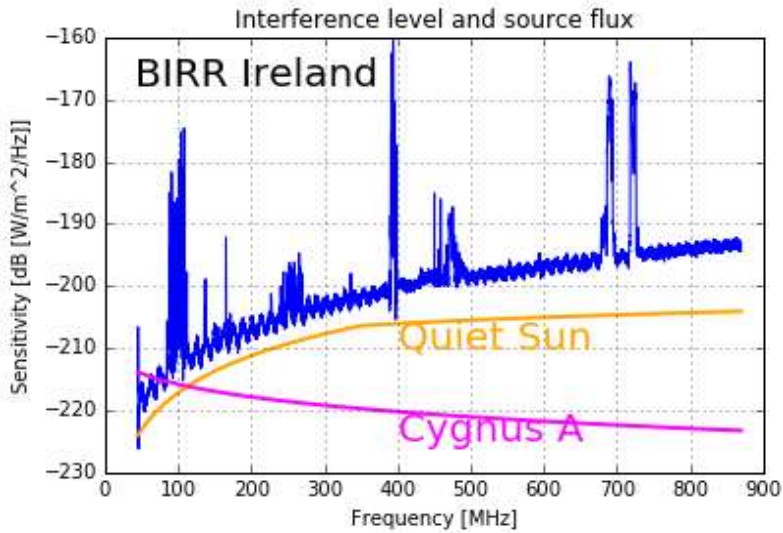


Figure 9 ~ Plot of the expected flux from the quiet radio Sun (orange solid trace) compared to Cygnus A flux (purple solid line) and measured level of rfi (blue solid trace) received by a Callisto and a bicone antenna (essentially a 0 dB gain antenna) at the Birr Observatory in Ireland during a radio frequency interference survey in 2016. This setup did not use an LNA and clearly is unable to detect the quiet Sun. Spikes are transmitters of various types including satellites (particularly around 250 MHz) and broadcast FM and TV stations. Image ©2016 C. Monstein.

7. Antenna Requirements

The antenna requirements for observing the quiet Sun can be determined by considering the system noise as a threshold and then calculating the antenna gain needed to boost the noise produced by the quiet Sun above that threshold. An important ingredient of the system noise calculations is the low noise amplifier noise figure. The calculations below are based on a typical value (1.1 dB) but other noise figures can be substituted.

System noise temperature: The system noise temperature T_{Sys} is the sum of the sky noise temperature T_{Sky} and the receiver system noise temperature T_{Rx} , or

$$T_{Sys} = T_{Sky} + T_{Rx} \text{ K} \quad (1)$$

The sky noise temperature is a composite of all background sources including the ground at the frequency of interest. For purposes here, it is assumed to be 300 K across the frequency range (the galactic radio background at the low end of the Callisto frequency range can be six times higher). The receiver system noise temperature T_{Rx} is

$$T_{Rx} = T_0 \cdot \left(10^{\frac{NF}{10}} - 1 \right) \quad (2)$$

where $T_0 = 290$ K is the reference temperature and NF is the low noise amplifier noise figure in dB. From eq. (2) for an amplifier noise figure of 1.1 dB (the noise figure is assumed flat across the frequency range and the LNA gain is assumed to be high enough to completely determine the system noise figure)

$$T_{Rx} = T_0 \cdot \left(10^{\frac{NF}{10}} - 1 \right) = 290 \cdot \left(10^{\frac{1.1}{10}} - 1 \right) = 83.6 \text{ K (84 K rounded)}$$

and from eq. (1)

$$T_{Sys} = T_{Sky} + T_{Rx} = 300 + 84 = 384 \text{ K}$$

System noise spectral density: The system noise spectral density NSD_{Sys} is determined from

$$NSD_{Sys} = k \cdot T_{Sys} \tag{3}$$

where k is the Boltzmann constant ($k = 1.38 \cdot 10^{-23} \text{ W Hz}^{-1} \text{ K}^{-1}$). Substituting the system noise temperature into eq. (3) gives the noise spectral density of the system noise floor, or

$$NSD_{Sys} = k \cdot T_{Sys} = 1.38 \cdot 10^{-23} \cdot 384 = 5.3 \cdot 10^{-21} \text{ W Hz}^{-1}$$

With a 1 W reference the noise spectral density in dBW Hz⁻¹ is

$$NSD_{Sys} \text{ (dBW / Hz)} = 10 \cdot \log \left(\frac{NSD_{Sys}}{NSD_{Ref}} \right) = 10 \cdot \log \left(\frac{5.3 \cdot 10^{-21}}{1} \right) = -202.8 \text{ dBW Hz}^{-1}$$

Noise spectral density from the antenna: For the quiet Sun to be detected, the antenna output noise spectral density NSD_{Ant} must be higher than the system noise floor. This can be expressed in terms of a margin M in dB such that

$$NSD_{Ant} \text{ (dBW / Hz)} \geq NSD_{Sys} + M \text{ dBW Hz}^{-1} \tag{4}$$

Example 1: Find the noise spectral density at the antenna for emissions that are $M = 5$ dB above the system noise floor. Assume the LNA noise figure is 1.1 dB.

Solution: Using eq. (4), the input to the low noise amplifier from the antenna (assuming zero loss in the connection) needs to be

$$NSD_{Ant} \text{ (dBW / Hz)} \geq -202.8 + 5 = -197.8 \text{ dBW Hz}^{-1}$$

As a linear ratio, the required input noise spectral density from the quiet Sun for this example is

$$NSD_{Ant} = 10^{\left(\frac{NSD_{Ant} \text{ (dBW/Hz)}}{10} \right)} \geq 10^{\left(\frac{-197.8}{10} \right)} = 1.7 \cdot 10^{-20} \text{ W Hz}^{-1}$$

The required noise spectral density at the antenna is related to the quiet Sun spectral flux density S_{Quiet} and antenna effective area A_{Eff} by

$$NSD_{Ant} = \frac{S_{Quiet} \cdot A_{Eff}}{2} \text{ W Hz}^{-1} \quad (5)$$

where S_{Quiet} is the spectral flux density of the quiet Sun at the frequency of interest in $\text{W m}^{-2} \text{ Hz}^{-1}$ and A_{Eff} is the antenna effective area in m^2 . The divisor 2 takes into account that a linear polarized antenna captures only one-half the total flux from a randomly polarized radio source.

Solving eq. (5) for the antenna effective area gives

$$A_{Eff} = \frac{2 \cdot NSD_{Ant}}{S_{Quiet}} \quad (6)$$

Antenna gain: The antenna gain G with respect to an isotropic antenna is related to the antenna effective area and wavelength by

$$G = A_{Eff} \cdot \frac{4 \cdot \pi}{\lambda^2} \quad (7)$$

where the antenna gain is a linear ratio. The wavelength is related to the frequency by

$$\lambda = \frac{c}{f} \quad (8)$$

where c is the speed of light ($3 \cdot 10^8 \text{ m s}^{-1}$) and f is the frequency in Hz. The antenna effective area is related to its physical aperture area A_{Phys} by

$$A_{Eff} = \eta \cdot A_{Phys} \quad (9)$$

where η is the aperture efficiency (for ordinary parabolic dish antennas η is typically 0.5 to 0.55).

Substituting eq. (6) in (7) and simplifying gives the required antenna gain in terms of the system noise spectral density, quiet Sun spectral flux density and wavelength, as in

$$G = \frac{8 \cdot \pi \cdot NSD_{Ant}}{S_{Quiet} \cdot \lambda^2} \quad (10)$$

Example 2: Find the antenna gain required to detect the quiet Sun at 200 MHz with a 5 dB margin.

Solution: From eq. (8), the wavelength at 200 MHz is

$$\lambda = \frac{c}{f} = \frac{3 \cdot 10^8}{200 \cdot 10^6} = 1.5 \text{ m}$$

From table 1, the spectral flux density of the quiet Sun S_{Quiet} at 200 MHz is 8.1 sfu or $8.1 \cdot 10^{-22} \text{ W m}^{-2} \text{ Hz}^{-1}$. The required antenna noise spectral density for margin $M = 5 \text{ dB}$ from Example 1 is $1.7 \cdot 10^{-20} \text{ W Hz}^{-1}$. Substituting values for the wavelength, quiet Sun spectral flux density and required antenna noise spectral density into equation (10) gives

$$G = \frac{8 \cdot \pi \cdot NSD_{Ant}}{S_{Quiet} \cdot \lambda^2} = \frac{8 \cdot \pi \cdot 1.7 \cdot 10^{-20}}{8.1 \cdot 10^{-22} \cdot 1.5^2} = 234.4$$

The gain in dB with respect to an isotropic antenna is

$$G(\text{dB}) = 10 \cdot \log(G) = 10 \cdot \log(234.4) = 23.7 \text{ dBi}$$

A higher or lower margin requires a higher or lower antenna gain; however, when expressed in dB the two are not exactly proportional. In the example above, increasing M by 1 dB from 5 to 6 dB increases the required noise spectral density from $1.7 \cdot 10^{-20}$ to $2.1 \cdot 10^{-20} \text{ W Hz}^{-1}$. The required antenna gain as a linear ratio is increased from 234.4 to 288.1, corresponding to 24.6 dBi, an increase of 0.9 dB. Similar calculations for a 1 dB decrease in the margin show that the required antenna gain is decreased by 1.1 dB from 23.7 to 22.6 dBi.

Antenna beamwidth: The high gain antennas required to receive the quiet Sun have narrow beamwidths compared to ordinary dipole and LPDA antennas and will require tracking the Sun during the eclipse. The half-power beamwidths (HPBW) can be determined from the antenna directivity. Directivity is a calculated parameter similar to gain whereas gain is a measured parameter that includes antenna losses and is always smaller than directivity. The ratio of gain to directivity is the *antenna efficiency factor* k_{Ant} .

For an antenna with minor lobes (side lobes and back lobes found on all practical antennas) and non-ideal radiation patterns, the directivity D , from [Kraus], is

$$D \approx \frac{41000 \cdot \epsilon_M}{k_p \cdot \theta_{HP}^\circ \cdot \phi_{HP}^\circ} \quad (11)$$

where

ϵ_M beam efficiency, 0.6 to 0.9 for large antennas

k_p pattern factor, 1.0 for uniform field distribution, between 0 and 1 otherwise

- θ_{HP}° half-power beamwidth in θ plane (for example, E-plane) ($^\circ$)
- ϕ_{HP}° half-power beamwidth in ϕ plane (for example, H-plane) ($^\circ$)

Assuming the antenna efficiency factor k_{Ant} is close to 1, the pattern is uniform and symmetrical in any plane ($\theta_{HP}^\circ = \phi_{HP}^\circ$) and the beam efficiency is in the mid-range, eq. (11) reduces to

$$G \approx \frac{30750}{(\theta_{HP}^\circ)^2} \tag{12}$$

Solving for θ_{HP}° gives a reasonable estimate of the HPBW, or

$$\theta_{HP}^\circ \approx \left(\frac{30750}{G} \right)^{\frac{1}{2}} \tag{13}$$

Example 3: Estimate the half-power beamwidth for the antenna in Example 2.

Solution: The gain previously determined is 234.4 or 23.7 dB. The beamwidth calculation requires the gain as a linear ratio. From eq. (13)

$$\theta_{HP}^\circ \approx \left(\frac{30750}{G} \right)^{\frac{1}{2}} = \left(\frac{30750}{234.4} \right)^{\frac{1}{2}} = 11.5^\circ$$

Calculations for gain and beamwidth can be made for various spot frequencies previously given for the quiet Sun and summarized (table 2).

Table 2 ~ Antenna gains required for detecting the quiet Sun with 5 dB margin and corresponding half-power beamwidths. Quiet Sun data is from table 1. LNA noise figure = 1.1 dB, zero loss between the antenna and LNA.

Frequency (MHz)	Wavelength (m)	S _{Quiet} (sfu)	S _{Quiet} (W m ⁻² Hz ⁻¹)	Gain (dBi)	Gain (linear)	HPBW ($^\circ$)
50	6	0.54	0.54 · 10 ⁻²²	23.4	219.8	11.8
100	3	2.4	2.4 · 10 ⁻²²	23.0	197.8	12.5
150	2	5.1	5.1 · 10 ⁻²²	23.2	209.4	12.1
200	1.5	8.1	8.1 · 10 ⁻²²	23.7	234.4	11.5
300	1	14.9	14.9 · 10 ⁻²²	24.6	286.8	10.4
400	0.75	21.7	21.7 · 10 ⁻²²	25.4	350.0	9.4
600	0.5	32.1	32.1 · 10 ⁻²²	27.3	532.4	7.6
1000	0.3	41.3	41.3 · 10 ⁻²²	30.6	1149.5	5.2
10000	0.03	275	275 · 10 ⁻²²	42.4	17263	1.3

The required gains can be achieved in a number of ways. For example, a stacked array of multi-element Yagi antennas or a parabolic dish antenna may be used (figure 10). Yagi antenna bandwidth is only about 5% of the center frequency and stacking in an array increases the gain but usually reduces the bandwidth. An alternative with a bandwidth in the range of 50% of the center frequency is a stacked array of helical antennas (more specifically, monofilar, axial mode helical antennas). Detailed information on helical antennas can be found at [Kraus]. Both Yagi and helical antennas can be used as feeds on parabolic dish reflector antennas.



Figure 10 ~ 5m parabolic dish at radio astronomy facility of ETH Zurich in Bleien. Box behind feed contains band pass filters and a low noise amplifier. While tracking the Sun, the entire antenna rotates in azimuth and in elevation controlled by a standard Windows computer. The estimated gain of is 45 dBi in L-band. Tower carrying the dish is a spotlight structure from WW-II. The shade of the focal plane unit in the dish center proves that the dish is tracking the sun. This dish antenna was used to produce the light-curve plot, shown in figure 15. Image courtesy of C. Monstein.

The physical area of a parabolic dish antenna is

$$A_{phys} = \frac{\pi \cdot d^2}{4} \tag{14}$$

where d is the dish diameter. Using eq. (9) and assuming the aperture efficiency $\eta = 0.55$, the effective area of a parabolic dish antenna is

$$A_{eff} = \eta \cdot A_{phys} = 0.55 \cdot \frac{\pi \cdot d^2}{4} \tag{15}$$

Substituting eq. (15) in eq. (7) gives the gain in terms of the dish diameter and wavelength, or

$$G = \eta \cdot \frac{\pi \cdot d^2}{4} \cdot \frac{4 \cdot \pi}{\lambda^2} = \eta \cdot \frac{\pi^2 \cdot d^2}{\lambda^2} \tag{16}$$

Solving for the diameter d gives

$$d = \frac{\lambda}{\pi} \left(\frac{G}{\eta} \right)^{\frac{1}{2}} \quad (17)$$

Assuming $\eta = 0.55$,

$$d = 1.35 \cdot \frac{\lambda}{\pi} G^{\frac{1}{2}} = 0.43 \cdot \lambda \cdot G^{\frac{1}{2}} \quad (18)$$

Example 4: Determine the diameter of a parabolic dish antenna that provides the gain found in Example 2.

Solution: The required gain was found to be 23.7 dBi or linear ratio 234.4 for a wavelength of 1.5 m. Substituting these values in eq. (18) gives

$$d = 1.35 \cdot \frac{1.5}{\pi} 234.4^{\frac{1}{2}} = 9.9 \text{ m}$$

It is noted that this size of parabolic dish antenna usually is found only in professional observatories, although it is known that at least one amateur radio observatory has an antenna at least as large [{Astropeiler}](#).

Combining eq. (13) and (16), the beamwidth of a parabolic dish antenna in terms of its diameter and wavelength is approximately

$$\theta_{HP}^{\circ} \approx \frac{\lambda}{d} \left(\frac{30750}{\eta \cdot \pi^2} \right)^{\frac{1}{2}} \quad (19)$$

Assuming $\eta = 0.55$,

$$\theta_{HP}^{\circ} \approx 75.3 \frac{\lambda}{d} \quad (20)$$

The above calculations concerning parabolic dish antennas assume that all incoming flux is reflected toward and captured by their associated feed antennas. Antenna design is beyond the scope of this paper; readers are referred to [Kraus] and other antenna engineering books and online resources.

8. Ku Band Down-Converter for X-Band Observations

In this section we discuss using a low-cost Ku-band dish antenna and associated low noise block converter (LNB) designed for satellite television reception with Callisto to observe the solar eclipse. These can provide an inexpensive alternative to constructing an antenna array or large parabolic reflector antenna. The actual observation frequency will be closer to about 10.6 GHz (X-band), which will be down-converted by the LNB to the Callisto native frequency range. The advantage of using Callisto with this setup is its reliability, consistency and data collection and processing capability. The technical requirements are not critical but a bias-tee (also called *power inserter* or *power injector* in the satellite television industry) will be needed to power the LNB (figure 11).

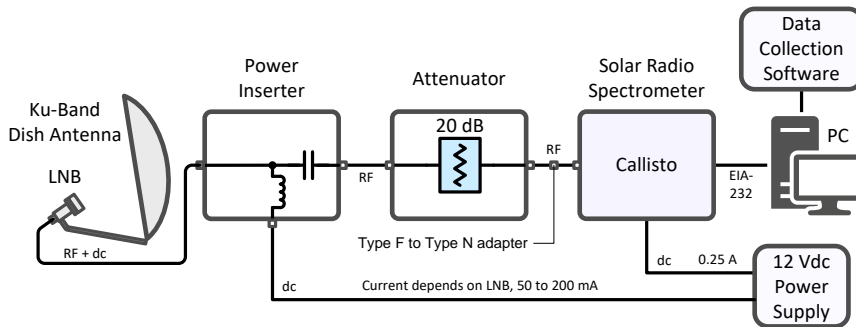


Figure 11 ~ Block diagram for observing at X-band using a Ku-band dish antenna, LNB and Callisto. An attenuator is optional to minimize receiver input overload. All coaxial cabling from the LNB to Callisto uses RG-6 (or equivalent) with type F connectors. A type F to type N adapter connects to the Callisto.

Example 5: Determine the diameter of a parabolic dish antenna that provides a 5 dB margin for detecting quiet Sun radio emissions at 10 GHz.

Solution: Table 2 shows that the necessary gain at 10 GHz is 42.4 dBi or 17 263 and the wavelength is 0.03 m. Substituting these values in eq. (18) gives

$$d = 1.35 \cdot \frac{0.03}{\pi} 17263^{\frac{1}{2}} = 1.7 \text{ m}$$

It is noted that a common commercial dish size is 1.65 m. A larger dish will provide a more pronounced Y-factor (ratio of Sun noise temperature-to-Sky noise temperature) and improve the detection margin as the Sun's flux is reduced during the eclipse.

Example 6: Determine the aperture efficiency, antenna noise temperature and half-power beamwidth at 10 GHz for an inexpensive 18 in diameter offset feed dish antenna (figure 12). The manufacturer's claim is its effective aperture is 18.1 in (46 cm).



Figure 12 ~ Inexpensive 46 cm diameter offset feed dish antenna and LNB originally designed for satellite television

Solution: The actual measured dimensions of this antenna from edge-to-edge are 18.25 W x 20.0 H in (46.4 W x 50.8 H cm). Assuming the antenna shape is an ellipse, its physical area

is $\pi \cdot \frac{W \cdot H}{4} = 287 \text{ in}^2$ (0.185 m²). Also, assuming the

manufacturer's claim applies to a circular aperture, the

aperture area is $\pi \cdot \frac{d^2}{4} = 257 \text{ in}^2$ (0.166 m²) and the aperture

efficiency $\eta = \frac{A_{\text{Eff}}}{A_{\text{Phys}}} = \frac{257}{287} = 0.9$ (this seems to be overstated by a factor of 2).

From table 1 (or table 2) the spectral flux density from the quiet Sun at 10 GHz is 275 sfu or, equivalently, 275 · 10⁻²² W m⁻² Hz⁻¹. Based on the effective area previously calculated, the noise spectral density at the antenna from eq. (5) is

$$NSD_{\text{Ant}} = \frac{S_{\text{Quiet}} \cdot A_{\text{Eff}}}{2} = \frac{275 \cdot 10^{-22} \cdot 0.166}{2} = 2.28 \cdot 10^{-21} \text{ W Hz}^{-1}$$

The antenna noise temperature T_{Ant} is related to the antenna noise spectral density by the Boltzmann constant k , or

$$NSD_{\text{Ant}} = k \cdot T_{\text{Ant}}$$

Therefore, the antenna noise temperature is

$$T_{\text{Ant}} = \frac{NSD_{\text{Ant}}}{k} = \frac{2.28 \cdot 10^{-21}}{1.38 \cdot 10^{-23}} = 165 \text{ K}$$

Because this calculation is traceable to the manufacturer's claim of the antenna's effective aperture, the antenna temperature may be overstated. Assuming the aperture efficiency is as the manufacturer claims ($\eta = 0.9$), from eq. (19) the HPBW of the antenna is approximately

$$\theta_{\text{HP}}^{\circ} \approx \frac{\lambda}{d} \left(\frac{30750}{\eta \cdot \pi^2} \right)^{\frac{1}{2}} = \frac{0.03}{0.46} \left(\frac{30750}{0.9 \cdot \pi^2} \right)^{\frac{1}{2}} = 3.8^{\circ}$$

Based on the specification of a standard commercial wideband LNB with 10.41 GHz local oscillator frequency, the LNB intermediate frequency (IF) ranges from (10.7 – 10.41 GHz =) 290 MHz to (11.28 GHz – 10.41 GHz =) 870 MHz. However, there is hardly any bandpass filtering in either the RF or IF paths of the LNB, so observations are possible below the low band frequency (figure 13). This unadvertised but free feature allows us to use Callisto as a down-converter spectrometer to observe the X-band (X-band is 7 to 11.2 GHz for NATO or 8 to 12.0 GHz according to IEEE). The usable observation bandwidth is limited by Callisto’s maximum frequency to about 580 MHz. Taking into account the LNB’s high sensitivity and IF output within Callisto’s frequency range, we can define the received frequency range as $F_{min} = 10.6$ GHz to $F_{max} = 10.72$ GHz.

The corresponding observation parameters are:

- ⊗ RF input frequency range: 10 600 MHz to 10 720 MHz
- ⊗ IF output frequency range: 290 to 870 MHz
- ⊗ Callisto channelization: 200 channels
- ⊗ Callisto frequency resolution: 2.9 MHz (580 MHz/200 channels)
- ⊗ Callisto detection bandwidth: 300 kHz
- ⊗ Callisto time resolution: 0.25 s
- ⊗ Callisto integration time: 1 ms
- ⊗ Duration of observation: 3 h

The Callisto frequency file can be setup with light curve integration assigned on channels 10 to 199 (channels 1 to 9 are not used to avoid the redundant channels always placed at the beginning of the frequency file; refer to the Callisto Software Setup Guide {[CallistoSSG](#) for more information}. For this situation, the usable observational bandwidth is 190 used channels x 2.9 MHz frequency resolution = 163.9 MHz, and the radiometric bandwidth is 149 used channels x 300 kHz detection bandwidth = 44.7 MHz. For a quiet Sun flux of about 275 sfu we may expect an antenna temperature on the order of 40 K.

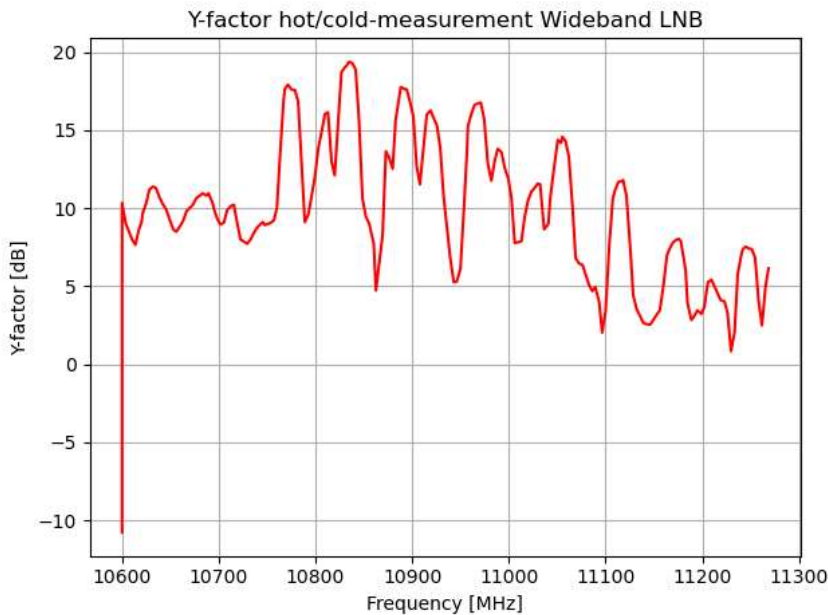


Figure 13 ~ Plot of the band pass characteristic and Y-factor of a wideband Ku-band LNB. Interestingly the LNB is most sensitive around 10.65 GHz below the regular band. Observations were performed with a hot/cold measurement. Hot while pointing to the sun and cold while pointing to the sky. Above 10.75 GHz we can see many satellite downlink transponders signals (TV), therefore we can only use frequencies below 10.75 GHz for radio astronomy.

There are three advantages to using an inexpensive LNB. First, is its very low cost (< 50 USD). Second, the noise figure of modern LNBs is less than 0.5 dB. The corresponding noise temperature is about 35 K, which is lower than the expected antenna noise temperature from the quiet Sun. Third, there is very little radio frequency interference (RFI) in the X-band and the observed spectrum is extremely clean, which allows undisturbed solar radio observations. From experience we do not expect high dynamic solar radio spectra in this frequency range, although some synchrotron radiation is remotely possible.

Unfortunately, there are negative aspects in such an observation concept. The satellite dish, providing a small beam angle on the order of a few degrees as determined from eq. (19) requires constant tracking of the Sun during the whole observation from sunrise to sunset. Without tracking, we will observe strong variations in the signal due to the convolution of the antenna beam pattern and the moving solar disc, and these are indistinguishable from the signal drop due to the eclipse itself. A way to avoid this is to use an existing optical telescope with a computer that allows tracking the Sun, and to replace the optics with a small satellite dish and LNB combination.

Most modern inexpensive Ku-band satellite dishes are offset feed dishes, which make the alignment difficult. Offset angles are typically 17 to 24° (figure 14). A dish with a central axis (prime focus) feed is of great advantage because alignment is much simpler. In any case, an alignment is required a few days before the eclipse to ensure that the dish is correctly pointing to the Sun. The easiest way to adjust the offset dish is to move the antenna so that the LNB horn (the part closest to the antenna) casts a shadow at the edge of the antenna next to the LNB mounting arm. Another method involves using double-sided tape to attach a small mirror to the center of the dish and adjusting the antenna until the Sun's reflection shines on the LNB horn (remove the mirror when done). The central axis dish is adjusted so the LNB casts a shadow at the center of the dish. Of course, the shadow method works only when the Sun is visible. Once adjusted just start the solar tracker for the coming eclipse day.

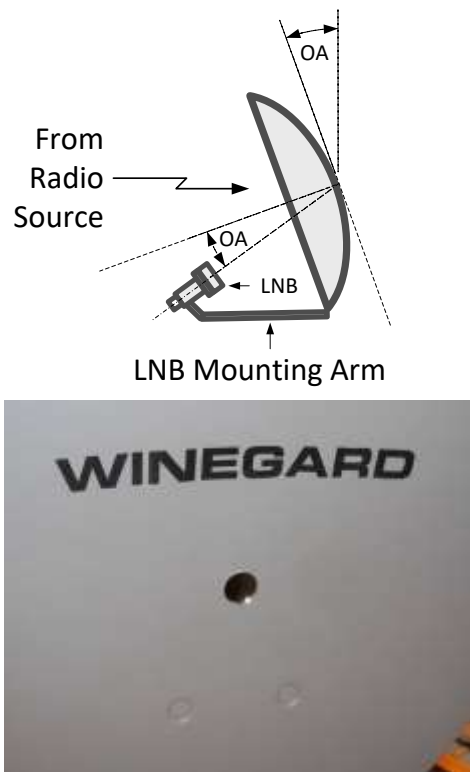


Figure 14 ~ Offset feed dish antenna. Left: Typical offset angles OA are 17 to 24°. Right: One method to align the antenna on a sunny day is to tape a small mirror to the dish center and then adjust the antenna so the Sun's reflection shines on the center of the LNB. A 25 mm diameter mirror from a local craft store is shown in this image attached to the center of a Winegard 46 cm dish.

Another difficulty is that inexpensive LNBS are sensitive to temperature and considerable drift can be expected if exposed to direct sunlight during observations. This can be at least partially mitigated by using a Sun shade on the LNB that is transparent to microwaves but this considerably complicates setting up. The least temperature disturbance can be expected on a cloudy day in which there is no direct sunlight on the LNB but this prevents alignment using the shadow method.

In spite of the above difficulties, a system composed of a satellite dish, LNB, Bias-T and Callisto is a quite convenient and attractive spectrometer to observe the quiet Sun and to estimate solar radio flux at microwave frequencies. It also is an easy way to observe the signal drop due to the eclipse. Afterwards, the data can be calibrated in solar flux units (sfu) (figure 15) by taking into account the solar radio flux published by NOAA, SWS [{Learmonth}](#) and others for the period. Observers considering this setup should look at the documents available for the Very Small Radio Telescope (VSRT) at [{Haystack}](#).

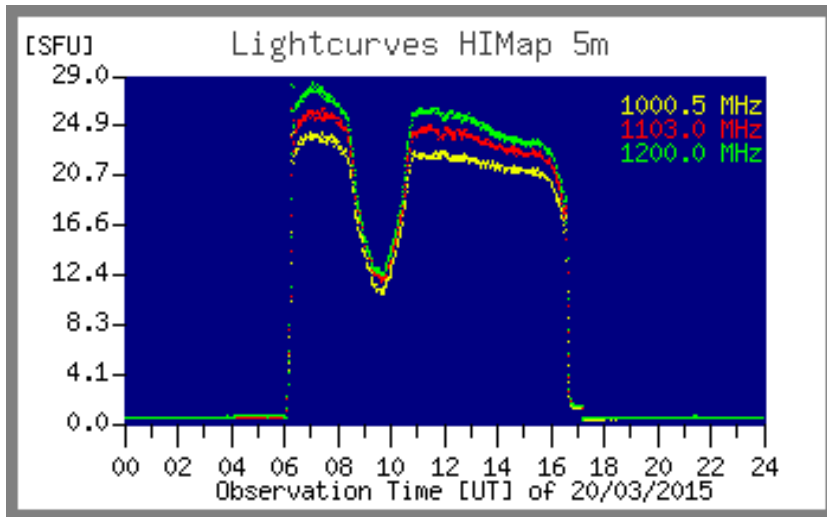


Figure 15 ~ Plot of an European eclipse on 20 March 2015, observed with a 5 m dish, tracking the Sun from Sunrise at around 06 UT until Sunset at 16:45 UT. The eclipse started around 08:30 with maximum obscuration at 09:30 and finished at 11:00. Calibration was performed based on reference values of the quiet Sun. Backend instrument was a Callisto frequency agile spectrometer, connected to a heterodyne converter which shifts 1-2 GHz down to 0-1GHz. For more details, see [Monstein]. We may expect a similar plot in X- or Ku-band performed with a ~60 cm satellite dish.

9. Scintillation Observations

This section briefly describes observations of satellite signals in the 250 MHz range to determine eclipse effects, if any, on radio wave scintillation. Additional information on scintillation can be found at [{SWS}](#).

Scintillation Effects: Scintillation is a random fluctuation in the intensity of celestial radio waves and satellite downlink signals on the time scale of a few seconds produced by ionospheric irregularities. Scintillation causes the familiar twinkling of visible light from stars and can be particularly detrimental at radio frequencies below a few gigahertz. A large amount of work has been done studying scintillation effects at L-band (1 to 2 GHz) on the accuracy of global navigation satellite systems (GNSS) such as the Global Positioning System (GPS). Signals from other satellites and spacecraft are affected as well. In the field of radio astronomy, scintillation can introduce undesired variations in the measurements of celestial radio objects.

Scintillation effects are broadly classified as refraction and diffraction. Both originate in the group delay and phase advance that a radio wave experiences as it interacts with free electrons along its transmission path through the ionosphere. The following discussion will focus on satellite signals because they are easily received by Callisto with an ordinary antenna and preamplifier.

The number of free electrons is usually expressed as *total electron content* (TEC), which is the number of free electrons in a rectangular solid with a one square meter cross-sectional area extending from the receiver to the satellite. Given by physics, the product of the group velocity and phase velocity of the satellite signals is equal to the speed of light squared. If the TEC increases, the signal's group velocity decreases and its phase velocity

The Total Electron Content (TEC) is the total number of electrons present along a path between a radio transmitter and receiver. Radio waves are affected by the presence of electrons. The more electrons in the path of the radio wave, the more the radio signal will be affected. TEC is a good parameter to monitor for possible space weather effects.

increases to keep their product a constant. A slower group velocity produces ranging errors in GPS systems while a faster phase velocity causes unexpected phase shifts. If the phase shifts are rapid enough, they can overwhelm the tracking loops in GPS receivers' phase-lock loops. Variations in group delay and phase advance caused by large-scale variations in electron density are defined as signal refraction.

Scintillation through signal diffraction is more complicated. When ionospheric irregularities form at scale lengths of a few hundred meters, they begin to scatter satellite signals causing the radio wave to follow multiple paths to the receiver. The signals on each path will add or subtract in phase, causing fluctuations in the signal amplitude and phase. The same process occurs with light and can be seen in the fuzzy image passing through jet exhaust from an airliner. Diffractive scintillation can seriously challenge GPS receivers, causing signal power fades exceeding several dB and fast phase variations.

The upcoming total solar eclipse will not affect all regions of the earth equally, and the physics behind the space weather in different regions can be dramatically different. The change in density and thickness of the ionosphere during the eclipse could potentially change radio waves traversing the ionosphere along the path of the shadow to a receiver.

Scintillation is quantified by an S4 index defined by

$$S4 = \sqrt{\frac{\langle I^2 \rangle - \langle I \rangle^2}{\langle I \rangle^2}} \quad (21)$$

where I is the signal intensity and the brackets ' $\langle \rangle$ ' denote time averages.

The S4-index can vary from 0 to 1.0 and is typically estimated over an interval of 60 seconds. The index can be considered weak or strong, roughly corresponding to the amount of scattering in the ionosphere. Strong scintillation corresponds to $S4 > 0.6$ and weak scintillation is $S4 < 0.6$. It has been determined that $S4 < 0.3$ is unlikely to have a significant effect on GPS signals.

A Python script [{S4FITS}](#) has been made available to perform the S4-index calculations from the FITS files produced by the Callisto spectrometer. For a moving satellite such as GPS or Iridium the calculations are applied over a time period of typically 5 to 10 s while for geostationary satellites the period can extend up to 60 seconds. The latter corresponds to a few hundred samples (480 samples at 100 channels/sweep or 240 samples at 200 channels/sweep; note: 1 sweep requires 0.25 s) per S4-index based on a Callisto system. We will concentrate on geostationary satellites because no tracking mechanism is needed, and the frequencies fall within the Callisto frequency range. The S4-index will be plotted with respect to the elapsed time of observation.

Observing scintillation: Observing signals in the upper-VHF band from geostationary satellites provides a significant advantage over celestial emissions because the spectral flux density of the satellite signals is much higher at about $-190 \text{ dBW m}^2 \text{ Hz}^{-1}$. The high received power levels allow the use of relatively small and cheap antennas fixed in sky-position (azimuth and elevation) while pointing to the geostationary path of the desired

satellites. In addition to a 'normal' sensitivity receiver like Callisto, a standard low noise amplifier (LNA) is recommended between the antenna and Callisto to provide an adequate system noise figure. Of course, other receivers can be used for this experiment in a single frequency or single channel mode, but the Python script provided is based on reading FITS files.



Figure 16 ~ Log periodic dipole array antenna (LPDA) mounted on a mast with a rotator and low noise amplifier. The 21-element Creative Design CLP5130-1N antenna frequency range is 50 to 1300 MHz and its free space gain is 6 to 8 dB. This antenna installation has a fixed elevation but can be turned to any hour angle with the rotator. The low noise amplifier has a noise figure of about 1.0 dB and a gain of about 20 dB. Setup at University of Glasgow, UK. Image ©2012 C. Monstein.

For receiving satellite signals we can use a simple Yagi antenna or a logarithmic periodic dipole array, LPDA (figure 16) fixed in azimuth and elevation and pointing to the geostationary satellite path over Earth's equator. An example is provided below. The azimuth and elevation will need to be separately determined for each location along the path of the eclipse. An online tool to find these angles can be found at [{GeoSat1}](#) and [{GeoSat2}](#). Also, we provide a Python script [{GeoAzEl}](#) for calculating the necessary parameters for military satellites over North America. Each observer should try to choose a satellite near their local meridian.

It should be possible to observe downlinks in the frequency range 240 MHz to 270 MHz from UFO-*, Skynet, Fltsatcom, Sicral, ComsatBW and Milstar satellites. For example, see [{UHFSatNA}](#) for a list of satellites and their approximate longitudes that may be observable over North America. For a more comprehensive list of satellites worldwide see [{UHFSat}](#).

Example 7: Suppose we would like to detect the satellite signals with a 5 dB signal-to-noise ratio (equivalent to a 5 dB margin used in the example quiet Sun calculations shown previously). The noise figure of our low noise amplifier is 1.1 dB, as before. Find the required antenna gain.

Solution: The system noise spectral density was previously found in section 7 to be -202.8 dBW Hz $^{-1}$ and to provide a 5 dB margin, the required antenna spectral density was -197.8 dBW Hz $^{-1}$. In linear terms

$$NSD_{Ant} = 10^{\left(\frac{NSD_{Ant}(dB)}{10}\right)} \geq 10^{\left(\frac{-197.8}{10}\right)} = 1.7 \cdot 10^{-20} \text{ W Hz}^{-1}$$

The estimated received spectral flux density from the satellites is $S_{Sat} = -190$ dBW m 2 Hz $^{-1}$ or in linear terms

$$S_{Sat} = 10^{\frac{S_{Sat}(dB)}{10}} = 10^{\frac{-190}{10}} = 1.0 \cdot 10^{-19} \text{ W m}^2 \text{ Hz}^{-1}$$

From equation (6), the required antenna effective area is

$$A_{Eff} = \frac{2 \cdot NSD_{Ant}}{S_{Sat}} = \frac{2 \cdot 1.7 \cdot 10^{-20}}{1.0 \cdot 10^{-19}} = 0.340 \text{ m}^2$$

For a mid-range frequency of 255 MHz, the wavelength from equation (8) is

$$\lambda = \frac{c}{f} = \frac{3 \cdot 10^8}{255 \cdot 10^6} = 1.18 \text{ m}$$

From equation (7), the antenna gain in terms of its effective area and wavelength is

$$G = A_{Eff} \cdot \frac{4 \cdot \pi}{\lambda^2} = 0.340 \cdot \frac{4 \cdot \pi}{(1.18)^2} = 3.09$$

As a logarithmic ratio in dB with respect to an isotropic antenna, the required gain is

$$G(dB) = 10 \cdot \log(G) = 10 \cdot \log(3.09) = 4.9 \text{ dBi}$$

Thus, with the assumptions given above, we find the antenna requirements are quite modest and can be easily fulfilled with almost any Yagi or log periodic antenna.

The scanning strategy for these satellites can use a Callisto frequency configuration file with 100 channels. In this case, each channel would cover $(270 - 240) \text{ MHz} / 100 \text{ channels} = 0.3 \text{ MHz}$, which equals the radiometric bandwidth of the Callisto radio spectrometer. Such a strategy will ensure we do not miss any transmission channels from the observed satellites.

For comparison purposes, Callisto should be setup to observe before and after the eclipse using a similar routine as described for observing the solar emissions in section 4. After the FITS files are saved and post-processed by the above-mentioned {S4FITS} Python script the S4 scintillation index is plotted versus time for any channel in the above frequency range. While we expect a change in the S4-index during the eclipse, it is yet to be proven to what extent the change will be.

10. Conclusions

The total solar eclipse on 8 April 2024 provides a great opportunity for solar radio observations in the VHF and UHF bands using the Callisto instrument. As the Moon's shadow crosses the United States it will block radio emissions from the quiet Sun. Callisto stations will need to add a low noise amplifier, if not already equipped, and upgrade their antennas to detect the quiet Sun. Two inexpensive alternative observations also are discussed, one to use a dish antenna and LNB designed for satellite television reception to observe the quiet Sun and another to observe geostationary satellite transmissions in the upper-VHF band and determine changes, if any, in the S4 scintillation index during the eclipse. To be most successful observers should start planning and rehearsing now for the event.

11. Weblinks and References

- {Astropeiler} <https://astropeiler.de/>
- {Callisto} <http://www.reeve.com/Solar/e-CALLISTO/e-callisto.htm>
- {CallistoSSG} <http://www.reeve.com/Documents/CALLISTO/CALLISTOSoftwareSetup.pdf>
- {eCallisto} <https://www.e-callisto.org/>
- {GE-Eclipse} http://xjubier.free.fr/en/site_pages/solar_eclipses/TSE_2017_GoogleMapFull.html
- {GeoAzEl} <https://e-callisto.org/Software/GeoAzEl.py>
- {GeoSat1} <http://www.csgnetwork.com/geosatposcalc.html>
- {GeoSat2} <http://www.dishpointer.com/>
- {Haystack} <http://www.haystack.edu/edu/pcr/vsrt-ret/index.html>
- {Learmonth} <http://www.sws.bom.gov.au/Solar/3/4>
- {MICA} <http://aa.usno.navy.mil/software/mica/micainfo.php>
- {NASA} <http://eclipse.gsfc.nasa.gov/SEgoogle/SEgoogle2001/SE2017Aug21Tgoogle.html>
- {NOAA} <https://www.esrl.noaa.gov/gmd/grad/solcalc/>
- {Path} <https://eclipse.gsfc.nasa.gov/SEpath/SEpath2001/SE2017Aug21Tpath.html>
- {Solar} <http://www.timeanddate.com/eclipse/list.html%3Fstarty%3D1950>
- {S4FITS} <https://e-callisto.org/Software/S4FITS.zip>

{SWS} <http://www.sws.bom.gov.au/Satellite/6/3>
{UHFSat} <http://www.uhf-satcom.com/uhf/>
{UHFSatNA} <http://www.crypto.com/misc/uhf-sats/>

[Benz] Benz, A., Chapt. 4.1.1.6 Radio Emission of the Quiet Sun, Solar System, Springer, DOI: 10.1007/978-3-540-88055-4_5, 2009
[Kraus] Kraus, J., Antennas, 2nd Ed., McGraw-Hill Inc., 1988
[Kundu] Kundu, M., Solar Radio Astronomy, John Wiley & Sons, 1965
[Monstein] Monstein, C., European Solar Eclipse Observed by Radio Waves, *Radio Astronomy*, March- April 2015, pages 21-27
[ReeveLNA} Reeve, W., Packaging a Low Noise RF Amplifier Module, *Radio Astronomy*, September-October 2015
[Smerd] Smerd, S., Radio-Frequency Radiations from the Quiet Sun, Australian Journal of Scientific Research A, vol. 3, p.34, 1950 (available at: <http://adsabs.harvard.edu/full/1950AuSRA...3...34S>)

Catalogue of the brightest astrophysical maser sources

Eduard Mol

Updated 6-3-2023

This document lists the properties of the strongest maser sources, which may be of interest to amateur radio astronomers. The data is collected from the publicly available maser database MaserDB [1] using the objects search tool, except where noted otherwise. The lists are limited to masers with minimum flux densities >200 Jy. For water masers a minimum flux cutoff of 500 Jy was used, because atmospheric noise and attenuation are significantly higher at 22.2 GHz. Objects with only one observation listed in MaserDB were also excluded.

1612 MHz OH masers (circumstellar)

Table 1: 1612 MHz OH masers around OH/IR stars

Note: because circumstellar OH masers typically have a distinct double-peaked spectrum with blue- and redshifted peaks, velocities and fluxes for both the blueshifted and the redshifted peaks of each source are listed.

Name	RA	DEC	V blue (km/s)	V red (km/s)	Period (d)	Fmax blue (Jy)	Fmax red (Jy)	Fmin blue (Jy)	Fmin red (Jy)	Fmean blue (Jy)	Fmean red (Jy)
NML Cygni	20 46 25.540	+40 06 59.40	-24.1	21.8	*	1920	328	500	97.8	1.002	198.6
VY Canis Majoris	07 22 59.1	-25 46 08	-4	45	*	1283	426	200	100	593.11	215.6

sources: Database of Circumstellar Masers [2], except the period column. Period data is from the Nancay 1612 MHz OH/IR star monitoring program (NRT) [3] and AAVSO Variable Star Index (VSX) [4]

*These stars have no particular variation or period according to the NRT monitoring program or the VSX database. **No periodicity information available for this star

Explanation of columns

Table 1

Name: name of OH/IR star

RA: right ascension

DEC: declination

V blue: velocity blueshifted peak, in km/s (Vlsr)

V red: velocity redshifted peak, in km/s (Vlsr)

Period: If the star has a known periodic brightness variation, the period is listed here in days.

Fmax blue: maximum peak flux density blueshifted peak in Jansky (Jy)

Fmax red: maximum flux density redshifted peak in Jy

Fmin blue: minimum flux density blueshifted peak in Jy

Fmin red: minimum flux density redshifted peak

Fmean blue: averaged flux density blueshifted peak

Fmean red: averaged flux density redshifted peak

6, 7 GHz methanol masers

G#	Source name	RA	DEC	Vmean (km/s)	Fpeak (Jy)	Fmin (Jy)	Vi	Nobs	type
G9.6208+0.1951	009.619+0.193	271.5617	-20.5257	1.69	5196	65	79.938	8	SFR
G323.7401- 0.2628	15278-5620	232.9396	-56.5139	-49.8	3450	2860	1.206	4	MIXED
G323.7400- 0.2544	323.77-0.213	232.9308	-56.5073	-48.54	2721	977.17	2.785	2	SFR
G81.8775+0.7820	81.87+0.78	309.6534	42.6332	8.96	1080	225.7	4.785	3	MIXED
G35.2008-1.7370	35.20-0.73	285.4398	1.226667	44.5	965.2	519.9	1.857	5	MIXED
G49.4898-0.3876	049.490-0.388	290.9327	14.50983	57.815	852.1	656.9	1.297	5	SFR
G25.7095+0.0438	025.710+0.044	279.5131	-6.40417	95.6	607	268.6	2.26	4	SFR
G328.2541- 0.5322	15541-5349	239.4993	-53.967	-37	440	425	1.035	4	SFR
G25.6954+0.0279	18353-0628	279.5206	-6.42416	96	364	225	1.618	2	SFR

Explanation of columns

G#: Object identifier (with galactic coordinates)

Source name: common name of the source (if applicable)

RA: right ascension

DEC: declination

Vmean: Average peak velocity of the source (with respect to Local Standard of Rest)

Fpeak (Jy): Highest flux density listed in MaserDB, in Jansky. If there is only one observation listed it is noted under Fpeak

Fmin (Jy): Lowest flux density listed in MaserDB, in Jansky.

Vi: Variability index; $Vi = F_{peak}/F_{min}$

Nobs: Number of observations listed in MaserDB

12 GHz methanol masers

G#	Source name	RA	DEC	Vmean (km/s)	Fpeak (Jy)	Fmin (Jy)	Vi	Nobs	type
G351.4170+0.6451	17175-3544	260.2226	-35.7837	-10.1	1210	692	1.749	3	MIXED
G339.8842-1.2590	16484-4603	253.02	-46.1428	-36.2	850	846	1.005	2	SFR
G323.7401-0.2628	15278-5620	232.9396	-56.5139	-49.8	530	396	1.338	3	MIXED
G188.9461+0.8874	06058+2138	92.22392	21.64158	10.79	235	230	1.022	2	MIXED
G133.9487+1.0647*	W3(OH)*	18 38 03.1*	-06 24 32*	-44*	793*	-	-	1	SFR*

*Source: Blazkiewicz and Kus, 2004 (Supplementary information on Visier) [5]

No observations of the 12.2 GHz line of W3(OH) are listed on maserDB, even though it is known as one of the strongest 12.2 GHz sources.

22 GHz water masers

G#	Source name	RA	DEC	Vmean (km/s)	Fpeak (Jy)	Fmin (Jy)	Vi	Nobs	type
G208.9928-19.3847	KL IRC2	83.81031	- 5.37311	7.9	7400000	2875.8	2573.197	12	MIXED
G43.1668+0.0106	190752.1+090108	287.5563	9.103979	10.2	575439.9	4020	143.144	9	MIXED
G133.9487+1.0647	G133.9476+01.0648	36.76911	61.87376	-48.2	30902.95	796.8	38.784	6	SFR
G49.4894-0.3690	6896	290.9164	14.51837	59.9	7413.1	1528.5	4.85	6	SFR
G351.2421+0.6698	351.243+0.671	260.0745	- 35.9161	-76.95	5700	2361.5	2.414	3	SFR
G49.4898-0.3876	G049.489-00.386	290.9327	14.51011	55.4	4662.4	1449.6	3.216	4	SFR
G351.4170+0.6451	NGC6334A	260.2214	- 35.7856	-8.8	855.01	661.5	1.293	2	MIXED

References:

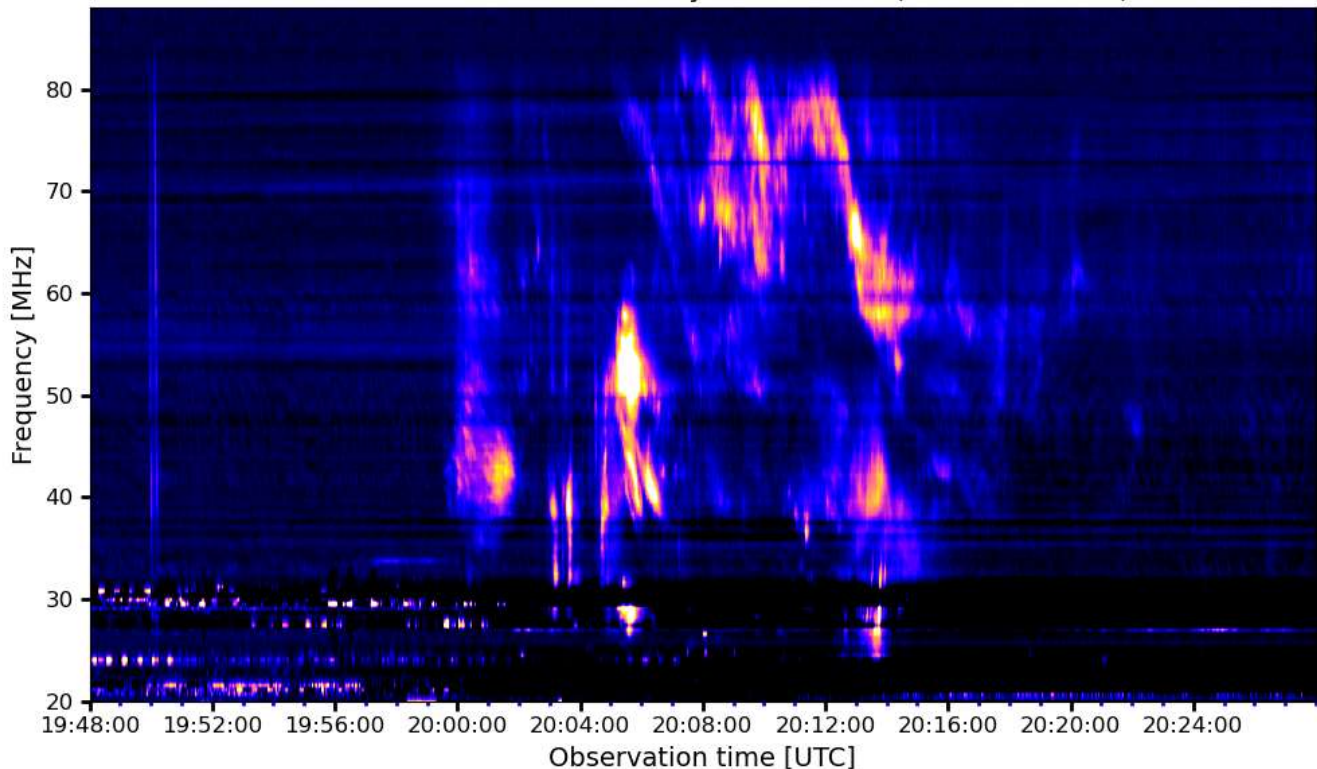
- 1) MaserDB: Databas of astrophysical masers: <https://maserdb.net/>
Ladeyschikov D.A., Bayandina O.S., Sobolev A.M., *Astronomical Journal*, 2019, Vol. 158, P. 233
- 2) Database of Circumstellar Masers (Engels et al.): <https://hsweb.hs.uni-hamburg.de/projects/maserdb//>
- 3) Nancay 1612 MHz maser monitoring program, D. Engels: https://hsweb.hs.uni-hamburg.de/projects/nrt_monitoring/index.html
- 4) AAVSO Variable Star Index: <https://www.aavso.org/vsx/>
- 5) Błaszkiwicz, L., & Kus, A. J. (2004). 12.2 GHz survey towards 6.7 GHz methanol masers-A comparison of 12.2 GHz and 6.7 GHz spectra. *Astronomy & Astrophysics*, 413(1), 233-240.
https://vizier.cds.unistra.fr/viz-bin/VizieR-3?-source=J/A%2bA/413/233/table2&-out.max=50&-out.form=HTML%20Table&out.add=_r&-out.add=_RAJ,_DEJ&-sort=_r&-oc.form=sexa

Observation Reports

Observations in Alaska of Solar Radio and Magnetic Activity During February 2023 Whitham D. Reeve

Type II Slow Radio Sweep on 17 February: The radio sweep was observed at the HAARP and Coho Radio Observatories by Callisto spectrometers and LWA Antennas but the associated received spectra are shown only for HAARP in the image below. The radio event started at 2000 and ended at about 2020. Harmonics usually accompany Type II sweeps in ratios of about 1.8 to 2.0 and some are visible in the image. The received spectra have a complicated structure and may include overlapping Type III and other radio phenomena. A double Type III radio burst is visible in the spectra at about 1950. See <https://reeve.com/Solar/Solar.htm> for burst definitions. The Sun position from HAARP was 153.3° true azimuth and 12.9° elevation at the time of reception.

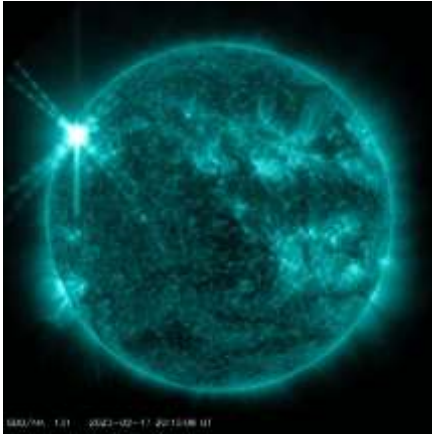
2023/02/17 Radio flux density, e-CALLISTO (ALASKA-HAARP)



Space Weather Prediction Center (SWPC) reported that solar active region 3229 produced an X2.2 x-ray flare at 2016 (see image of the Sun below). The flare, in turn, produced a coronal mass ejection (CME). Type II radio sweeps are very often observed with CMEs. In addition to the Type II, the flare produced radio emissions over a very wide bandwidth.

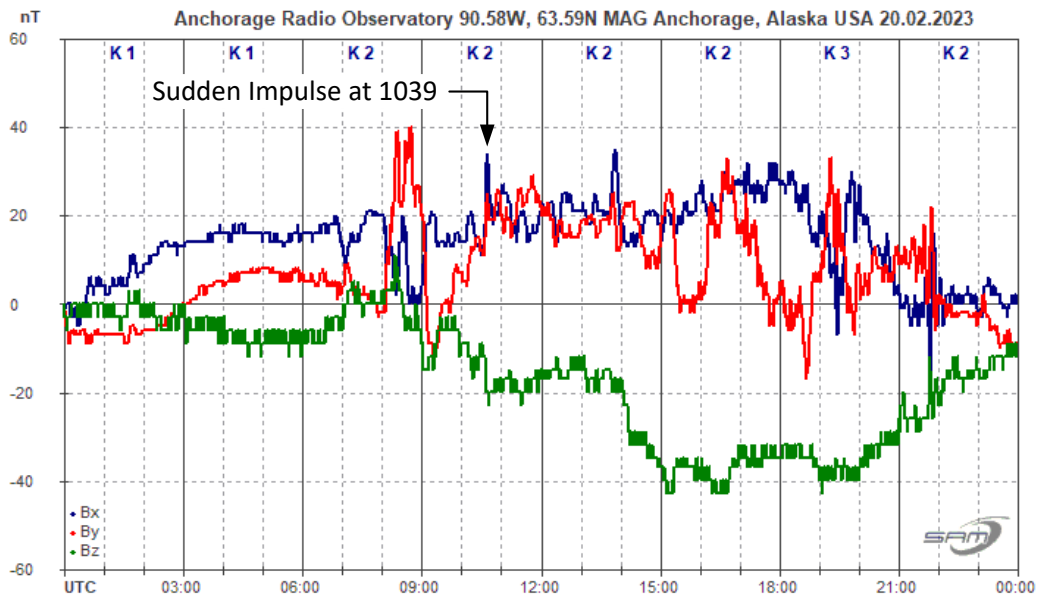
Based on CME imagery and the radio sweep characteristics, SWPC estimated the CME velocity to be $2,407 \text{ km s}^{-1}$. Assuming the estimate was along the Sun-Earth line, the CME would arrive at Earth in 17.3 h, or approximately 1343 on 18 February. However, the actual arrival time was 1039 on 20 February, a time of flight of 62.1 h. Therefore, the average speed toward Earth was closer to 671 km s^{-1} . The interplanetary shock from the CME

arrived at the DSCVR spacecraft at 0952 on 20 February, 47 minutes before a sudden impulse was observed at Earth's magnetosphere. The DSCVR spacecraft is approximately 1.5 million km inside Earth's orbit in a line with the Sun. Assuming the magnetosphere's radius was $8R_E$ (51 thousand km), the distance the shock traveled from the spacecraft to the magnetosphere (to produce the sudden impulse) was approximately 1.45 million km. Therefore, the average speed in that segment of travel was about 514 km s^{-1} . The difference in calculated speeds most likely is due to the assumptions and approximations.



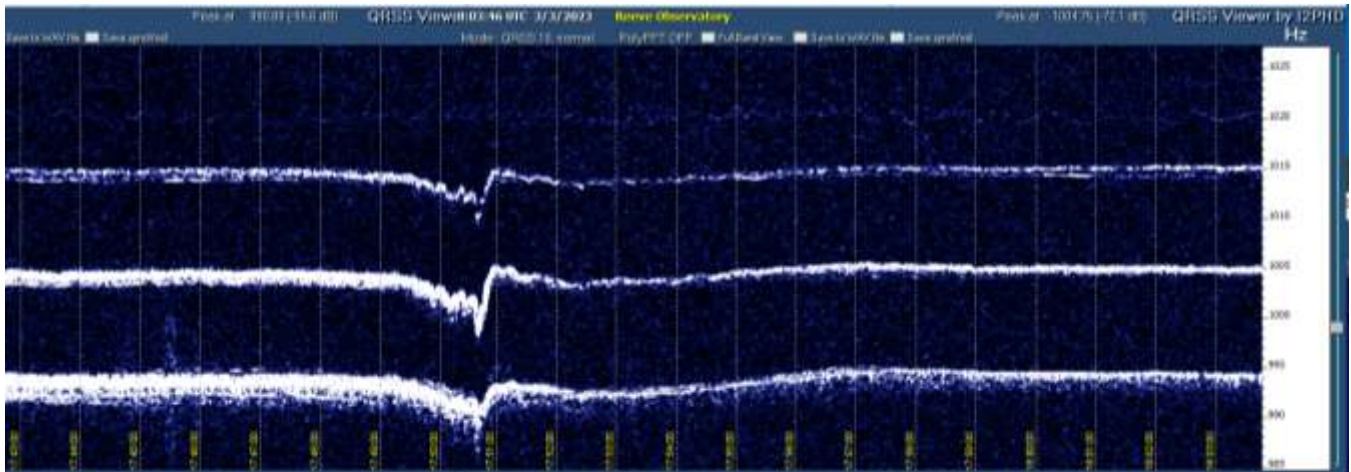
Solar Dynamics Observatory (SDO) image of the Sun at 13.1 nm wavelength showing the flare near the northeast limb at 2015. This wavelength emphasizes a spectral line emitted by iron atoms that have lost 19 and 22 electrons at temperatures of 10 000 000 K and is used to study solar flares and other high-energy solar phenomena. Image source: NASA

Geomagnetic Sudden Impulse on 20 February resulting from the 17 February CME: The sudden impulse mentioned above was recorded on the HAARP SAM-III magnetometer at 1039; see magnetogram below. The magnetometer sensors are located about 50 m from the LWA Antenna used to capture the radio sweep. The sudden impulse was strongest on the x-axis (east-west, blue trace) but also recognizable on the y-axis (north-south, red trace). A small negative deflection on the z-axis (vertical, green trace) barely exceeded the background noise level. A geomagnetic storm sometimes follows a sudden impulse but not in this case. An almost identical magnetic response was recorded on the Anchorage SAM-III magnetometer about 300 km southwest of HAARP. HAARP magnetograms may be viewed in real-time at: https://reeve.com/SAM/SAM-HAARP/SAM-HAARP_simple.html .

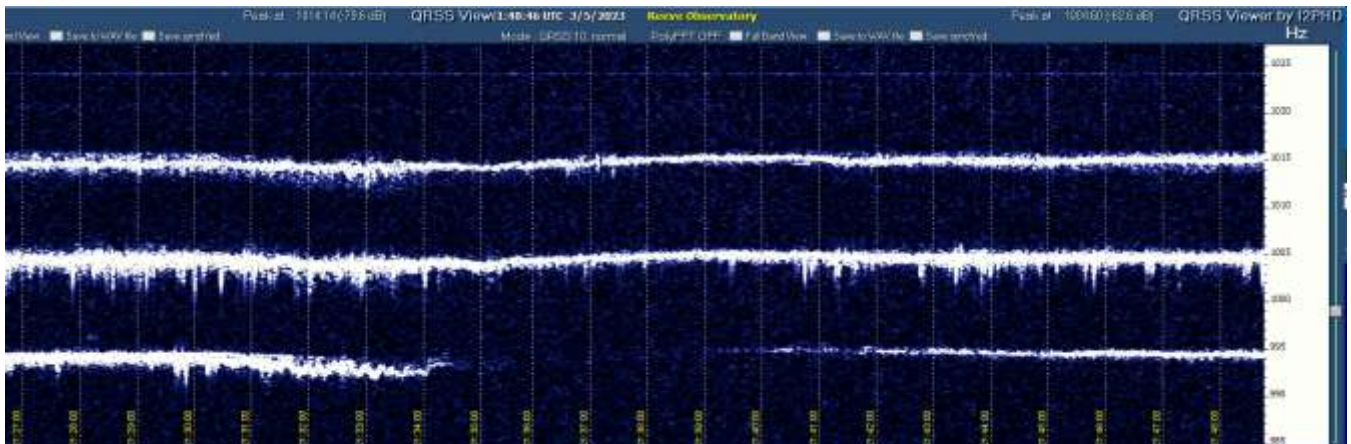


Solar Radio Observations at Anchorage, Alaska in March 2023 Whitham D. Reeve

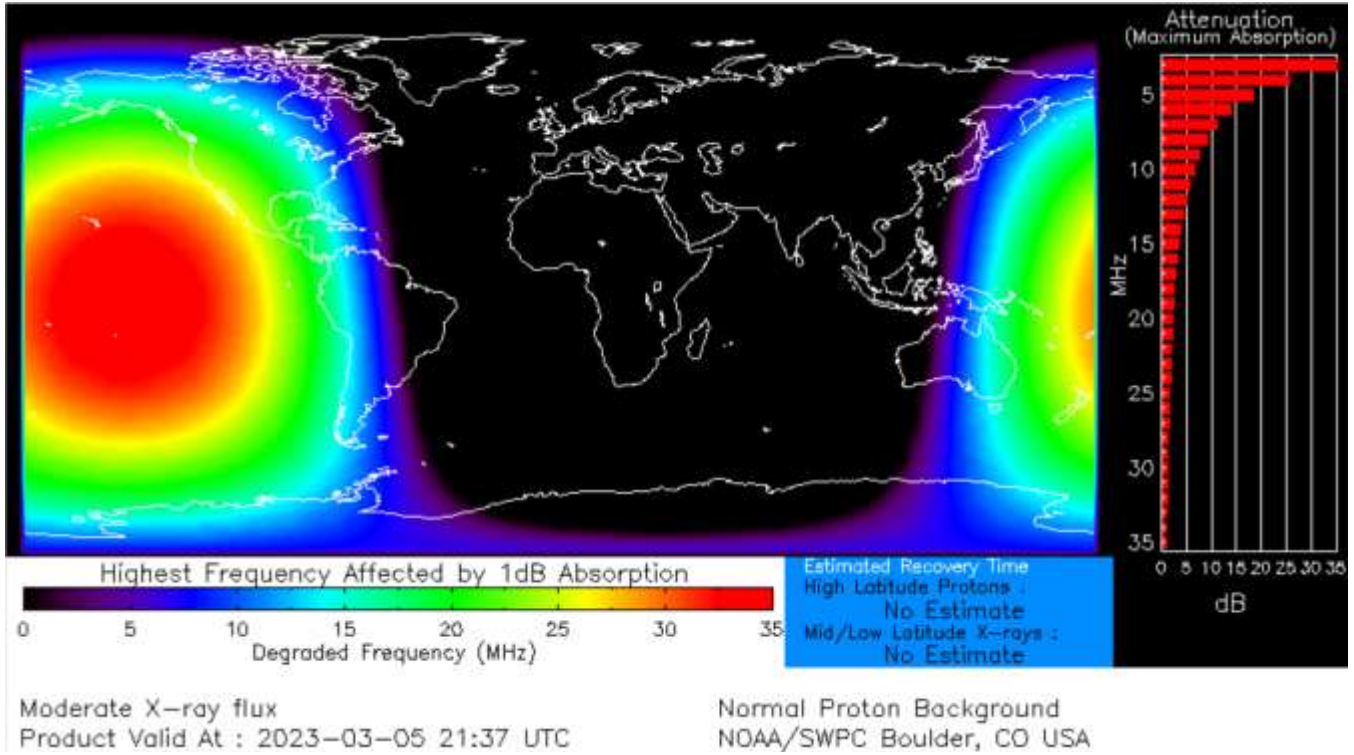
Sudden Frequency Deviations at 15, 20 and 25 MHz on 3 March 2023: The sudden frequency deviations (SFD) were observed to start at 1749 with peak effects at 1750:40 and recovery about 10 minutes later; see Argo plot below. The bottom trace at 995 Hz represents the 15 MHz carrier, the middle trace at 1005 Hz represents the 20 MHz carrier and the upper trace at 1015 Hz represents the 25 MHz carrier. All carriers are from the WWV or WWVH time-frequency stations. The SFDs were caused by the radiation from an X2.1 x-ray flare at solar active region 3234. The flare radiation began at 1742, peaked at 1752 and ended at 1759. The Sun position from Anchorage at 1751 was 115° true azimuth and 5.6° elevation; sunrise had been about 1 h before.



Radio Blackout at 15 MHz on 5 March 2023: Solar active region 3243 produced an M5.0 x-ray flare starting at 2129, peaking at 2136 and ending at 2141. The radiation from the flare enhanced the ionosphere's D-region electron density, thereby increasing the absorption at 15 MHz and producing a radio blackout. Referring to the Argo plot below, the radio blackout at 15 MHz, represented by the 995 Hz trace, was observed to start at Anchorage at 2134 with partial recovery about 10 minutes later. The carrier frequencies at 20 and 25 MHz (middle and upper traces at 1005 and 1015 Hz, respectively) also were affected but not severely enough to produce a radio blackout at those frequencies in the path to Anchorage.



The D-Region Absorption Prediction (D-RAP) plot produced by Space Weather Prediction Center for 2137 (below) shows 3 – 4 dB attenuation at 15 MHz and somewhat less at 20 and 25 MHz as seen in the histogram on the right side of the plot. These values take into account the radio wave’s 2-way passage through the D-region. The Sun position from Anchorage at 2137 was 171° true azimuth and 22.6° elevation.



Journal Archives and Other Promotions

The rich and diverse legacy of member contributed content is available in the SARA Journal Archives. Table of contents for journals is available online at: [SARA-Journal-Master-Index.xlsx \(live.com\)](#)

The entire set of The Journal of The Society of Amateur Radio Astronomers is available by online download. It goes from the beginning of 1981 to the end of 2022 (over 6000 pages of SARA history!)

All SARA journals and conference proceedings are available through the previous calendar year.

SARA Store (radio-astronomy.org/store.)

SARA offers the above USB drives, DVDs, printed Proceedings and Proceedings on USB drive and other items at the SARA Store: <http://www.radio-astronomy.org/e-store>. Proceeds from sales go to support the student grant program. Members receive an additional 10% discount on orders over \$50 US. Payments can be made by sending payment by PayPal to treas@radio-astronomy.org or by mailing a check or money order to SARA, c/o Brian O'Rourke, 337 Meadow Ridge Rd, Troy, VA 22974-3256

SARA Online Discussion Group

SARA members participate in the online forum at <http://groups.google.com/group/sara-list>. This is an invaluable resource for any amateur radio astronomer.

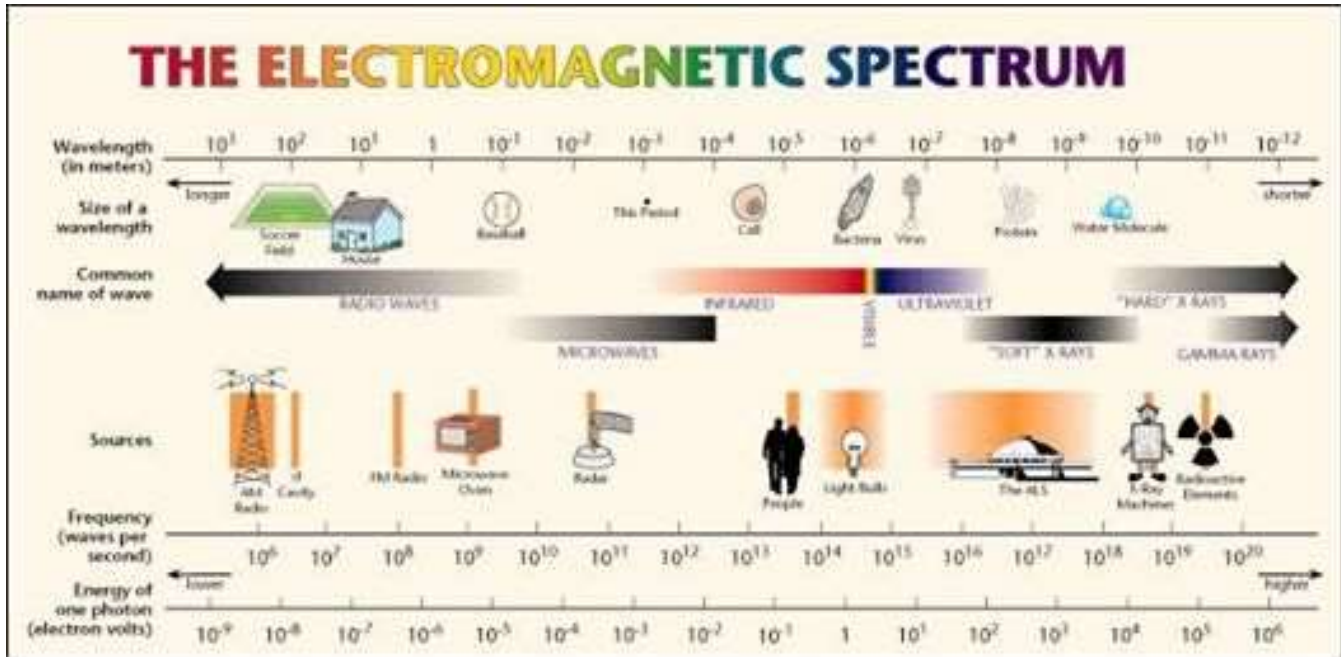
SARA Conferences

SARA organizes multiple conferences each year. Participants give talks, share ideas, attend seminars, and get hands-on experience. For more information, visit <http://www.radio-astronomy.org/meetings>.

What is Radio Astronomy?

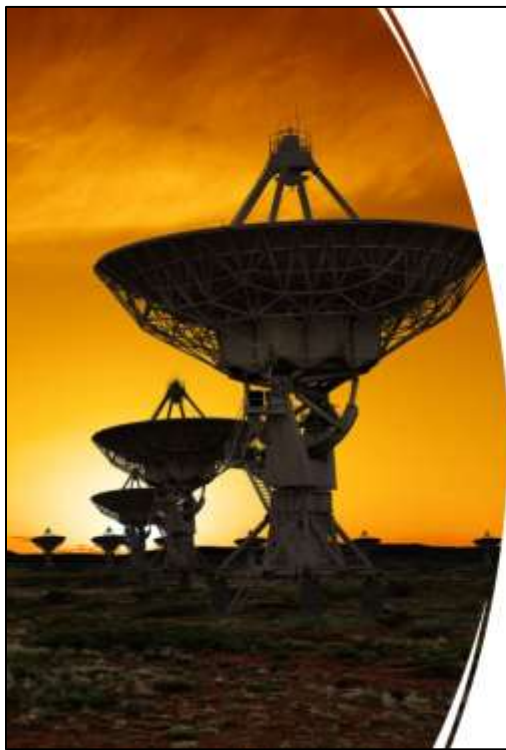
This link is for a booklet explaining the basics of radio astronomy.

<http://www.radio-astronomy.org/pdf/sara-beginner-booklet.pdf>



Radio Astronomy Constants, Variables and Formulas – Parabolic Dish Gain

SARA YouTube Channel: https://youtu.be/2bx5K9jUc_w



Society of Amateur Radio Astronomers

Radio Astronomy

Constants, Variables, and Formulas



Lesson 1

Parabolic Dish Antenna Gain

Parabolic Dish

- A parabolic dish collects radio waves and redirects them to a focus.
- The shape reflects the radio waves to a focus
- The antenna feed is located at the focus to collect the concentrated signal



Antenna Gain

- Antenna gain is the measure of the directionality of the antenna

$$G(dBi) = 10 \text{Log}_{10} \left(\eta x \left(\frac{\pi D}{\lambda} \right)^2 \right)$$

η Efficiency of the antenna (50%-85%)

π Pi (3.14259)

D Diameter of the antenna

$\lambda = c / f$ Wavelength = speed of light/ frequency

Example Problem #1

Given:

$D=1m$ $\eta = 50\%$, $f=1420$ MHz, $c= 299,792,458$ m/s $\approx 3 \times 10^8$ m/s

Calculations:

$$\lambda = \frac{c}{f} = \frac{3 \times 10^8 \text{ m/s}}{1420 \times 10^6 / \text{s}} = .21 \text{ m}$$

$$G(dBi) = 10 \text{Log}_{10} \left(\eta x \left(\frac{\pi D}{\lambda} \right)^2 \right)$$

$$G(dBi) = 10 \text{Log}_{10} \left(.5 x \left(\frac{3.14259 x 1 \text{ m}}{.21 \text{ m}} \right)^2 \right) = 20.49 \text{ dBi}$$

Example Problem #2

Given:

$D=3m$, $\eta = 65\%$, $f=1260 \text{ MHz}$, $c= 299,792,458 \text{ m/s} \approx 3 \times 10^8 \text{ m/s}$

Calculations:

$$\lambda = \frac{c}{f} = \frac{3 \times 10^8 \text{ m/s}}{1260 \times 10^6 / \text{s}} = .24 \text{ m}$$

$$G(\text{dBi}) = 10 \text{Log}_{10} \left(\eta x \left(\frac{\pi D}{\lambda} \right)^2 \right)$$

$$G(\text{dBi}) = 10 \text{Log}_{10} \left(0.65 x \left(\frac{3.14259 x 3 \text{ m}}{0.24 \text{ m}} \right)^2 \right) = 30.01 \text{ dBi}$$



Like and Subscribe!

Join SARA to start your hobby of
Amateur Radio Astronomy

www.radio-astronomy.org

Administrative

Officers, directors, and additional SARA contacts

The Society of Amateur Radio Astronomers is an all-volunteer organization. The best way to reach people on this page is by email with SARA in the subject line SARA Officers.

President: Dr. Rich Russel, AC0UB, <https://www.radio-astronomy.org/contact/President>

Vice President: Jay Wilson, <https://www.radio-astronomy.org/contact/Vicepresident>

Secretary: Bruce Randall, NT4RT, <https://www.radio-astronomy.org/contact/Secretary>

Treasurer: Brian O'Rourke, K4UL, <https://www.radio-astronomy.org/contact/Treasurer>

Past President: Dennis Farr

Founder Emeritus and Director: Jeffrey M. Lichtman, KI4GIY, jeff@radioastronomysupplies.com

Board of Directors

Name	Term expires	Email
Ed Harfmann	2024	edharfmann@comcast.net
Dr. Wolfgang Herrmann	2023	messbetrieb@astropeiler.de
Tom Jacobs	2023	tdj0@bellsouth.net
Charles Osborne	2023	k4cso@twc.com
Bob Stricklin	2024	bstrick@n5brg.com
Steve Tzikas	2024	Tzikas@alum.rpi.edu
Jon Wallace	2023	wallacefj@comcast.net
David Westman	2024	david.westman@engineeringretirees.org

Other SARA Contacts

All Officers	http://www.radio-astronomy.org/contact-sara	
All Directors and Officers	http://www.radio-astronomy.org/contact/All-Directors-and-Officers	
Eastern Conference Coordinator	http://www.radio-astronomy.org/contact/Annual-Meeting	
All Radio Astronomy Editors	http://www.radio-astronomy.org/contact/Newsletter-Editor	
Radio Astronomy Editor	Dr. Richard A. Russel	drrichrussel@netscape.net
Contributing Editor	Whitham D. Reeve	whitreeve@gmail.com
Educational Outreach	http://www.radio-astronomy.org/contact/Educational-Outreach	
Grant Committee	Tom Crowley	grants@radio-astronomy.org
Membership Chair	http://www.radio-astronomy.org/contact/Membership-Chair	
Technical Queries (David Westman)	http://www.radio-astronomy.org/contact/Technical-Queries	
Webmaster	Ciprian (Chip) Sufitchi, N2YO	webmaster@radio-astronomy.org

Resources

Great Projects to Get Started in Radio Astronomy

Radio Observing Program

The Astronomical League (AL) is starting a radio astronomy observing program. If you observe one category, you get a Bronze certificate. Silver pin is two categories with one being personally built. Gold pin level is at least four categories. (Silver and Gold level require AL membership which many clubs have membership. For the bronze level, you need not be a member of AL.)

Categories include

- 1) SID
- 2) Sun (aka IBT)
- 3) Jupiter (aka Radio Jove)
- 4) Meteor back-scatter
- 5) Galactic radio sources

This program is a collaboration between NRAO and AL. Steve Boerner is the Lead Coordinator and a SARA member.

For more information:

Steve Boerner

2017 Lake Clay Drive

Chesterfield, MO 63017

Email: sboerner@charter.net

Phone: 636-537-2495

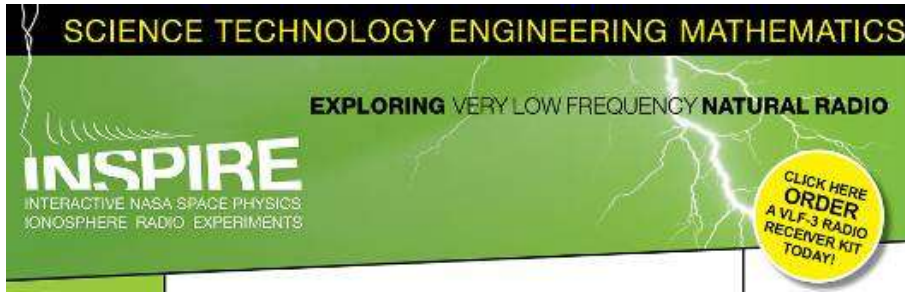
<http://www.astroleague.org/programs/radio-astronomy-observing-program>

Radio Jove



The Radio Jove Project monitors the storms of Jupiter, solar activity and the galactic background. The radio telescope can be purchased as a kit, or you can order it assembled. They have a terrific user group you can join. <http://radiojove.gsfc.nasa.gov/>

INSPIRE Program



The INSPIRE program uses build-it-yourself radio telescope kits to measure and record VLF emissions such as tweeks, whistlers, sferics, and chorus along with man-made emissions. This is a very portable unit that can be easily transported to remote sites for observations.

<http://theinspireproject.org/default.asp?contentID=27>

SARA/Stanford SuperSID



Stanford Solar Center and the Society of Amateur Radio Astronomers have teamed up to produce and distribute the SuperSID (Sudden Ionospheric Disturbance) monitor. The monitor utilizes a simple pre-amp to magnify the VLF radio signals which are then fed into a high definition sound card. This design allows the user to monitor and record multiple frequencies simultaneously. The unit uses a compact 1-meter loop antenna that can be used indoors or outside. This is an ideal project for the radio astronomer that has limited space. To request a unit, send an e-mail to supersid@radio-astronomy.org

Radio Astronomy Online Resources

SARA YouTube Videos: https://www.youtube.com/channel/UC-SzptAQZ-20c9CkRb9ZPpw/videos	Pisgah Astronomical Research Institute: www.pari.edu
AJ4CO Observatory – Radio Astronomy Website: http://www.aj4co.org/	A New Radio Telescope for Mexico - ORION 2021 01 20. Dr. Stan Kurtz https://www.youtube.com/watch?v=Q9aBWr1aBVc
Radio Astronomy calculators https://www.aj4co.org/Calculators/Calculators.html	National Radio Astronomy Observatory http://www.nrao.edu
Introduction to Amateur Radio Astronomy (presentation) http://www.aj4co.org/Publications/Intro%20to%20Amateur%20Radio%20Astronomy,%20Typinski%20(AAC,%202016)%20v2.pdf	NRAO Essential Radio Astronomy Course http://www.cv.nrao.edu/course/astr534/ERA.shtml
RF Associates Richard Flagg, rf@hawaii.rr.com 1721-1 Young Street, Honolulu, HI 96826	Exotic Ions and Molecules in Interstellar Space -- ORION 2020 10 21. Dr. Bob Compton https://www.youtube.com/watch?v=r6cKhp23SUo&t=5s
RFSpace, Inc. http://www.rfspace.com	The Radio JOVE Project & NASA Citizen Science – ORION 2020.6.17. Dr. Chuck Higgins https://www.youtube.com/watch?v=s6eWAXjywp8&t=5s
CALLISTO Receiver & e-CALLISTO http://www.reeve.com/Solar/e-CALLISTO/e-callisto.htm	UK Radio Astronomy Association http://www.ukraa.com/
Deep Space Exploration Society http://DSES.science	CALLISTO software and data archive: www.e-callisto.org
Deep Space Object Astrophotography Part 1 -- ORION 2021 02 17. George Sradnov https://www.youtube.com/watch?v=Pm_Rs17KlyQ	Radio Jove Spectrograph Users Group http://www.radiojove.org/SUG/
European Radio Astronomy Club http://www.eraonet.org	Radio Sky Publishing http://radiosky.com
British Astronomical Association – Radio Astronomy Group http://www.britastro.org/baa/	The Arecibo Radio Telescope; It's History, Collapse, and Future - ORION 2020.12.16. Dr. Stan Kurtz, Dr. David Fields https://www.youtube.com/watch?v=rBZIPOLNX9E
Forum and Discussion Group http://groups.google.com/group/sara-list	Shirleys Bay Radio Astronomy Consortium marcus@propulsionpolymers.com
GNU Radio https://www.gnuradio.org/	SARA Twitter feed https://twitter.com/RadioAstronomy1
SETI League http://www.setileague.org	SARA Web Site http://radio-astronomy.org
NRAO Essential Radio Astronomy Course http://www.cv.nrao.edu/course/astr534/ERA.shtml	Simple Aurora Monitor: Magnetometer http://www.reeve.com/SAMDescription.htm
NASA Radio JOVE Project http://radiojove.gsfc.nasa.gov Archive: http://radiojove.org/archive.html https://groups.io/g/radio-jove	Stanford Solar Center http://solar-center.stanford.edu/SID/
National Radio Astronomy Observatory http://www.nrao.edu	

For Sale, Trade and Wanted

At the SARA online store: radio-astronomy.org/store.

SARA Polo Shirts

New SARA shirts have arrived.

We now have a good selection of X, XX, and XXX shirts available in all colors including white! Shirts are \$20 at the conference and \$25 shipped.

Contact the treasurer at treas@radio-astronomy.org for availability and shipping.



Scope in a Box

radio-astronomy.org/store.

Kit of parts and software to build a working Radio Telescope to detect Hydrogen Line emissions. Available to USA addresses only at this time.

SuperSID Complete Kit

radio-astronomy.org/store.



SARA Publication, Journals and Conference Proceedings (various prices)

radio-astronomy.org/store.

SARA Journal Online Download

radio-astronomy.org/store.

The USB drive covers the society journal "Radio Astronomy" from the founding of the organization in 1981 thru 2020. Articles cover a wide range of topics including: cosmic radiation, pulsars, quasars, meteor detection, solar observing, Jupiter, Radio Jove, gamma ray bursts, the Itty Bitty Telescope (IBT), dark matter, black holes, the Jansky antenna, methanol masers, mapping at 408 MHz and more. This CD contains all of the above and more with over 4800 pages of articles on radio astronomy. Also included is a copy of Grote Reber's handwritten, 34 page document "Carriage and Mirror Detail" of his historic antenna now on display at the National Radio Astronomy Observatory (NRAO) in Greenbank, WV. You also get an electronic copy of the 109 page "Basics of Radio Astronomy" from JPL Goldstone-Apple Valley Radio Telescope. Also included is the NRAO 40-foot radio telescope "Operators Manual", which by the way, you get to operate if you attend the Eastern SARA conference in July.

SARA Advertisements

There is no charge to place an ad in Radio Astronomy; but you must be a current SARA member. Ads must be pertinent to radio astronomy and are subject to the editor's approval and alteration for brevity. Please send your "For Sale," "Trade," or "Wanted" ads to edit@radio-astronomy.org. Please include email and/or telephone contact information. Please keep your ad text to a reasonable length. Ads run for one bimonthly issue unless you request otherwise.

Radio-Astro-Machine, zblac@gmail.com

Elevation rotation adapter plate for Scope in a Box and custom machining. For further information visit <https://radio-astro-machine.wixsite.com/my-site> or send an email.

Typinski Radio Astronomy, Inc., info@typinski.com

Antenna systems and feed line components for HF radio astronomy

Jeff Kruth, WA3ZKR, kmec@aol.com

RF components from HF to MMW, various types including mixers, RF switches, amplifiers, oscillators, coaxial components, waveguide components, etc. I have a very large collection of stuff and the facilities to test and provide data. Please email with your needs and I will see if I have something for you. Have fun!

Stuart and Lorraine Rumley, sales@valontechnology.com

The Valon Technology 2100 Downconverter, when combined with our 5009 frequency synthesizer module, provides a high-performance, compact receiver downconverter system. Applications include hydrogen line studies at 1420MHz and radio astronomy in the protected 30MHz segment of the 21 cm band. For more information visit <http://www.valontechnology.com/2100downconverter.html> or send an email.

Radio2Space, filippo.bradaschia@primalucelab.com

SPIDER radio telescopes and turn-key-systems designed specifically for education.

<https://www.radio2space.com>

We developed our SPIDER radio telescopes as turn-key-system just to avoid the problem you perfectly highlighted in your website: "Purchasing a radio telescope isn't like buying an optical telescope. They are harder to find, and usually require assembly and software troubleshooting. In some cases, a radio telescope must be built from components." Our SPIDER radio telescopes are not designed for amateurs that prefer to build a radio telescope but to schools, universities, museums, and other science institutes that needs for a complete and ready-to-use system, just like the optical telescopes they can normally buy!

Membership Information

Annual SARA dues Individual \$20, Classroom \$20, Student \$5 (US funds) anywhere in the world. Membership includes a subscription to Radio Astronomy, the bimonthly Journal of The Society of Amateur Radio Astronomers, delivered electronically (via a secure web link, emailed to you as each new issue is posted). We regret that printing and postage costs prevent SARA from providing hardcopy subscriptions to our Journal.

We would appreciate the following information included with your check or money order, made payable to SARA:

Name: _____
 Email Address: _____
(required for electronic Journal delivery)
 Ham call sign: _____ (if applicable)
 Address: _____
 City: _____
 State: _____
 Zip: _____
 Country: _____
 Phone: _____

Please include a note of your interests. Send your application for membership, along with your remittance, to our Treasurer.

For further information, see our website at: <http://radio-astronomy.org/membership>

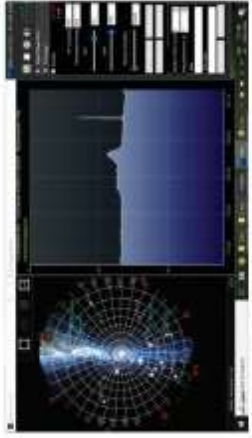


Society of Amateur Radio Astronomers, Inc.
 Founded 1981

Membership supported, nonprofit [501(c) (3)]
 Educational and Radio Astronomy Organization
**Knowledge through Common Research,
 Education and Mentoring**

How to get started?

SARA has a made a kit of software and parts to detect the Hydrogen line signal from space. This is an excellent method to get started in radio astronomy. It teaches the principles of antenna design, signal detection, and signal processing. Read more about this and other projects on our web site.



SARA members have been privileged to use this forty foot diameter drift-scan hydrogen line radio telescope every year at their annual meeting in Green Bank.



<http://radio-astronomy.org>

Why Radio Astronomy?

Because about sixty five percent of our current knowledge of the universe has stemmed from radio astronomy alone. The discovery of quasars, pulsars, black holes, the 3K background from the "Big Bang" and the discovery of biochemical hydrogen/carbon molecules are all the result of professional radio astronomy.



The Society of Amateur Radio Astronomers

SARA was founded in 1981, with the purpose of educating those interested in pursuing amateur radio astronomy.

The society is open to all, wishing to participate with others, worldwide.

SARA members have many interests, some are as follows:

SARA Areas of Study and Research:

- Solar Radio Astronomy
- Galactic Radio Astronomy
- Meteor Detection
- Jupiter
- SETI
- Gamma Ray/High Energy Pulse Detection
- Antennas
- Design of Hardware / Software

The members of the society offer a friendly mentor atmosphere. All questions and inquiries are answered in a constructive manner. No question is silly!

SARA offers its members an electronic bi-monthly journal entitled Radio Astronomy. Within the journal, members report on their research and observations. In addition, members receive updates on the professional radio astronomy community and, society news.

Once a year SARA meets for a three-day conference at the Green Bank Observatory in Green Bank West Va.

There is also a spring conference held at various cities in the Western USA. Previous meetings have been at the VLA in Socorro, NM and at Stanford University.



How do amateurs do radio astronomy?

Radio astronomy by amateurs is conducted using antennas of various shapes and sizes, from smaller parabolic dishes to simple wire antennas. These antennas are connected to receivers and most of these receivers are software defined radios these days. Data from the receivers are collected by computers, and the received signals will be displayed as charts, graphs or maybe even sky maps. As diverse as the observed objects, so is the instruments and tools used. SARA members will always be supportive to find good solutions for what one wishes to observe.

Is amateur radio astronomy instrumentation expensive?

Technical information freely circulated in our monthly journal helps amateurs to obtain good low noise equipment from off the shelf assemblies, or to build their own units. The actual cash investment in radio astronomy equipment need not exceed that of any other hobby.

What are amateurs actually looking for in the received data?

The aim of the radio amateur is to find something new and unusual. Just as an amateur optical observer hopes to notice a supernova or a new comet, so does an amateur radio observer hope to notice a new radio source, or one whose radiation has changed appreciably.

How do I get started?

Just as a long journey begins with the first step, the project you elect must start with a clear idea of your objectives. Do you wish to study the sun? Jupiter? Make meteor counts? Do you wish to engage in imaging radio astronomy? What you decide will not only determine the type of equipment you will need, but also the local radio spectrum.



The Reber Telescope at NRAO. Constructed by Grote Reber in 1937 in his back yard in Wheaton, Illinois



SARA Members discussing the IBT (Itty Bitty Telescope)

